CAMERI - Coastal and Marine
Engineering Research Institute

המכון הישראלי
לחקר הנדסה ימית בע"מ

Marine Policy Plan for Israel:

Physical Oceanography, Deep Sea and Coastal zone Overview

P.N. 800/14

August 2014

Technion City, Haifa

CAMERI - Coastal and Marine
Engineering Research Institute

המכון הישראלי
לחקר הנדסה ימית בע"מ

Marine Policy Plan for Israel:

Physical Oceanography, Deep Sea and Coastal zone Overview

P.N. 800/14

Prepared for: Technion Research and Development Foundation Ltd.

By: Eliezer Kit

Uri Kroszynski

August 2014

Technion City, Haifa

Table of contents

1 – INTRODUCTION

This document is an attempt at outlining the present state of knowledge about the Mediterranean sea in the Israeli Exclusive Economic Zone (EEZ). The outline is based on first hand scientific and professional knowledge based on research and engineering project work dealing with the Israeli coastal waters, as well as on references to relevant works found in technical literature and in the Internet. The Coastal and Marine Engineering Research Institute (CAMERI) staff, composed by academic researchers and engineers has gained experience and reputation in research and consultancy work for public, governmental and private bodies.

The document is intended to aid the effort to develop a Marine Spatial Plan for the Israeli Mediterranean EEZ. CAMERI was sub-contracted to deal with the Physical Oceanography part of phase 1 of the Plan.

We found it relevant to outline very broadly some phenomenological description and focus on pointing out data collected from observations, with references to the source where the measured data can be found. Nevertheless, one section deals with the generation of synthetic data by means of models. The reason for that is the necessity to describe the oceanographic data for the huge bodies of water in the offshore where only scarce measurements can be conducted. These models are solved numerically by up-to-date software programs running on modern digital computers/clusters.

The sections deal with the following subjects:

- A general introductory outline of the Mediterranean Sea geography and climate;
- The bathymetry, or seafloor topography in the EEZ area;
- Water masses and general circulation patterns;
- Winds, which are the main forcing for sea surface layer flow in deep waters and for currents in shallower waters, as well as being the main cause for the generation of waves.
- Waves, which are responsible for mixing the sea surface layer and causing uniform density waters in shallower areas, as well as causing coastal currents and thus sediment transport;
- Temperature and salinity, whose distribution governs water density gradients leading to the formation and flow of water masses and to the vertical buoyancy gradients leading to the displacement of deep waters;
- Coastal currents, generated by wind stress and breaking waves. These currents transport sediment and therefore govern coastal morphology;
- Tides and sea level;
- Bed sediment, granulometry and sediment transport;
- Numerical models and operational forecasting systems;
- Tsunamis and
- New technologies for oceanographic measurements;

Final remarks point out what information gaps need to be filled and outlines some recommendations concluding the document.

The report contains semi-independent sections dealing with the different aspects mentioned. However, the sections follow a logical thread. Within each section, the large scale deep sea description is done before going into more detailed scale as the coast is approached. At the end of each section there is a list of references and quite often links to appropriate Internet sites.

Some of the subjects might be outside the established scope. Some other subjects were not addressed. A comprehensive coverage of *all* subjects is not possible given the time and volume limits of the report. So, the present document is largely a result of choice and compromise. It is

hoped that the document is informative enough for an overview, and that it is useful at the same time and will allow the reader to deepen his knowledge by reading the suggested references.

At the beginning of the nineties, oceanographers were aware of how little knowledge there was about the eastern Mediterranean

> "… *The general conclusion is that very little is known of the Eastern Mediterranean in comparison with other interesting regions of the world's ocean. The phenomenological evidence is still inconclusive and contradictory, and leaves unsolved the major questions concerning the basic physical mechanisms and driving forces of the circulation itself (wind versus thermohaline driven). The role of tracer distributions in determining circulation patterns is still poorly understood. Modelling efforts are scanty and often provide contradictory results. We address the major and critical questions which must be answered to obtain a basic understanding of the dynamics of the Eastern Mediterranean; we review the present knowledge of its phenomenology and of the modelling research carried out up to now, critically assessing what is still poorly known or ambiguous.*"
>
> Extract from *Large-scale properties of the Eastern Mediterranean: a review,* by Paola Malanotte-Rizzoli and Artur Hecht, published in Oceanologica Acta 1988, Vol. 11 – No. 4, pp. 323-335.

Among the important points to be clarified at that time, the authors mention:

> "*1) What is the dominant driving force of the Eastern Mediterranean circulation: a) the wind stress field; b) thermohaline fluxes; or c) source/sink distribution of flow?*
> *2) Is there a quasi-steady, yearly component of the circulation or is the seasonal cycle the dominating pattern?*"

These and other researchers initiated the Physical Oceanography in the Eastern Mediterranean (POEM) program that, during a decade, made a huge contribution to the current knowledge of physical oceanography in this area. Today, the general circulation patterns in the Eastern Mediterranean are much better understood thanks to planned measurement campaigns undertaken during the last 20 years. It is precisely the aim of this document to outline these observations.

Geography

As its name indicates, the Mediterranean Sea is surrounded by land: Europe on the north, the (Asian) Near East on the east and Africa on the south. It communicates on the west with the Atlantic Ocean through the 14 Km wide and only 300 m. deep Gibraltar Straight, on the north-east with the Black Sea through the Dardanelles (200 m. deep) entrance to the Sea of Marmara and then the 50 m. deep Bosphorus to the Black Sea. Finally, on the south-east, it communicates with the Red Sea through the man made, 20 m. deep, Suez Canal. The Mediterranean is approximately 3800 Km. long and about 1600 Km. at its widest, with an average depth of 1.5 Km. (the deepest point is at a depth of about 5.2 Km). Its area is about 2.5 million square Km and its volume about 3.7 million cubic Km.

A population of 400 million people lives along the 46.000 Km of Mediterranean coastline (40% of which are island perimeters), belonging to 22 countries.

Its borders are very irregular, so several regions of the Mediterranean are known by different names, like the Adriatic Sea, the Aegean Sea, etc., as shown in Fig. 1.1. Similarly, the seafloor is also very irregular forming different basins separated by large and small islands and submerged mount chains. In particular, the tip of the Italy boot, Sicily and the Sicilian strait sill, separate the Mediterranean in Western and Eastern basins, which are, in turn, subdivided into sub-basins, each with it's own particular characteristics. In the north part of the Eastern Basin we have the Adriatic between Italy and the Balkans, and the Aegean. In the southern part, we have the Ionian basin (between the Strait of Sicily and the Cretan Passage) and the Levantine basin. Israel's EEZ is in the south-east corner of this latter basin.

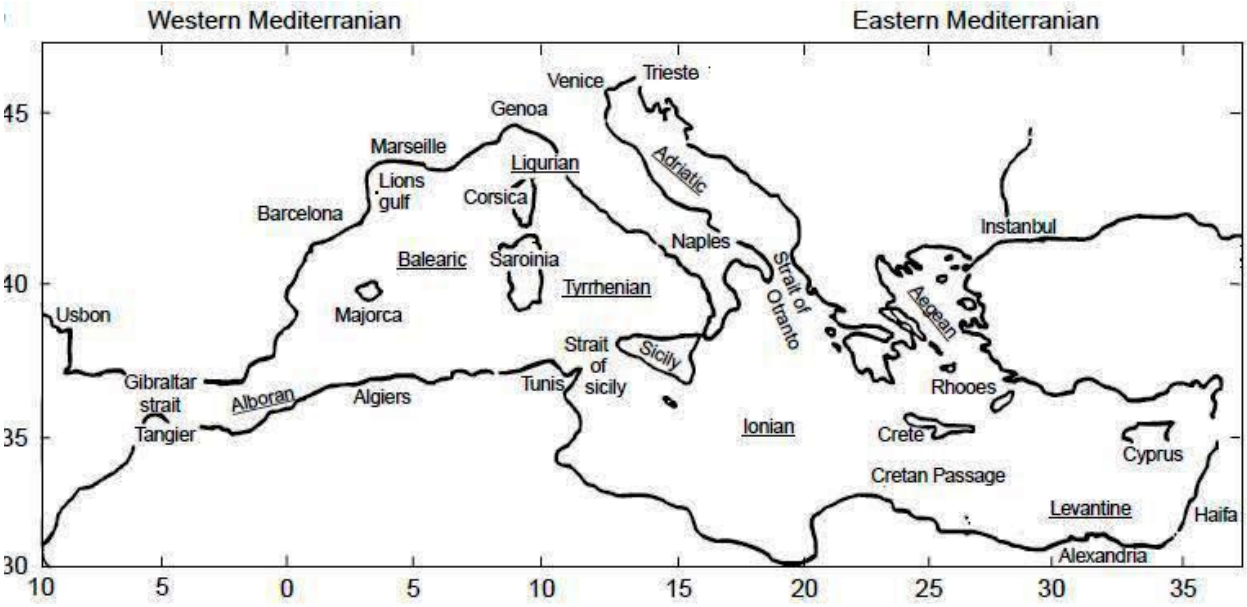

Fig. 1.1 – Mediterranean Sea geography: Straits and sub-basins (latitude and longitude in degrees). Source: *Robinson et al.* (2001)

Local climate

The climate in the Eastern Mediterranean is characterized by mild, rainy winters and dry, hot summers. Precipitation amounts decrease from west to east and from north to south, ranging from 1000-1250 mm around Antalya to 600-800 mm Iskenderun Bay. In the coastal plains of the southern part, precipitation may reach 600-850 mm around Beirut, Akko, and Tzfat, and decreases to about 400 mm or less in the arid southern Israel (*Hogan C., 2013*). Droughts are becoming more frequent and extended.

An assessment of climatic change in the Eastern Mediterranean (*CIMME, 2011*), predicts increasing temperatures, particularly in the northern part (Turkey, Greece) with 1-3°C by 2030, 3-5°C by 2050 and 3.5-7°C by the end of the century. This means warming at a faster rate than the global 2.8°C predicted by the end of the century. In addition, it predicts heat waves and extreme high summer temperature peaks. Another predicted trend is of decreasing rain. 10-50% less rain is expected the north during this century, with even drier springs and summers. An increase of about 5 dry days per year by mid century is predicted for Israel, which seems modest compared with 20 more dry days per year in Turkey.

The Mediterranean coastal area of Israel has a climate characterized by properties imposed by the sub-tropic "highs" (regions of semi-permanent high atmospheric pressure). These "highs", located between latitudes 25°N and 30°N move with the sun: southward in winter and northward in summer. Consequently, the summer climate is under the influence of the tropic "highs", while in winter the climate of the region is sandwiched between the sub-tropic "highs" in the south and the "conditioned weather" in the north. The conditioned weather area is characterized by moving "lows" (storms) which cause precipitations and bad weather conditions when they "succeed" in penetrating into the Mediterranean. Therefore, the weather is characterized by (sometimes very strong) precipitations with calm conditions between them.

In addition to these general patterns the region is influenced by other geographic factors, which can be divided in two categories: (a) bodies of air and (b) monsoons.

(a) Since the coast of Israel is located on the eastern boundary of the Mediterranean Sea, only westerly winds are humid (warm in winter and cool in summer). Winds from other directions bring dry air (warm in summer and cold in winter).

(b) The Mediterranean coast of Israel can be under the influence of monsoons from either NE or SE. In both cases, the pressure systems generated improve the weather conditions in this region. These systems are the Indian monsoon in summer, the Siberian "high" in winter and the Sudanese-Ethiopian "low" active during all seasons, especially in autumn (*Stiassnie, 1987*).

References

Hogan C., 2013; "Levantine Sea". Retrieved from Encyclopedia of Earth http://www.eoearth.org/view/article/166646

CIMME, *2011*: "Climatic change and impacts in the Eastern Mediterranean and the Middle East", CIMME Annual Report, The Cyprus Institute, 12pp. Found as pdf file in the Internet.

Malanotte-Rizzoli P. and Hecht A., *1988*; "Large-scale properties of the Eastern Mediterranean: a review", Oceanologica Acta **11**/4, 323-335

Robinson A.R., Leslie W.G., Theocharis A., Lascaratos A., *2001*; "Mediterranean Sea Circulation", OCEAN CURRENTS, Academic Press, 19 pp.

Stiassnie M., *1987*: "Safe Heavens for Avoidance of Dangerous Weather and Sea State in Mediterranean, Ashdod Port", CAMERI report P.N.188/87, Technion City, Haifa

2 – BATHYMETRY

There are several datasets of measured Mediterranean Sea bathymetry. For example, depths can be obtained from global sources like the General Bathymetric Chart of the Oceans, GEBCO, featuring 30 arc-second and 1 arc-minute gridded bathymetry data for the entire Mediterranean. These data were generated by combining quality-controlled ship depth-soundings with interpolation between sounding points guided by satellite-derived gravity data. However, in areas where they improve on the existing grid, data sets generated by other methods have been included. Land data are largely based on the Shuttle Radar Topography Mission (SRTM30) gridded digital elevation model. (https://www.bodc.ac.uk/data/online_delivery/gebco/).

One of the most comprehensive and detailed collection of bathymetry datasets for the entire Mediterranean and its sub-areas is presented as maps and metadata in the European Marine Observation and Data Network (EMODNET) portal, at the website http://www.emodnet-hydrography.eu/#.

Israel's offshore region

Concerning the south-eastern Levantine Sea, Israel has contributed to the EMODNET database a very detailed bathymetry survey, undertaken by the Geological Survey of Israel (GSI), together with the Israel Oceanographic and Limnological Research (IOLR) and the Survey of Israel, in the National Bathymetric Survey project, initiated in 2001 (*Hall, 2013*). Utilizing sophisticated equipment and research vessels, an area approximately 160 Km long along the coast by 70 Km wide has been surveyed, leaving unmapped only that part of Israel's Mediterranean EEZ deeper than 1600 m. By 2005, 440 million soundings had been done from IOLR's vessel R/V Etziona, all along the coast, from Gaza to Lebanon, between 15 and 700 m depth. Then, during the fall of 2010, an additional strip of deeper waters up to 1600 m depth (8700 square Km) was mapped with a rented multi-beam sonar system aboard EcoOcean's vessel R/V Mediterranean Explorer (*ECOOCEAN, 2010*).

According to *Hall* (2013), The gas fields offshore Israel have been or are under development with specific, very high resolution surveys being carried out by foreign ships and underwater vehicles. These should eventually be integrated into the 25 m Digital Terrain Model (DTM) of Israel's offshore, which remains classified except at grid resolutions of ~50 m.

The horizontal resolution of the measurements is 2-5 m up to a depth of 100 m and 10-25 m on the continental slope to 700 m depth. As an example of the resolution of the survey, the kurkar ridges offshore Yafo, as well as other seafloor details are shown in Fig. 2.1.

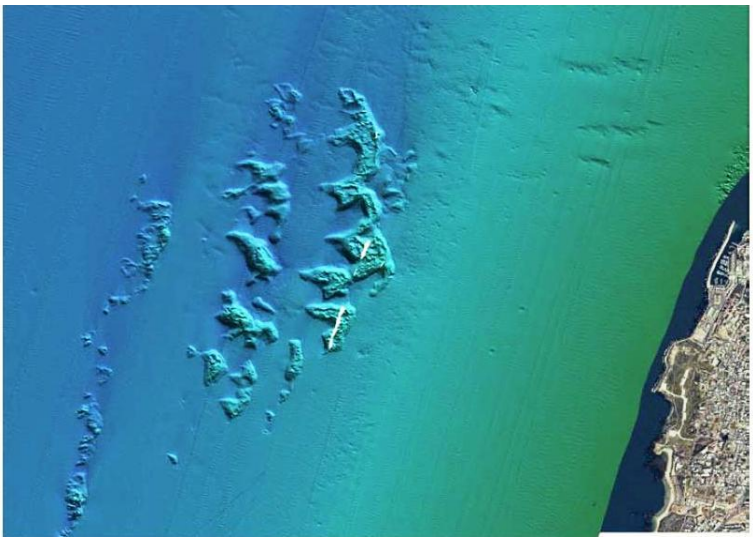

Fig. 2.1 – Kurkar ridges and other seafloor details offshore Yafo, National Bathymetric Survey project. Source: *Hall* (2009)

The bathymetry of the south-eastern Levantine basin, zoomed-in from the interactive map at the EMODNET website, is reproduced in Fig. 2.2. In the upper Fig. 2.2 (a), some details of the seafloor topography can be appreciated, like the submerged Mount Erathostenes south of Cyprus. Fig. 2.2 (b) shows the different surveyed areas more clearly. The region surrounding the yellow Israeli area is left gray, indicating the absence of detailed data. In that region, GEBCO data is used.

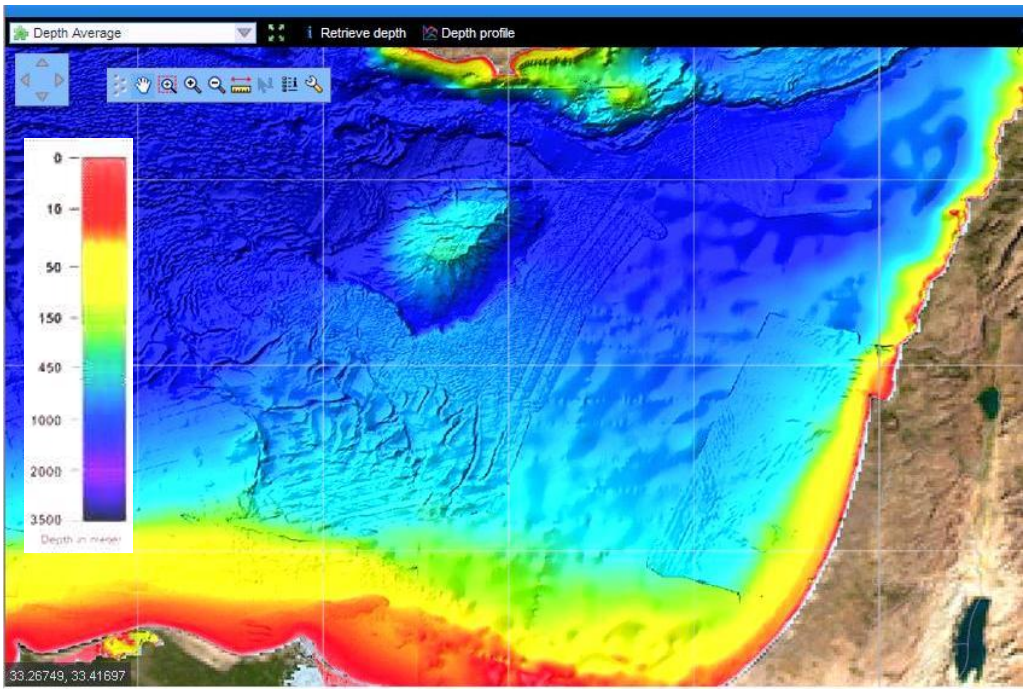

(a)

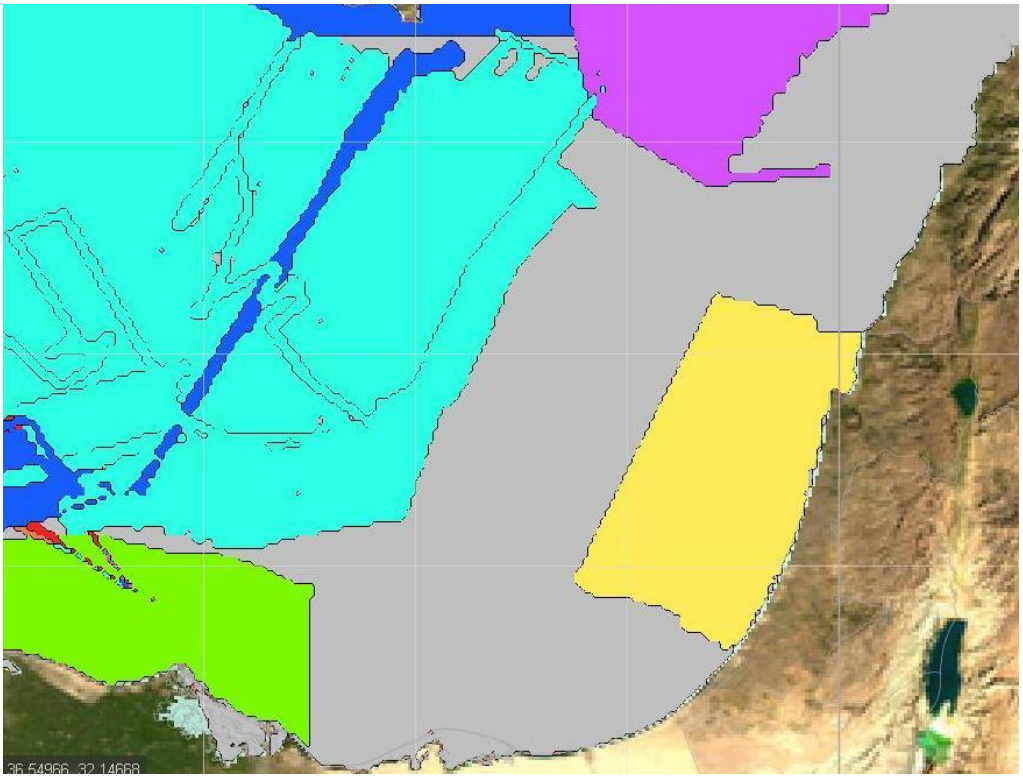

(b)

Fig. 2.2 – South-Eastern Mediterranean bathymetry map: (a) features of the seafloor. A closer look at the coast of Israel reveals the rectangular area with the contribution of the National Bathymetric Survey; (b) the yellow rectangular area along the Israeli coast is clearly marked, as well as colored areas for the contributions from other survey programs. Grey areas indicate lack of detailed surveys. Source: www.emodnet-bathymetry.eu/

Detailed bathymetry maps at various sites in the coastal region

In the immediate vicinity of the shoreline, more detailed bathymetry maps exist in the context of particular coastal development projects and construction of marine structures. These are changing as soon as e.g. dredging or sand deposition works are undertaken, a breakwater is prolonged, etc., as is the case for Haifa Port in recent years (see *Levin et al., 2014*). Fig. 2.3 shows an example of the changes in bathymetry of the area surrounding Haifa Port from 2007 to 2013.

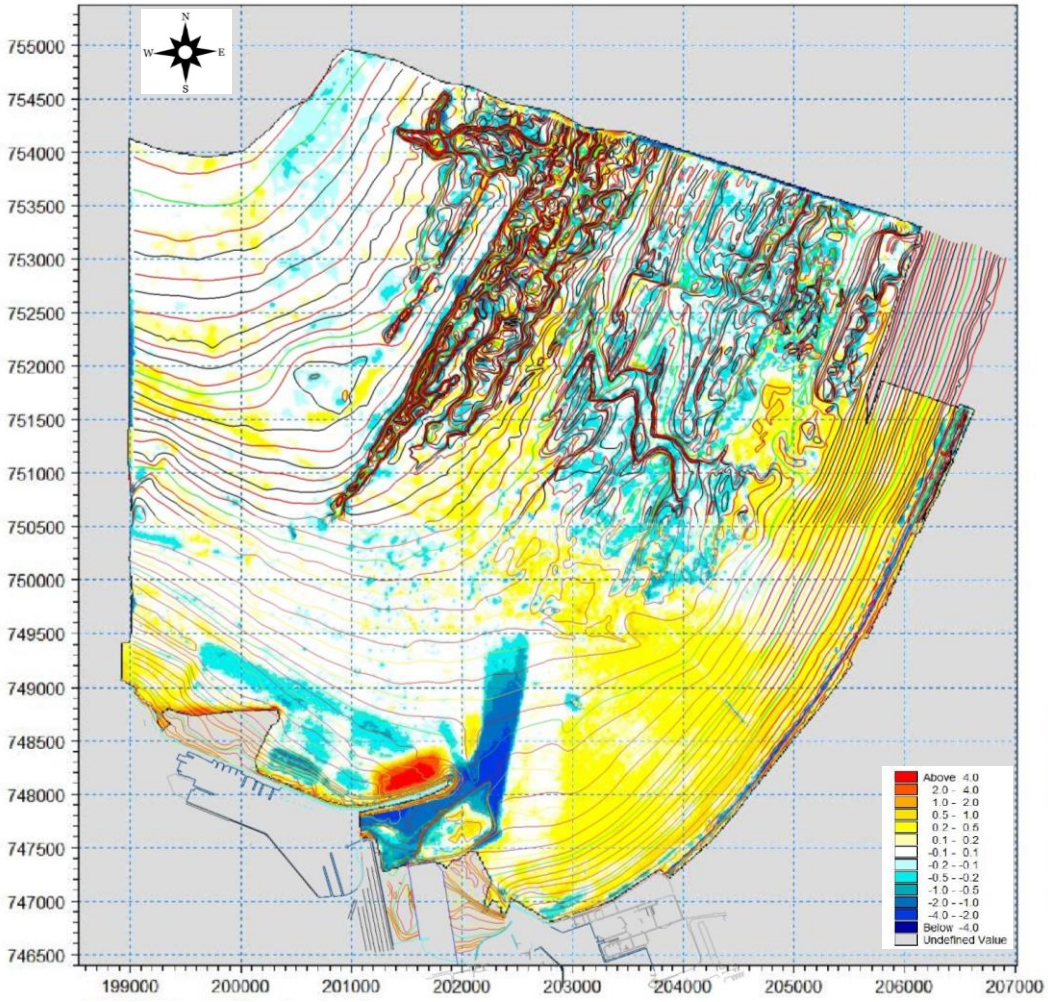

Fig. 2.3 – Changes in bathymetry in the vicinity of Haifa Port between 2007 and 2013. Blue shades indicate deepening, while yellow and red indicate that area became shallower. Color scale is in meters, Coordinates (also in meters) follow the New Israeli Grid. Source: *Levin et al.* (2014)

Similar detailed bathymetry maps exist for Ashkelon region in the vicinity of Rutenberg Power station settling basin (CAMERI report P.N.781/13), Ashdod Port development projects (CAMERI report P.N.795/14 = differential maps; CAMERI report P.N.762/12 = Sand Mining EIA for Haifa Port development; CAMERI report P.N.706/09 = DHV), Tel Aviv – Herzliya region new protection scheme (CAMERI report P.N.790/14), Netanya cliff protection project (CAMERI report P.N.760/12) and in the vicinity of Hadera Power station settling basin (CAMERI report P.N.747/11), Haifa Port development projects (CAMERI report P.N.799/14 = Channel monitoring; CAMERI report P.N.782/13 = Channel hindcast model; CAMERI report P.N.761/12 = Sand Mining EIA).

Geological research into the retreat of the coastal cliff and other hazards has resulted in the Geological Survey of Israel, GSI, carrying out a complete mapping of the coastal zone by LIDAR (laser beam LIght and raDAR) technology, producing a basic 50 cm grid (*Hall, 2013*).

References

Drimer N., Glozman M., Kit E., Levin A., and Sladkevich M., *2009*: "Processing of Hydrographic Data for the Ashdod Port Extension Project", CAMERI report P.N.706/09, Technion City, Haifa.

ECOOCEAN, *2010*; "Deep multi-beam survey offshore Israel", ECOOCEAN, Marine Research and Education http://www.ecoocean.org/?PageId=588

Hall J.K. et al., *2009*; "The Israel National Bathymetric Survey Almost Completed", FIG Working Week 2009, Surveyors Key Role in Accelerated Development, Note and Presentation, Hydrographic Surveying in Practice, 3-8 May 2009, Eilat, Israel

Hall J.K., *2013*; "Israel National Report", presented at the Mediterranean and Black Seas Hydrographic Commission (MBSHC) 18th Meeting, 25-27 September 2013, Istanbul, Turkey

Khudyakova V., Kroszynski U., Levin A., Sladkevich M., and Kit E., *2012*: "Netanya Coast and Cliff Protection Study: Modeling Stage", CAMERI final report P.N.760/12, Technion City, Haifa.

Levin A. et al., *2014*; "Monitoring activities after completion of works for deepening the marine entrance channel to Haifa Port", CAMERI report P.N. 799, 162 pp., Technion City, Haifa (in Hebrew)

Levin A., Glozman M., Keren Y., Sladkevich M., Kroszynski U., and Kit E., *2013*: "The Environmental Impact of Shallow Water Dredging of Sand (Tasks 1.3.3, 1.4.1, 1.4.2 and 1.4.3), Haifa Region, *National Master Plan 13/B/1/1*", CAMERI report P.N.761/12, Technion City, Haifa.

Levin A., Glozman M., Keren Y., Sladkevich M., Kroszynski U., and Kit E., *2013*: "The Environmental Impact of Shallow Water Dredging of Sand (Tasks 1.3.3, 1.4.1, 1.4.2 and 1.4.3), Nitzanim Region, *National Master Plan 13/B/1/1*", CAMERI report P.N.762/12, Technion City, Haifa.

Levin A., Jensen A., Christensen B. B., Dorge J., Glozman M., Sladkevich M., Kroszynski U., and Kit E., *2013*: "The Environmental Impact of Shallow Haifa Port Channel Dredging Works, *Hindcast Modeling*", CAMERI report P.N.782/13, Technion City, Haifa.

Sladkevich M., Glozman M., Keren Y., Levin A., and Kit E., *2013*: "Rutenberg Power Station and Ashkelon Desalination Plant: I. Statistical Analysis of Waves; II. Engineering Assessment of Brine and Warm Water Spreading", CAMERI report P.N.781/13, Technion City, Haifa.

Sladkevich M., Glozman M., Levin A., Keren Y., and Kit E., *2011*: "Spreading of Warm Water Issued from the Hadera Power Station Diluted with Brine Released from the Hadera Desalination Plant", CAMERI report P.N.747/11, Technion City, Haifa.

Sladkevich M., Levin A., and Kit E., *2013*: "Morphological Changes within the Ashdod Port Region", CAMERI report P.N.795/14, Technion City, Haifa.

Sladkevich M., Levin A., and Kit E., *2013*: "Sedimentological Numerical Model for Studying the Protection Schemes of the Herzliya Coast and Cliff, *Models Calibration*", CAMERI report P.N.790/14, Technion City, Haifa.

3 – WATER MASSES AND GENERAL CIRCULATION

Circulation in the Mediterranean is very active, not only at surface level, but also in deep water. The reasons for the circulation of water masses are many, ranging from Coriolis forces to topographic and geographic constraints, to water mass displacement and density currents due to temperature and salinity gradients, to wind stress and waves on the surface, etc.

Due to climatic conditions, the Mediterranean is an evaporation basin. The inflow of fresh water from big rivers (like the French Rhone, the Spanish Ebro, the Italian Po, and the Egyptian Nile) and smaller rivers (see Fig. 3.1), added to rainfall (average ~500 mm/year or 1250 cubic Km per year), and seepage from coastal aquifers are insufficient to balance evaporation. Fresh water is an essential factor in replenishing the upper layer of the sea, reduce its salinity and provide sediment, nutrients (and pollution). Its discharge to the sea, however, has been drastically reduced in the last 50 years due to climatic changes and to accelerated human development activities and consumption. For instance, the Nile discharges a mere 150 cubic meters per second i.e. less than 5 cubic Km per year after construction of the Aswan dam. The total annual fresh water discharge into the Mediterranean is about 315 cubic Km from rivers, and about 70 cubic Km from coastal aquifers, (*UNEP/MAP*, *2012*).

Thus, the volumetric balance is kept by sea water inflow. The contribution from the Black Sea is rather small (less than 300 cubic Km per year) and the one from the Red Sea through the Suez Canal is much smaller. The main inflow is therefore from the Atlantic Ocean.

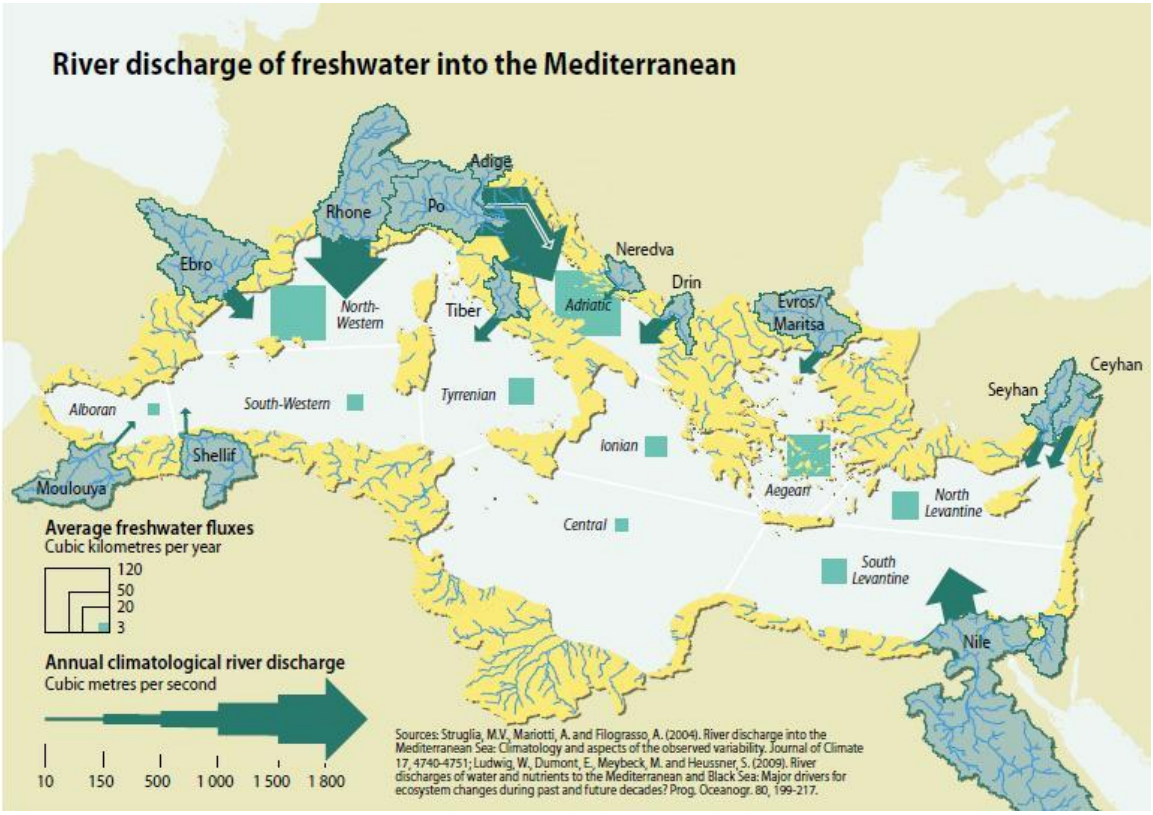

Fig. 3.1 – Drainage basins and discharge of rivers into the Mediterranean Sea (2004). Source: *UNEP/MAP* (2012)

Mediterranean waters are warmer and saltier than the inflowing ocean water. Evaporation increases the salinity of surface waters. When warm saline surface water cools after the summer season, it may become denser than deeper waters, which are perhaps slightly less saline but still keep warm. This unstable buoyancy gradient gives rise to the (vertical) termohaline circulation.

The formation of water masses and their interaction has been the subject of intense study. An important effort in this direction has been undertaken in the POEM (Physical Oceanography in the Eastern Mediterranean) international project during the last decade of the former millennium (*Robinson et al., 2001*, *Malanotte-Rizzoli and Bergamasco, 1989*, *Malanotte-Rizzoli and Hecht, 1988*, and *Robinson et al., 1992*).

Schematically, the Mediterranean Sea comprises three main water masses (*UNEP/MAP, 2012*) as illustrated in Fig. 3.2:

- The MAW (Modified Atlantic Water), formed in the surface layer with a thickness of 100-200 m. and salinity of 36.2 psu (near Gibraltar) to 38.6 psu (in the Levantine basin).
- The LIW (Levantine Intermediate Water), formed in the Levantine Basin between 200 and 800 m. depth and with salinity 38.4-39.1 psu, which is the most saline water mass of the eastern Mediterranean Basin. LIW is formed in late winter at several locations of the Levantine Sea as well as in the southern Aegean Sea.
- The MDW (Mediterranean Deep Water) is the deep layer of dense water. In the Eastern basin, the deep water mass (EMDW) is characterized by a temperature below 13.6°C and a salinity of 38.7 psu (slightly cooler and less saline than the LIW).

The incoming Atlantic water (left of figure) crossing Gibraltar is continuously modified by evaporation and by mixing with more saline waters beneath as it flows east along Africa. With an already darker shade of blue for the eastern basin (see Fig. 3.2), the MAW is subject to seasonal warming or cooling but becomes much denser when it cools during autumn which causes it to sink in specific zones, contributing to the formation of intermediate and deep waters. The dense intermediate LIW, in turn, flows west and eventually out again to the ocean. This large scale circulation pattern has been named, by analogy, the "conveyor belt".

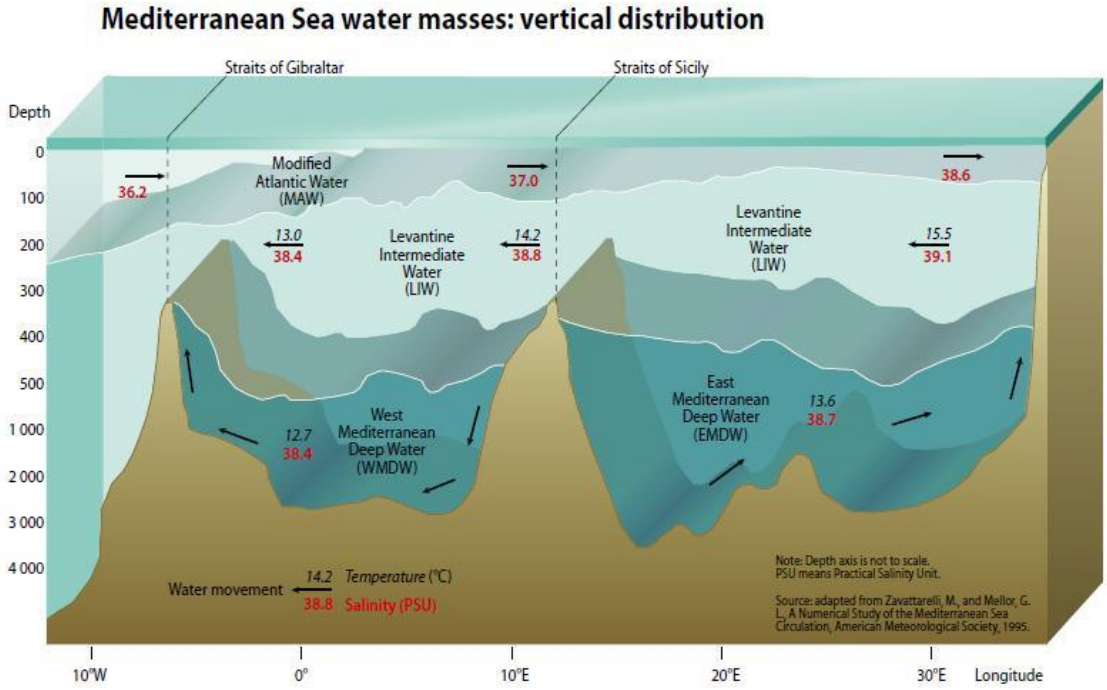

Fig. 3.2 – Schematic view of main water masses (black numbers indicate temperature in °C, red ones indicate salinity in psu and arrows indicate the direction of circulation). Note the gradual darkening of the uppermost layer from ocean salinity in the west to fully developed MAW in the east. Source: *UNEP/MAP* (2012)

The POEM research program had established that a single homogeneous water body filled the entire Eastern Basin below 1200 m depth. The deep water column had formed mainly from dense water exiting the Adriatic and was characterized by temperature and salinity slowly decreasing with depth, which implies low static stability. Considering the 1200 m. depth limit, it was calculated that the renewal period of the deep water mass would be about 126 years (*Roether and Shiltzer, 1991).*

Observations and intensive field measurements in the last decade of last century indicated another source of dense water in the Aegean Sea. This dense water flowing through the Cretan Arc straits with a salinity of 29.24 psu sunk into the bottom layer of the central regions of the Eastern basin, displacing the resident, less dense (29.18 psu) EMDW of Adriatic origin upwards (*Manca et al., 2002*). In the short period from 1987 to 1995, the new deep water mass, warmer and more saline than the old EMDW, had replaced about 20% of the deep water below 1200 m. This abrupt change in water mass characteristics and circulation was termed "the transient". The dense Aegean waters propagated northwards into the Ionian Sea and eastwards into the Levantine basin, affecting the properties of the Levantine Deep Water (designated LDW).

The LIW has been detected in several places of the Levantine basin. Meteorological and hydrological conditions within the Levantine Sea are generally favorable for the convergence and convective sinking of high salinity waters. The eastern Mediterranean generally, and the region between Rhodes and Cyprus more specifically, are areas of formation of the LIW.

During late fall and winter, cold, dry winds cause increased evaporation and cooling of the basin's surface sea layer. Moreover, cold waters from the (shallow) continental shelves also mix with the surface waters. At different places (in particular in the northern part of the basin), the more saline and colder surface waters become denser than the underlying ones and sink, causing formation of the LIW and contributing perhaps also of the LDW. The LIW reach the Western Mediterranean basin and, mixed with other saline water, eventually flow out to the Atlantic Ocean as a submerged, saline current through Gibraltar. According to *Millot et al.* (2006), the densest component of the outflow is Tyrrhenian Dense Water (TDW).

Thus, the circulation in the Mediterranean can be likened to an "engine" which transforms the lightly salted Atlantic water entering through the Strait of Gibraltar into dense, salty water known as Mediterranean water, which in turn leaves through the Strait of Gibraltar into the North Atlantic (*OCA/CNES, 2000*). The inflow from the Atlantic balances the Mediterranean total volume while the dense, salty water outflow balances the total amount of salt.

The large scale circulation features described have significant seasonal and geographical variability. Smaller scale (sub-basin and mesoscale) features, like gyres and eddies, are identified, as shown schematically in Fig. 3.3. These gyres and eddies can be present seasonally or more permanently.

In order to get an idea of the complexity of the Mediterranean currents pattern, the YouTube clip at https://www.youtube.com/watch?v=BeurUq0cRaM presents a visualization of an 11 month flow simulation constrained with measured data. The clip was prepared at NASA's Goddard Space Flight Center Scientific Visualization Studio. The time period for this visualization is 16 Feb 2005 through 16 January 2006. One second in the clip corresponds to about 2.75 days in the simulation. The colors of the flows represent their depths. White represents near surface flow while deeper currents are bluer. The flow field was produced by running a simulation using the MIT general circulation model (MITgcm), constrained with satellite and other data. Unfortunately, flow in the Levantine basin is not shown in the clip. Besides the capability of visualizing huge amounts of data in a compact and understandable fashion, the clip illustrates the power of numerical flow models and data synthesizing software.

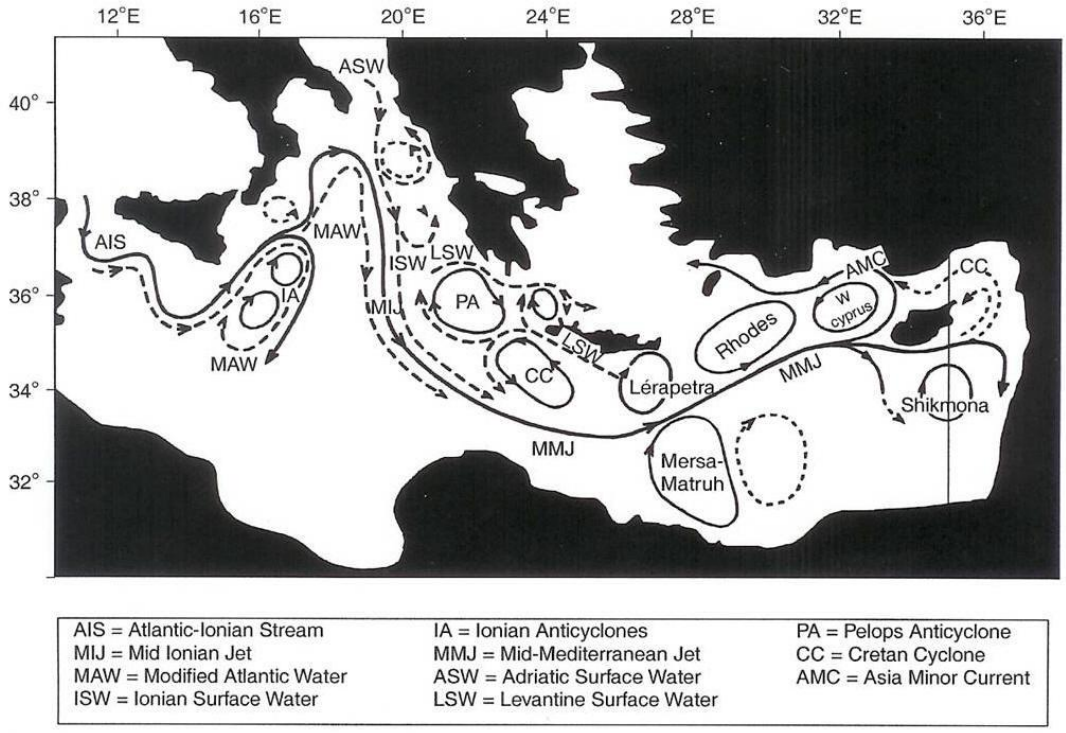

Fig. 3.3 – Schematic view of sub-basin and mesoscale features in the Eastern Mediterranean. Source: *Hogan* (2013)

There are three main sub-basin eddies within the Levantine basin, which interact dynamically, namely: The anti-cyclonic (clockwise) Mersa Matruh and Shikmona gyres; and the cyclonic Rhodes gyre east of Crete. The feature closest to Israel is the long lived (more than a month as shown in *Poulain et al., 2010*) is the Shikmona gyre. The meandering and bifurcating Mid-Mediterranean Jet-flow (MMJ) of the central Levantine basin current and the Asia Minor Current (AMC) feed these gyres and eddies (*Hogan, 2013*).

A comprehensive international project, NEMED (North Eastern Mediterranean), sponsored by the U.S. Office of Naval Research, deals with the satellite tracking of drifters released at different times and locations as a means to quantify the surface circulation and eddy variability in the eastern Levantine basin. Direct measurements of surface circulation were performed over a full seasonal cycle (summer 2009 to spring 2010) using low-cost satellite tracked drifters, with particular focus on the waters in the vicinity of Cyprus, Israel and Turkey (*Poulain et al., 2010*). IOLR participated as a main project partner. A total of 16 drifters were released. The first 6 drifters were released in August 2009, three of them about 20 Km offshore Ashdod, the other three along a line south of Cyprus (Fig. 3.4 a). Then, 7 drifters were released in November-December 2009, again, three of them offshore Ashdod and the other four along a line south of Cyprus (Fig. 3.4 b). The third deployment episode took place in March 2010, with three drifters released offshore Ashdod (Fig. 3.4 c). The following features were observed:

- A strong coastal current off the coasts of Israel, Lebanon and Syria, flowing northwards. Loops in the tracked trajectories indicate the presence of eddies generated by the coastal current.
- A long lived (more than a month) anti-cyclonic (clockwise) gyre at the north-west of Haifa. Its period is about 4 days and its diameter about 80 Km. (see Fig. 3.4 a).
- In Fig. 3.4 b, the gyre is circumvented but there is evidence of another eddy south of Cyprus, above the submerged Mount Erathostenes.

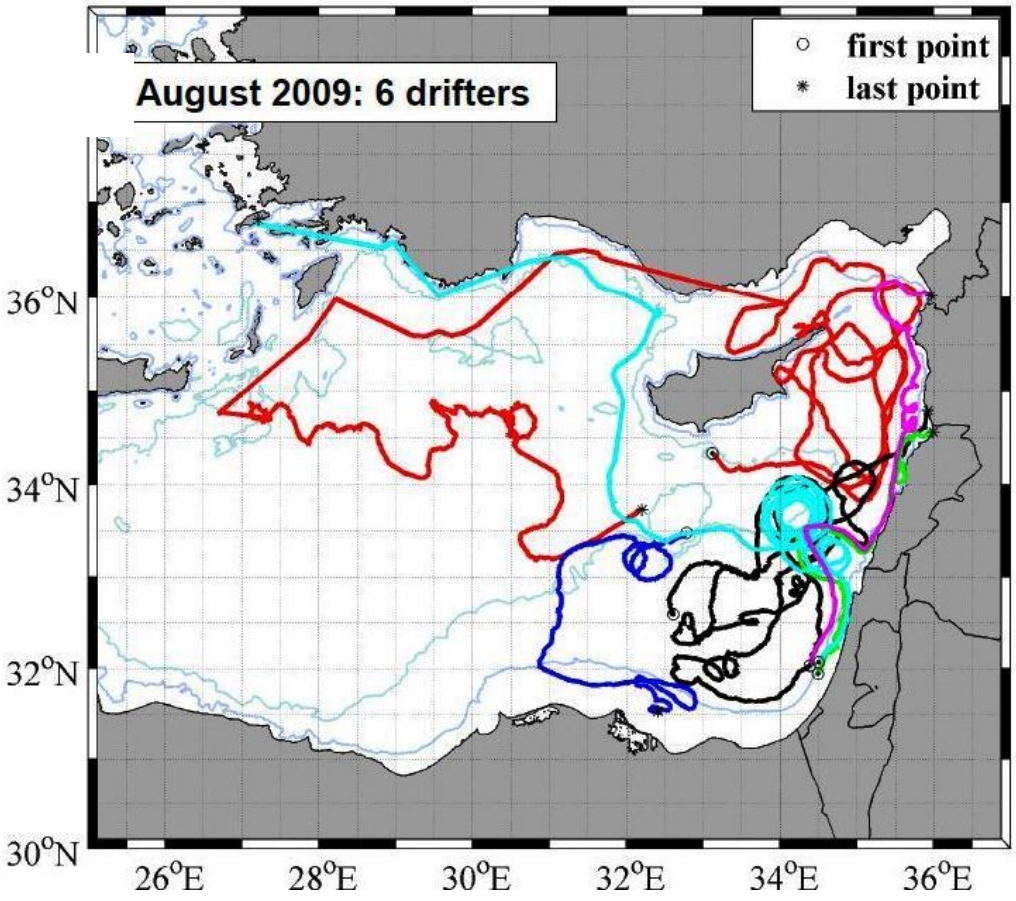
August 2009: 6 drifters
first point
last point
36°N
34°N
32°N
30°N
26°E
28°E
30°E
32°E
34°E
36°E

(a)

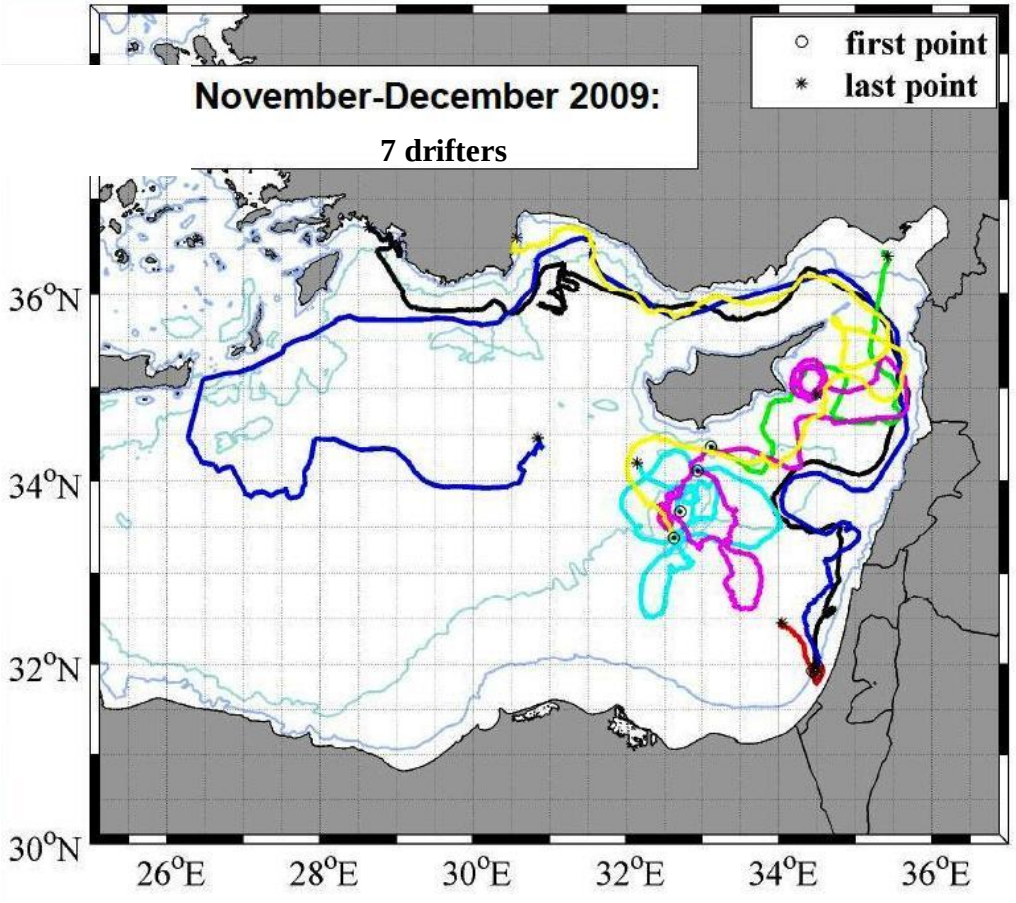
November-December 2009:
7 drifters
first point
last point
36°N
34°N
32°N
30°N
26°E
28°E
30°E
32°E
34°E
36°E

(b)

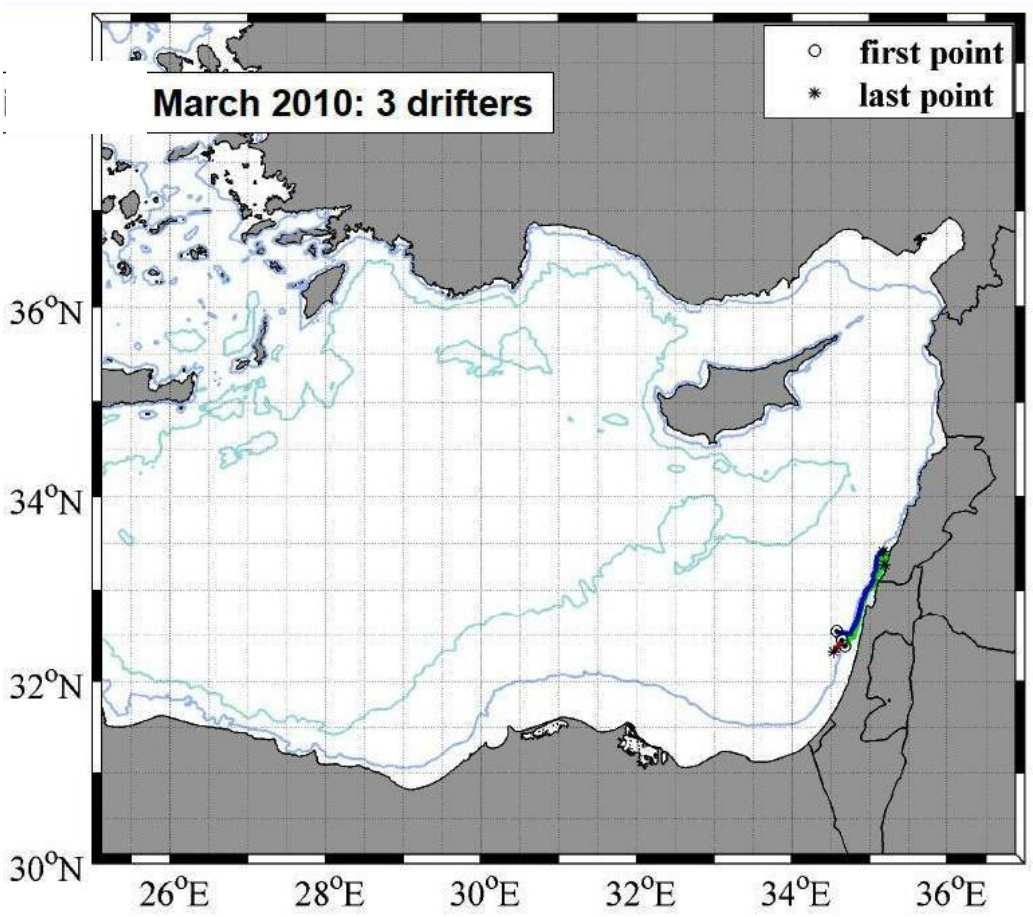

(c)

Fig. 3.4 – Surface drifter trajectories in the NEMED project: (a) first release in August 2009 (b) second release in November-December 2010 and (c) third release in March 2010. Source: *Poulain et al.* (2010)

These recent studies reveal strong evidence of the seasonal and more persistent trans-annual fluctuation of the AW, the MMJ, the Cyprus warm eddy and the non permanent Shikmona gyre recurrence (*Zodiatis et al., 2012*, *Menna et al., 2012*).

Drifter measurements are often collected in conjunction with the operation of HF coastal radars (see *Molcard et al., 2009*). Drifter data permit the calibration and validation of the radar measurements. The combination of both types of data (in practice, the radar data corrected by the drifters) represents the best description of the spatial structure and temporal evolution of the coastal circulation.

References

Hogan C., *2013*; "Levantine Sea". Retrieved from Encyclopedia of Earth, http://www.eoearth.org/view/article/166646

Malanotte-Rizzoli P. and Bergamasco A., *1989*; "The circulation of the Eastern Mediterranean: Part 1", Oceanologica Acta, **12/**4, 335-351

Malanotte-Rizzoli P. and Hecht A., *1988*; "Large-scale properties of the Eastern Mediterranean: A review", Oceanologica Acta, **11/**3, 323-335

Manca B.B., Ursella L. and Scarazatto P., *2002*; "New Development of Eastern Mediterranean Circulation based on Hydrological Observations and Current Measurements", Marine Ecology, **23**, Supplement I, 237-257

Menna M., Poulain P., Zodiatis G. and Gertman I., *2012*; "On the surface circulation of the Levantine sub-basin derived from Lagrangian drifters and satellite altimetry data", Deep Sea Research I, **65**, 46-58

Millot C., Candela J., Fuda J. and Tber Y., *2006*; "Large warming and salinification of the Mediterranean outflow due to changes in its composition", Deep Sea Research I, **53**, 656-666

Molcard A. et al., *2009*; "Comparison between VHF radar observations and data from drifter clusters in the Gulf of La Spezia (Mediterranean Sea)", Journal of Marine Systems, **78**, Supplement, S79–S89

OCA/CNES, *2000*; "The Mediterranean Sea". Extract from: The Geonauts inquire the oceans educational CD, 7 pp. Found as pdf file in the Internet.

Poulain P., Menna M., Gertman I. and Zodiatis, G., *2010*; "Surface circulation in the eastern Levantine Basin as deduced from satellite-tracked drifters", Presentation at the 42nd International Liege Colloquium on Ocean Dynamics, 26-30 April 2010, Liege, Belgium, 39 slides. Found as pdf file in the Internet.

Roether W. and Shiltzer R., *1991*; "Eastern Mediterranean deep water renewal on the basis of chlorofluoromethans and tritium", Dynamics of Atmospheres and Oceans, **15**, 333-354

Robinson A.R. et al., *1992*; "General circulation of the Eastern Mediterranean", Earth Science Reviews, **32**, 285-309

Robinson A.R., Leslie W.G., Theocharis A. and Lascaratos A., *2001*; "Mediterranean Sea Circulation", OCEAN CURRENTS, Academic Press, 19 pp.

UNEP/MAP, *2012*; "State of the Mediterranean Marine and Coastal Environment", 2012 United Nations Environment Program / Mediterranean Action Plan, Barcelona Convention, Athens, 2012, 96 pp.

Zodiatis G., Hayes D., Gertman I. and Nikolaides A., *2012*; "The mesoscale circulation in the South-Eastern Levantine Basin", Cyprus Oceanography Center. Presentation, 24 slides. Found as pdf file in the Internet.

4 – WINDS

The typical winds affecting the Mediterranean Sea are sketched in Fig. 4.1. Best known are the Sirocco and the Mistral. Both can reach gale force and cause storms and high seas. In our area, the hot, dry and dusty Hamsin, comes usually from the south east and is seldom strong. It is not limited to any single wind direction, but is associated, rather, with the dryness, the heat and the dust-laden atmosphere.

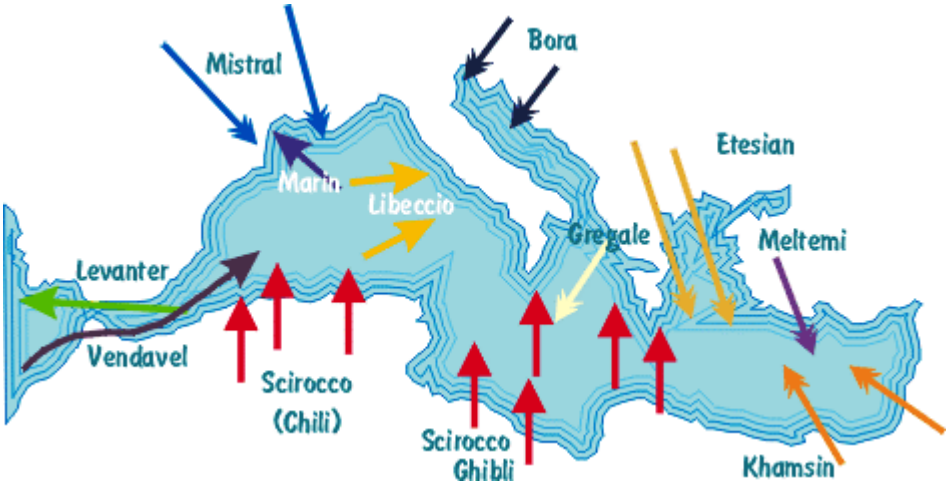

Fig. 4.1 – Mediterranean local winds. Source: Mediterranean Marinas & Sailing website: http://1yachtua.com/Medit-marinas/Mediterranean_Sailing/mediterranean_winds.shtm

Long term wind (and wave) records over the Mediterranean are mainly obtained from three sources: satellite observations, buoys and coastal/land based meteorological stations. Using these together with computer models, *Cavalieri and Sclavo* (2006) produced localized 10 year long calibrated time series at a large number of points at 0.5 arc-degree intervals.

The meteorological services of most Mediterranean countries, as well as institutions dealing with ocean and atmosphere have collaborated in different frameworks to provide and share information about climatic and weather conditions in their countries (and in particular in their coastal and sea areas). In Israel, the source of long term wind measurements is the Israel Meteorological Service, IMS. In the IMS website http://www.ims.gov.il/IMSEng/Tazpiot, last-day hourly wind speed (and direction) is available online at the coastal stations (Hadera, Tel Aviv west, Ashkelon). An example is given in Fig. 4.2. An hourly value of speed and direction in the figure is, in fact, the last 10 minutes average of that hour.

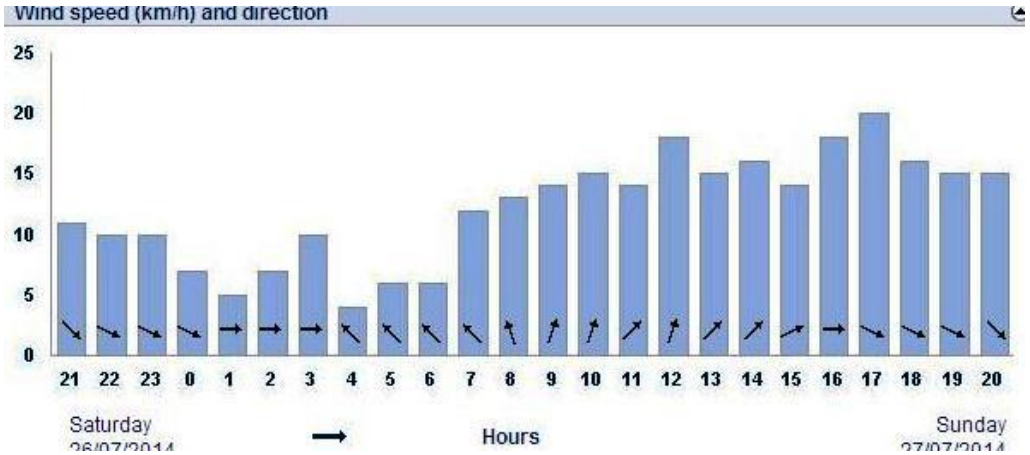

Fig. 4.2 – Measured hourly wind at Hadera harbor between July 26 and 27, 2014. The little arrows indicate direction.(up is north). The ordinate is in Km/hour. Source: IMS website.

The winds at Hadera harbor, Tel Aviv west and Ashkelon harbor are measured at 5, 10 and 4 m above sea level, respectively. However, it is customary to convert raw data in order to specify wind at standard height of 10 m above sea level for communication and use in applications.

There are some other sources too. Winds are measured at Haifa port employing the Atlas system. The wind is measured 47 m above sea level. An hourly averaged time series of speed and direction converted to standard 10 m above sea level is produced. A one month long time series is shown in Fig. 4.3. The Israel Port Company, IPC, owns the data.

Even though in winter, wind is light, with speed seldom above 6 m/s and not above 8 m/s. The dominant direction seems to be 135 degrees i.e. SE.

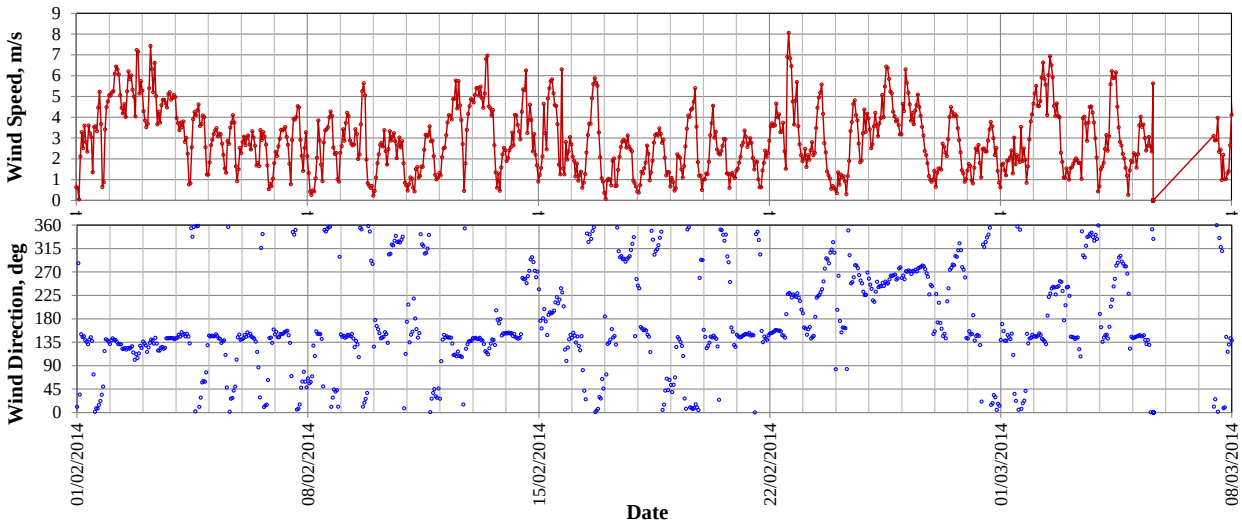

Fig. 4.3 – Hourly averaged wind time series at Haifa port from February 1 to March 8, 2014. Speed (red curve) is in m/s while direction (blue) is in degrees clockwise from north. Source: *Levin et al.* (2014)

CAMERI obtained from IMS wind time series recorded at what used to be the tip of the Haifa port main breakwater. The historical data consists of an hourly averaged wind time series spanning 7 years, between 01.04.1995 – 31.03.2002, and a (higher resolution) 10 minute averaged time series spanning 9 years, from 01.04.2002 – 31.03.2011. The first time series has large gaps where data records are missing; the largest gap is half a year long. Thus, this time series was ignored. Fig. 4.4 shows a wind rose diagram for the 10 min. time series.

Approximately 88% of annual winds, 83% of winter winds and 90% of summer winds, are light (wind speed below 6 m/s). About 12% of annual winds, 16% of winter winds and 9.4% of summer winds are fresh (wind speed between 6 and 10 m/s). In general, only 0.67% of annual winds, 1.2% of winter winds and 0.34% of summer winds are strong and exceed 10 m/s.

The direction of winds with speed above 6 m/s is N (2.03% occurrence). The dominant direction in general is SE, and that of strong winds (above 10 m/s) able to generate wave storms and strong currents is W (0.15% occurrence).

According to *Levin et al.* (2012b), the strongest winds are in reasonable agreement with wave storm events in deep water. The maximum wind speed, 19.1 m/s, was recorded during the winter storm event on 21.01.2007. In that storm, the significant wave height from records at CAMERI's Haifa waverider buoy location was larger than 5 m. The corresponding wind direction was NNW.

An analysis of extreme events indicate wind speed of 18 m/s with return period of 10 years, 18.5 m/s for 20 years, 19.5 for 50 years and 20.3 m/s with return period of 100 years. These values cannot be employed for applications that need higher resolution than the 10 min averages.

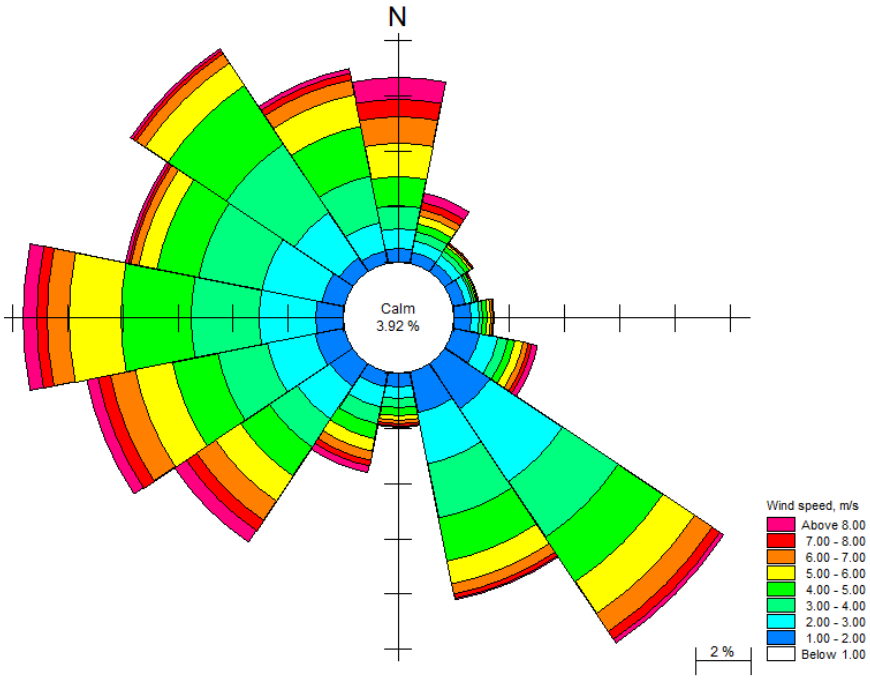

Fig. 4.4 – Wind rose diagram for 9 years of 10 min averaged wind records at Haifa. Source: *Levin et al.* (2012b)

The situation at Ashdod is similar. CAMERI obtained from IMS a 10 min averaged time series of 10 m wind spanning 18 complete hydrographic years, from 01.04.1993 to 31.03.2011. Fig. 4.5 shows a wind rose diagram for the entire time series.

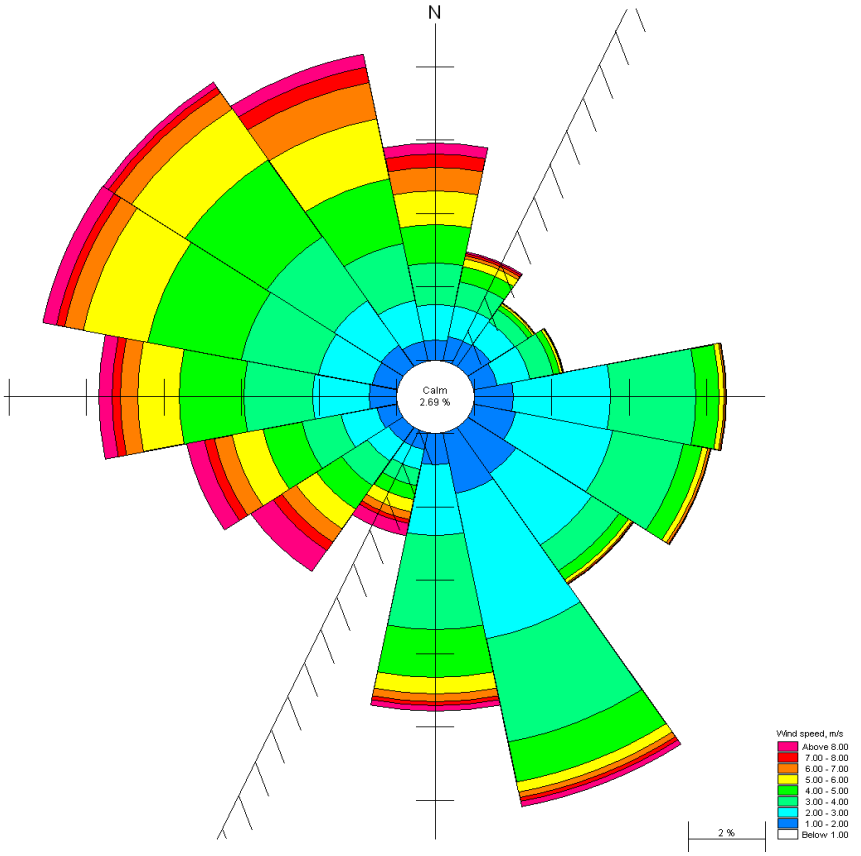

Fig. 4.5 – Wind rose diagram for 18 years of 10 min averaged wind records at Ashdod. Source: *Levin et al.* (2012a)

Approximately 90% of annual winds, 86% of winter winds and 93% of summer winds, are light (wind speed below 6 m/s). About 9% of annual winds, 12% of winter winds and 7% of summer winds are fresh (wind speed between 6 and 10 m/s). In general, only 1.2% of annual winds, 2.7% of winter winds and 0.26% of summer winds are strong and exceed 10 m/s.

The direction of winds with speed above 6 m/s is NW (1.64% occurrence). The dominant direction in general is SSE, and that of strong winds (above 10 m/s) able to generate wave storms and strong currents is SW (0.30% occurrence).

According to *Levin et al.* (2012a), the strongest winds are in reasonable agreement with wave storm events in deep water. The maximum wind speed, 21.8 m/s, was recorded during the winter storm event on 12.12.2010. In that storm, the significant wave height from records at CAMERI's Ashdod waverider buoy location was larger than 6 m. The corresponding wind direction was SSW.

An analysis of extreme events indicate wind speed of 22.7 m/s with return period of 10 years, 24 m/s for 20 years, 25.5 for 50 years and 27 m/s with return period of 100 years. These values cannot be employed for applications that need higher resolution than the 10 min averages.

Weather forecasts based on computer operational models also provide wind speed and direction (as well as wave height and direction) covering the entire Mediterranean. IMS is conducting research on numerical meteorological forecast of the weather employing a regional model adapted from the German Meteorological Service model. The area of application includes also the entire Levantine basin. The horizontal resolution is 13 Km, and it includes 38 layers on the vertical. Three and a quarter day forecasts are produced twice daily. More details can be found in the IMS website, at http://www.ims.gov.il/IMSEng/RESEARCH.

References

Levin A. et al., *2012a*; "Processing of Hydrographic Data at the Ashdod Region", CAMERI report P.N. 736, 271 pp., Technion City, Haifa

Levin A. et al., *2012b*; "Processing of Hydrographic Data for the Haifa Region", CAMERI report P.N. 737, 329 pp., Technion City, Haifa

Levin A. et al., *2014*; "Monitoring activities after completion of works for deepening the marine entrance channel to Haifa Port", CAMERI report P.N. 799, 162 pp., Technion City, Haifa (in Hebrew)

5 – WAVES

Satellite measurement in open sea

One of the techniques employed for wave measurement in oceans and sea basins is satellite altimetry (*Challenor et al., 2006*). The European Space Agency, ESA launched in the early 90s the European Remote Sensing ERS-1 and ERS-2 satellites, featuring also radar altimetry and sea surface sensing instruments. Also NASA and the French space agency CNES jointly launched the TOPEX/Poseidon mission in 1992, followed later by the Jason-1 (2001) and Jason-2 (2008) missions, to map the sea surface topography, among other ocean observation tasks. *Galanis et al.* (2011) collected all available wave satellite data derived from these missions and performed statistical calculations in order to compare with results from numerical wave models with and without the influence of sea surface circulation flow. The study covered the entire Mediterranean, with particular focus on the Levantine Sea. Concerning accuracy of satellite data, bias uncertainty is a non-negligible factor in altimeter error budgets.

Another source of long term observed wave data are in-situ buoys. These are almost exclusively located in near-shore coastal areas of the different countries. In Israel, for example, several wave measuring devices are distributed along the coastline.

Internal waves in the weakly stratified very deep eastern Mediterranean trenches were addressed by *van Haren and Gostiaux* (2011). Such waves are outside the scope of this document.

Instrumental directional wave measurements in coastal region

More than 20 years of wave measurements at Haifa and Ashdod have been continuously recorded by Datawell directional waverider buoys operated by CAMERI. The recordings are done on behalf of the Israel Port Company, IPC. The buoys are deployed offshore Haifa and Ashdod ports, at locations where sea depth is 24 m. The raw data is processed and stored, as explained in detail in an Appendix in *Levin et al.* (2012a). An example of a wave time series recorded during the month of February 2014 at the Haifa buoy is presented in Fig. 5.1. The figure shows the significant wave height in meters (mean height of the highest third of the waves).and direction (in degrees measured clockwise from north) as functions of time. During that winter month, wave heights were seldom larger than 2 m, arriving mostly from west.

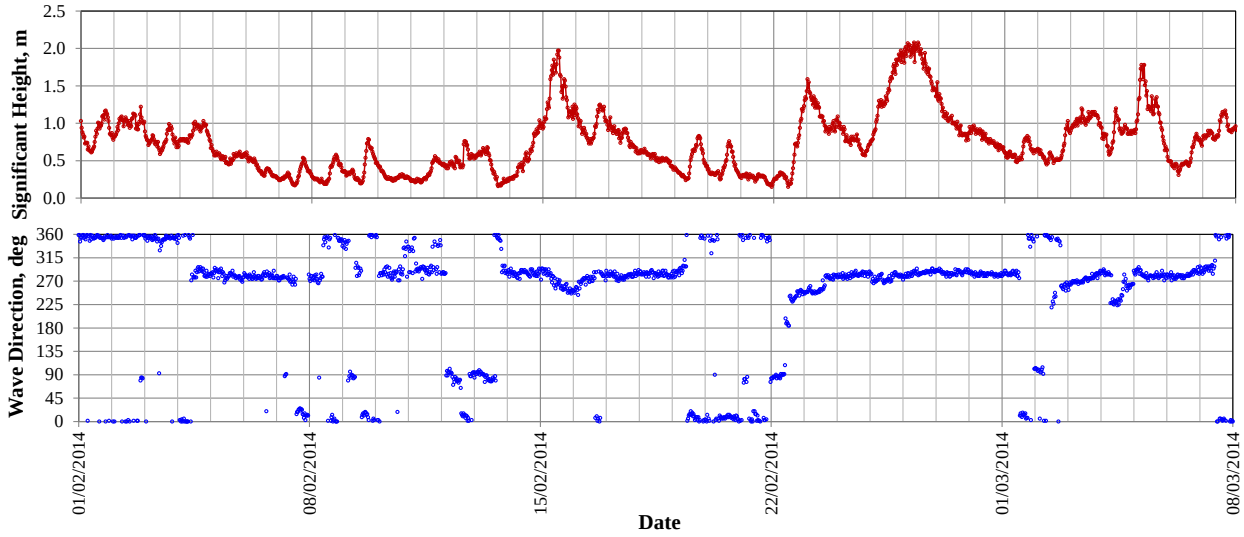

Fig. 5.1 – Significant height (red) and direction (blue) of waves recorded at Haifa in the period 01.02.2014 – 08.03.2014. Source: *Levin et al. (2014)*

Just north of the Haifa port extended main breakwater tip, where sea depth is 16 m, waves are measured since mid August 2007 with an ADCP Workhorse TRDI device (manufactured by Teledyne RD Instruments) belonging to IPC and maintained by IOLR. The primary function of an

ADCP (Acoustic Doppler Current Profiler) is to measure depth profiles of flow velocity and other parameters. This model, though, can also measure wave height and direction.

Levin et al. (2014) presents long term statistics for the Haifa waverider (19 years, 3 hour time series) and ADCP (5 years, 2 hour time series). A very detailed description of the waverider instrumentation and analysis procedures for the CAMERI long term wave time series is found in *Levin et al.* (2012b).

Other wave measurements are continuously conducted at Hadera and Ashkelon (IOLR) and Ashdod (CAMERI). The former can be obtained for the three-last-days at the ISRAMAR website http://isramar.ocean.org.il/isramar2009/#, under the tab: Near-Real-Time. The three-last-day graphs are updated 8 times daily. Fig 5.2 shows three-last-day measurements at Hadera and Ashkelon. The abscissa is local summer time with hourly markings. The left hand side ordinates are for wave period in seconds (green curves) while the right hand side ordinates are maximum (purple) and significant (black) wave heights in m. The figure depicts a typical summer situation with waves below 1 m high and periods between 6 and 8 s.

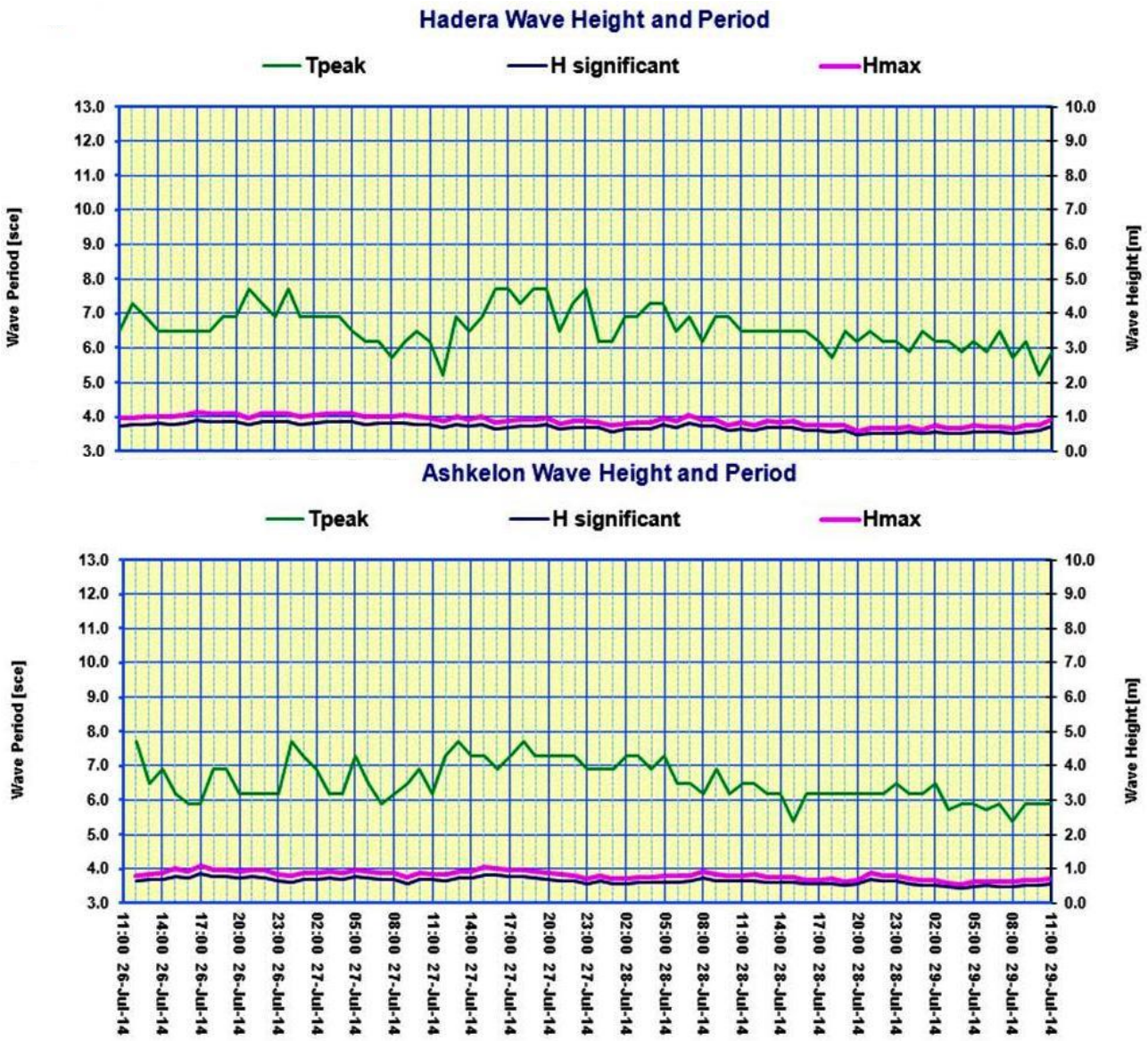

Fig. 5.2 – Three-last-days wave measurements at Hadera (above) and Ashkelon (below). Source: ISRAMAR website http://isramar.ocean.org.il/isramar2009/#

At Ashdod, wave measurements are done continuously by CAMERI with a Datawell waverider buoy identical to the one in Haifa. A very detailed account and long term analysis is given in *Levin et al.* (2012a).

The analysis of wave recorded data at Haifa and Ashdod is based on 19 year long 3 hour wave time series extracted from the processed recorded data.

Wave conversion formulas for deep water were presented in *Perlin and Kit* (1999), as a tool that allows inferring deep water wave height and direction at a selected target location along the Israeli coast given the deep water wave height and direction at another location. The transformation parameters for the Ashdod and Haifa data sets are reproduced in Table 5.1.

Table 5.1 – Transformation parameters for calculating deep water significant wave height and wave direction at different target locations, from deep water significant wave data at Ashdod or Haifa (from *Perlin and Kit, 1999*)

Location	θ_s**-270°** (°N)	***L*** **(Km)**	R_h	$\delta\theta$ *(degrees) for wave height ranges (m)*						
				0-0.5	**0.5-1**	**1-1.5**	**1.5-2**	**2-2.5**	**2.5-3**	**>3**
Ashdod data set										
Ashkelon	36	-28	0.98	0	2.2	2.4	3.2	2.4	3.7	4.2
Ashdod	25	0	1.00	0	0	0	0	0	0	0
Tel-Aviv	17	26	1.02	0	-2.0	-2.2	-3.0	-2.2	-3.4	-3.9
Herzelia	16	37	1.03	0	-2.9	-3.2	-4.2	-3.2	-4.9	-5.6
Netanya	14	54	1.04	0	-4.2	-4.7	-6.1	-4.7	-7.1	-8.1
Hadera	12.5	66	1.05	0	-5.1	-5.7	-7.5	-5.7	-8.7	-9.9
Haifa	7	110	1.08	0	-8.5	-9.5	-12.5	-9.5	-14.5	-16.5
Haifa data set										
Ashkelon	36	138	0.91	0	1.07	11.9	15.7	11.9	18.2	20.7
Ashdod	25	110	0.93	0	8.5	9.5	12.5	9.5	14.5	16.5
Tel-Aviv	17	84	0.94	0	6.5	7.3	9.5	7.3	11.1	12.6
Herzelia	16	73	0.95	0	5.6	6.3	8.3	6.3	9.6	11.0
Netanya	14	56	0.96	0	4.3	4.8	6.4	4.8	7.4	8.4
Hadera	12.5	44	0.97	0	3.4	3.8	5	3.8	5.8	6.6
Haifa	7	0	1.00	0	0	0	0	0	0	0

In the table above, $\boldsymbol{L}$ denotes the distance between selected target location and source location (Haifa or Ashdod); $\boldsymbol{R_h}$ is the wave height correction coefficient; $\boldsymbol{\theta_s}$ is the shoreline direction at the selected target location; $\boldsymbol{\delta\theta}$ is the direction correction angle.

Wave statistics are based upon the recorded buoy time-series and its transformation to deep water. The transformation procedure of measured waves from the buoy to deep water employs the 2D wave transformation software STWAVE (*Smith et al., 2001*), which also needs the knowledge of the bathymetry up to deep water (100-150 m sea depth). STWAVE takes into account depth-induced wave refraction and shoaling, current-induced refraction and shoaling, depth- and steepness-induced wave breaking, diffraction, wind-wave growth, and wave-wave interaction and white-capping which redistribute and dissipate energy in a growing wave field.

This wave transformation procedure to and from deep water, in conjunction with the *Perlin and Kit* (1999) conversions in deep water, are very convenient in order to patch gaps in the Haifa time series with modified records in the Ashdod time series and vice-versa. They also allow deriving synthetic time series for other target locations.

For convenience, a statistical seasonal split in two extended seasons is considered: summer (7 months) from April through October and winter (5 months) from November through March.

For the analysis of wave storms the definition of what is considered a storm is essential. For the Ashdod and Haifa studies, a storm is identified as an event in which the peak significant wave height is at least 3.5 m (*Levin et al. 2012a*). The duration of a storm event is closely related to the storm definition and represents an important component of the wave climate. According to the

US Army Coastal Engineering Manual, CEM (2006), storm duration is defined as the continuous period of time during which the significant wave heights, H_{m0}, are above some fixed threshold. The recommended threshold should be determined so that 6% of the recorded long-term H_{m0} time-series exceeds this threshold. For Haifa and Ashdod a 2 m threshold is appropriate (*Levin et al. 2012a, 2012b*). Whenever two successive significant wave height peaks are less than 48 hours apart, they are considered as belonging to the same storm. Successive peaks separated by 5 or more days are considered to belong to two different storms.

The deep water annual rose diagrams for significant wave height and peak period for Ashdod are shown in Fig. 5.3. Similar ones for winter and summer, as well as histograms and tables, are presented and discussed in *Levin* (2012a).

The analysis results show that the dominant wave direction for Ashdod is WNW. Approximately 51% of the annual waves come from this direction.

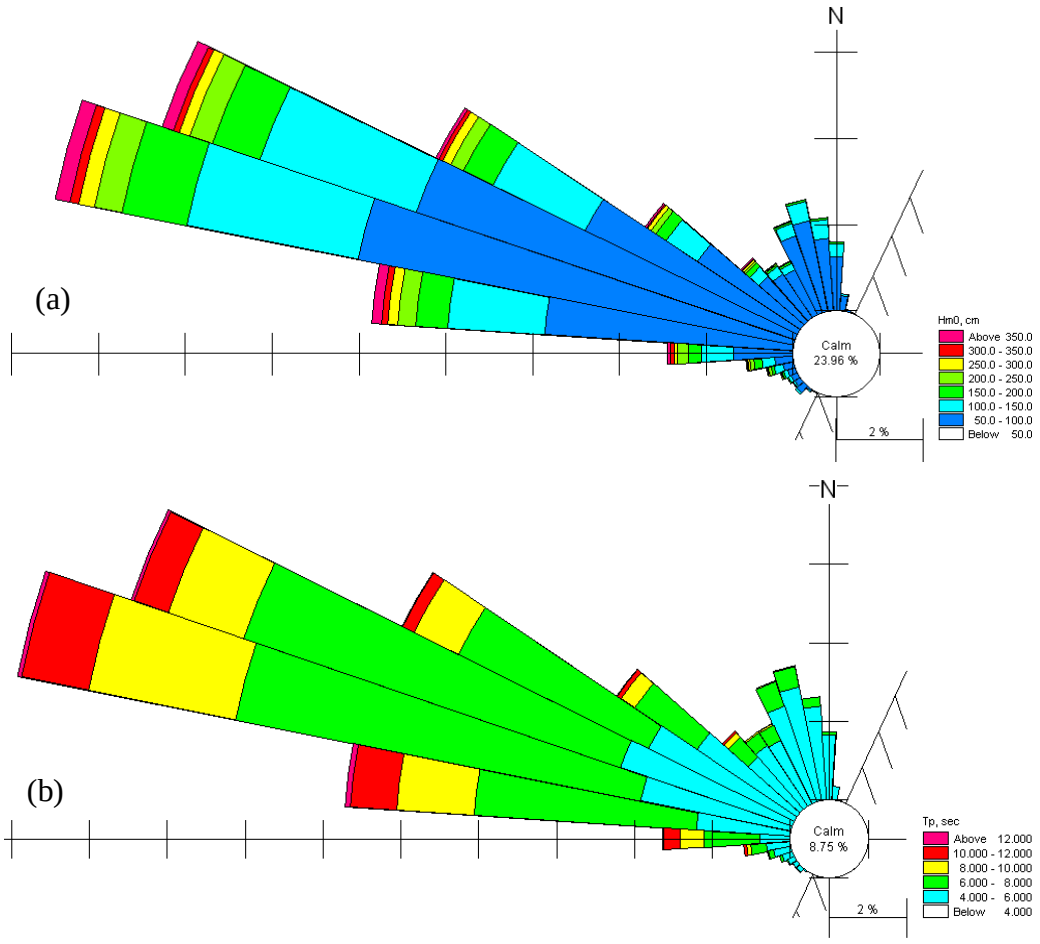

Fig. 5.3 – Annual rose diagram of (a) significant wave height (H_{m0}, meters) and (b) wave peak period (T_p, seconds) in deep water, Ashdod (01.04.1992-31.03.2011). Data coverage is 99.25%

The analysis of *extreme wave events* at Ashdod during the considered 19 hydrographic years shows that, according to the Weibull distribution with a 3.5 m threshold: (a) At the buoy location the extreme wave height with 50 years return period is about 7.2 m, the one with 100 years return period is about 7.6 m and with 200 years return period is about 8.0 m; (b) In deep water the extreme wave height with 50 years return period is about 8.1 m, with 100 years return period is about 8.7 m, with 200 years return period is about 9.2 m. More details can be found in Levin et al. (2012a).

The analysis of *storm events* in deep water at Ashdod during the period of measurements (02.04.1992-31.03.2011) shows that: (a) the total number of storms was 91; (b) the average number of storms per year is about 5, the minimum is 2 storms per year and the maximum is 9 storms per year; (c) three major storms with H_{m0}>6.5 m occurred on December 2002, January 2008 and December 2010. The highest significant wave in deep water was H_{m0} = 6.93 m (20.12.2002). The highest waves propagate from the dominant direction WNW; (d) the average storm duration was about 47 hours; and (e) the longest storm duration was approximately 100 hours and the shortest storm duration was 18 hours.

For the sake of comparison, the deep water annual rose diagrams for significant wave height and peak period for Haifa are shown in Fig. 5.4. Similar ones for winter and summer, as well as histograms and tables, are presented and discussed in *Levin* (2012b).

The analysis results show that the dominant wave direction for Haifa is W to WNW. Approximately 70% of the annual waves come from these directions. The directional distribution of waves in deep water is similar to that at Ashdod. However, waves are generally higher at Haifa (as implied by the 1.08 factor in Table 5.1).

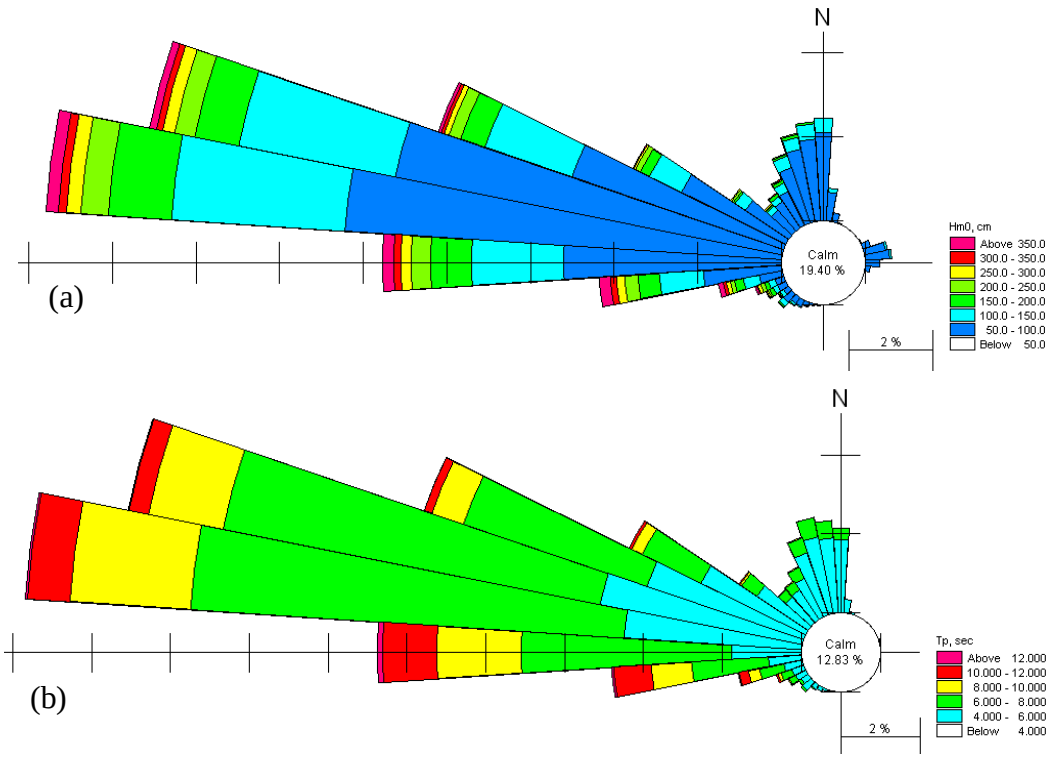

Fig. 5.4 – Annual rose diagram of (a) significant wave height (H_{m0}, meters) and (b) wave peak period (T_p, seconds) in deep water, Haifa (01.04.1992-31.03.2011). Data coverage is 99.50%

The analysis of *extreme wave events* at Haifa during the considered 19 hydrographic years shows that, according to the Weibull distribution with a 3.5 m threshold, the extreme wave height in deep water with 50 years return period is about 8.3 m, with 100 years return period is about 8.8 m, with 200 years return period is about 9.3 m. More details can be found in *Levin et al.* (2012b)

The analysis of *storm events* in deep water at Haifa during the period of measurements (25.11.1993-31.03.2011) shows that: (a) the total number of storms was 96; (b) the average number of storms per year is about 5, the minimum is 3 storms per year and the maximum is 8 storms per year; (c) three major storms with H_{m0}>7.5 m occurred on February 2001, December 2002 and December 2010. The highest significant wave in deep water was H_{m0} = 7.75 m (12.12.2010). The highest waves propagate from the dominant direction W-WNW; (d) the average storm duration was about 52 hours; and (e) the longest storm duration was approximately 125 hours and the shortest storm duration was 15 hours.

References

Challenor P., et al., *2006*; "Satellite altimetry: A revolution in understanding the wave climate", paper 453, 5pp, Found as pdf file in the Internet

Galanis G., et al., *2011*; "Wave height characteristics in the Mediterranean Sea by means of numerical modeling, satellite data, statistical and geometrical techniques", Mar Geophysical Research, 15pp., Springer. Found as pdf file in the Internet

Levin A. et al., *2012a*; "Processing of Hydrographic Data at the Ashdod Region", CAMERI report P.N. 736, 271 pp., Technion City, Haifa

Levin A. et al., *2012b*; "Processing of Hydrographic Data for the Haifa Region", CAMERI report P.N. 737, 329 pp., Technion City, Haifa

Levin A. et al., *2014*; "Monitoring activities after completion of works for deepening the marine entrance channel to Haifa Port", CAMERI report P.N. 799, 162 pp., Technion City, Haifa (in Hebrew)

Perlin A. and Kit E., *1999*; "Longshore sediment transport on Mediterranean Coast of Israel", *ASCE Journal of the Waterways, Port, Coastal and Ocean Division*, **125**/2, 80-87

Smith J.McK., Sherlock A.R., and Resio D.T., *2001*: "Modeling Nearshore Wave Transformation with STWAVE", Coastal and Hydraulics Engineering Technical Note I-64, Coastal and Hydraulics Laboratory (CHL), Vicksburg, Mississippi. The software is available for free download at: http://chl.erdc.usace.army.mil/chl.aspx?p=s&a=ARTICLES;279

Van Haren H. and Gostiaux L., *2011*; "Large internal waves advection in very weakly stratified deep Mediterranean waters", Geophysical Research Letters, **38**, L22603, 5pp. Found as pdf file in the Internet.

United States Army - Corps of Engineers, *2006*: "Coastal Engineering Manual (CEM)", Washington, D.C., U.S.

6 – SEA TEMPERATURE AND SALINITY

Salinity and temperature determine the density of sea water. Density gradients govern buoyancy and density flows in the sea. Many studies have dealt with measuring sea salinity and temperature over time in various areas of the Mediterranean. There are abundant records, particularly in coastal waters. Records of coastal surveys by IOLR, which also include temperature and salinity measurements, are kept in ISRAMAR's data repository (see website http://isramar.ocean.org.il/isramar2009/).

In an experimental program named MedArgo, about 25 autonomous drifting profilers were deployed from research and other vessels at various locations throughout the Mediterranean in order to collect temperature and salinity profile data and to measure subsurface currents (*Poulain et al., 2007*). More than 2000 profiles were measured between June 2004 and December 2006. The drifters were programmed for 5 day cycles. Each cycle consists of about four and a half day drifting at a parking depth of 350 m, followed by a "yo-yo" diving to either 700 or 2000 m depth depending on the region and rising thereafter to the sea surface while measuring the temperature and salinity profiles with CTD (Conductivity-Temperature-Depth) sensors. The parking depth was chosen where the core of the Levantine Intermediate Water mass, LIW, generally is, so the device would drift with it and the LIW path could be traced. At the end of each cycle, the drifter stayed at the sea surface for about 6 hours in order to be located by and to transmit the data collected to the Argos system, mounted on satellites, for distribution to the members of the program. Finally, the device descends again to its parking depth. IOLR participated in the program and was responsible for the deployment of 8 drifters. However, none of these drifters seem to have reached the Israeli EEZ.

One of the efforts undertaken in the framework of international sea data collection for the Mediterranean resulted in the metadata stored in the servers of the University of Liege, Belgium. Salinity and temperature records from many sources and methods (conductivity-temperature-depth CTD, bottle samples and other) done since 1900 and up to 2009 were collected in the database, and processed in various ways. Fig. 6.1 shows the distribution of conventional (CTD + bottles) profile data obtained from merging two data sets of different origin (25228 stations after quality control). It can be seen that the amount of stations in the deep sea portion of Israel's EEZ, (south east Levantine) is not very dense.

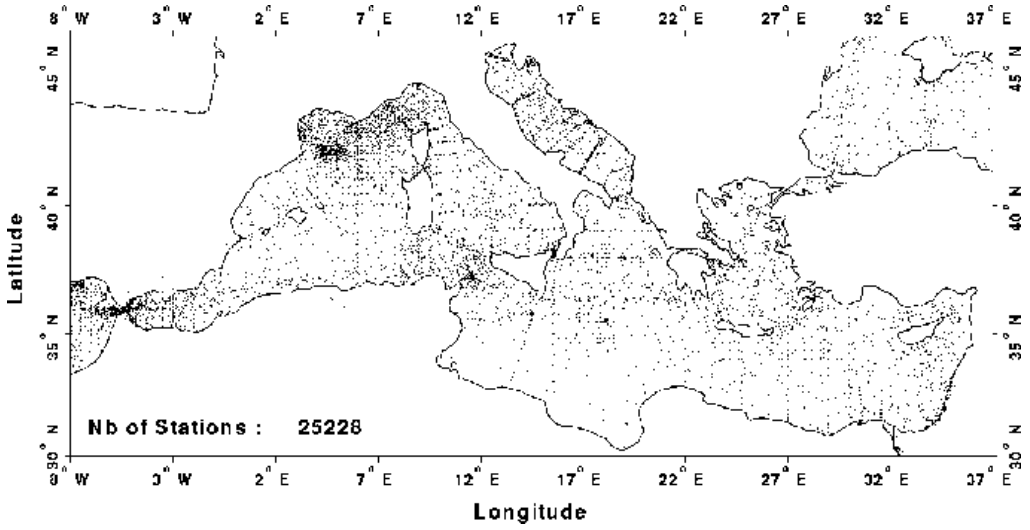

Fig. 6.1 – Distribution of conventional (CTD + bottles) profile data obtained from merging the MED-2 and the U.S. NODC data sets (25228 stations after quality control). Source: University of Liege servers (http://modb.oce.ulg.ac.be/backup/atlas/node27.html)

Gridded monthly temperature and salinity records have been produced by processing and interpolating the measured data. The gridded values are available (upon registration) from the Internet site: http://gher-diva.phys.ulg.ac.be/web-vis/clim.html. The grid has a horizontal resolution of 16 points per longitude (and latitude) arc-degree, and 33 depth levels, from sea surface to -5500 m at the deepest point, starting at 0, 10, 20, 30, 50, 75, 100, 125, 150, 200, 250 and 300 m, then each 100 m to 1500 m and then each 250 m to the seafloor. The grid also covers the south-eastern Levantine Sea and can be visualized online for a user defined vertical section or on a horizontal map, as illustrated in Fig. 6.2. The visualization allows also a 12 frame animation over the year. Seasonal temperature and salinity data files can be extracted directly from the Mediterranean Oceanic Database, MODB, at the website http://modb.oce.ulg.ac.be/backup/modb/welcome.html. Temperature and salinity depth profiles by year can also be found there, from measurements done at different surveys, at diverse times and locations. The compressed ASCII data files can be downloaded from the site via FTP access.

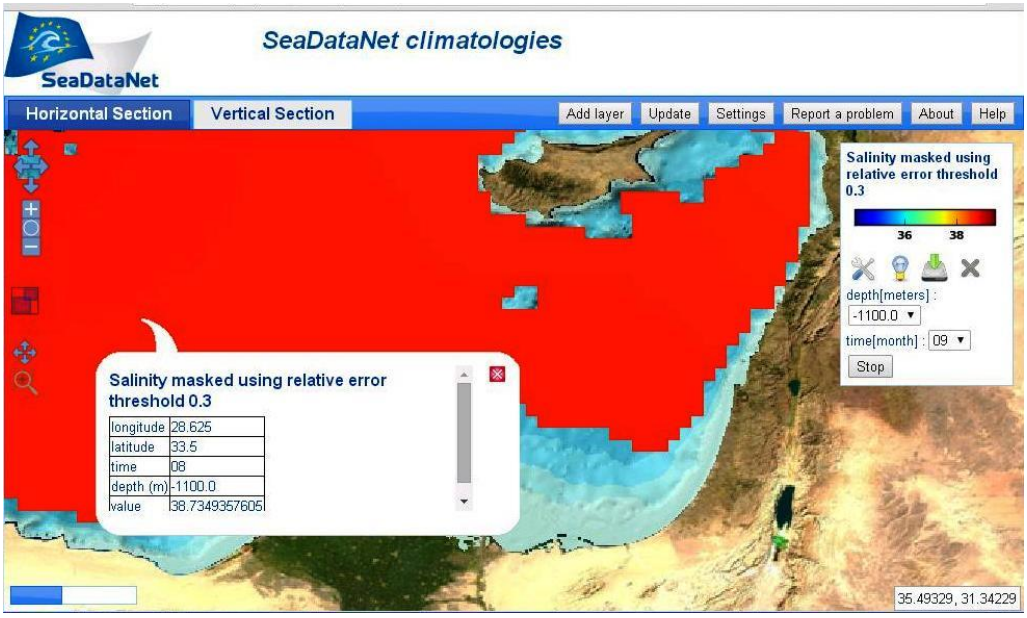

Fig. 6.2 – August salinity (about 39 psu) at 1100 m depth

A study by *Berman et al.* (2003) from the Hebrew University presents summer (July-August) versus winter (February) temperature vs. depth profiles for the south eastern Levantine Sea. In summer, the surface temperature is ~29°C, decreasing rapidly to about 16°C at 200 m depth, and thereafter gradually to the steady 14°C at 800 m depth and more. The winter distribution starts at about 17°C at the surface and coincides with the winter distribution already at 200 m depth. This shows a 12°C cyclic seasonal difference in sea surface temperature.

A recently released YouTube video clip produced by the European Space Agency, ESA, shows the Mediterranean Sea Surface Temperature (SST) evolution from January 2011 to May 2012. The SST is obtained from multiple satellite observation missions. The link to the video clip: https://www.youtube.com/watch?v=675HZxWzgTo.

The Datawell directional waveriders operated by CAMERI at Haifa and Ashdod have temperature gauges mounted on the bottom of the buoys, providing seawater temperatures about 40-50 cm below sea surface. Thus, sea surface temperatures were measured during approximately two decades at both Haifa and Ashdod (Waverider buoys are placed at locations where sea depth is approximately 24 m). The SST data coverage at Ashdod is 91% due to several months when the gauge didn't operate properly. Table 6.1 presents minimum, maximum and average seawater temperature near the sea surface (SST) for Ashdod (see Fig. 7.2 for buoy location). The SST values for Haifa are very similar. For convenience, the summer season spans 7 months (April through October) and the winter season spans 5 months, (November through March).

Table 6.1 – Minimum, maximum and average SST near Ashdod. (*Levin et al., 2012*)

Period	Sea Surface Temperature, °C			Records, % of year	
	Minimum	Maximum	Average	Total	Loss
Year	12.5	32.8	23.4	91.0	9.0
Winter	12.5	27.4	19.6	38.7	2.7
Summer	16.8	32.8	26.2	52.3	6.3

Only 10% of winter records show temperatures lower than 17.0°C, only 10% of summer records show temperatures lower than 20.0°C, and only 10% of annual records show temperatures lower than 17.5°C. Similarly, only 10% of winter records show temperatures larger than 24.0°C, only 10% of summer records show temperatures larger than 30.5°C, and only 10% of annual records show temperatures larger than 30.0°C.

Conductivity-Temperature-Depth CTD instruments are in continuous operation at Hadera and Ashkelon, operated by IOLR. Last four and a half day measurements are published online at the ISRAMAR Internet website http://isramar.ocean.org.il/isramar2009/#, as shown in Fig. 6.3.

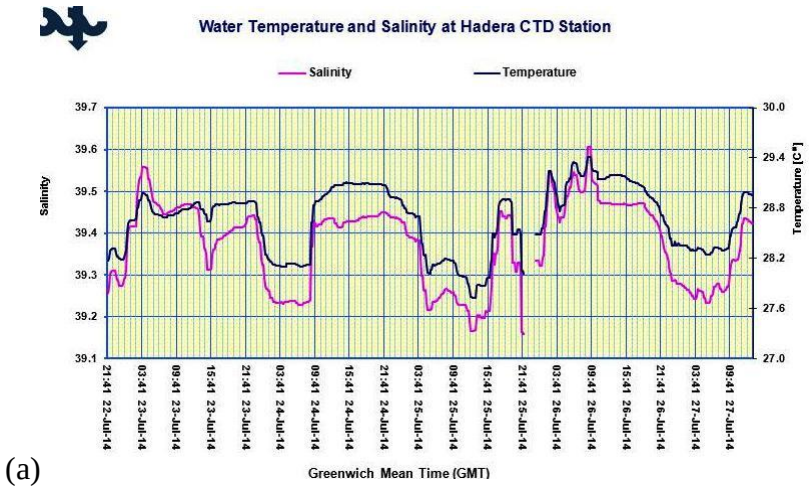

(a)

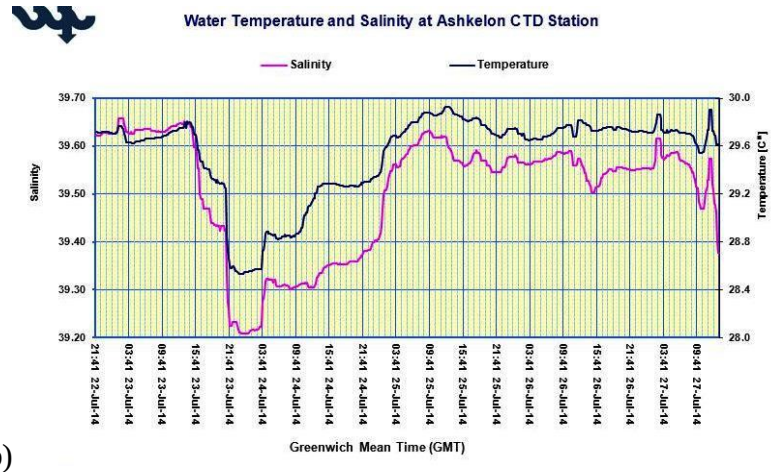

(b)

Fig. 6.3 – Near real time measured salinity and temperature at (a) Hadera and (b) Ashkelon during the last four and a half days. Time is GMT. Salinity in psu (magenta curve) reads on the left hand side ordinate, while temperature in °C reads on the right hand side scale. Source: ISRAMAR website http://isramar.ocean.org.il/isramar2009/#.

During the four and a half days period shown, salinity varies between 39.2 and 39.6 psu at both stations. Temperature varies between 27.6 and 29.4°C at Hadera and between 28.6 and 29.9°C at Ashkelon, which is typical for summer.

Using these data CAMERI researches carried out an *Engineering Assessment* for spreading of warm water issued from the Hadera and Rutenberg Power Stations diluted with brine released from the Hadera and Ashkelon Desalination Plants (see Sladkevich et al. 2011 and 2013).

Further offshore, in Israel's EEZ, available sea surface temperature fields, as well as water circulation, salinity and temperature are mostly computer generated by running numerical model simulations or forecasts. An example can be seen in Fig. 6.4, obtained interactively at the ISRAMAR Internet website: http://isramar.ocean.org.il/isramar2009/selips/.

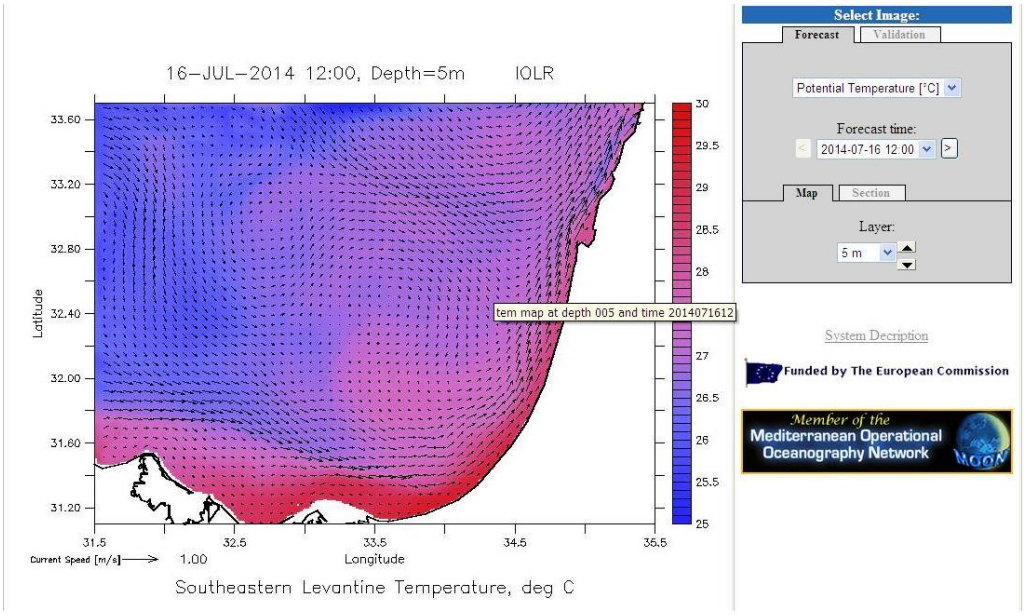

Fig. 6.4 – SELIPS (South Eastern Levantine Israeli Prediction System) forecast of potential temperature (5 m. below sea surface). Arrows represent computed flow speed and direction at computational grid points at that depth. The level can be chosen up to 300 m below sea surface.

References

Berman T., Paldor N. and Brenner S., *2003*; "Annual SST cycle in the Eastern Mediterranean, Red Sea and Gulf of Eilat", Geophysical Research Letters, Vol. **30**, No. 5, 1261,

ISRAMAR Internet site; http://isramar.ocean.org.il/isramar2009/

Levin A. et al., *2012*; "Processing of Hydrographic Data at the Ashdod Region", CAMERI report P.N. 736, 271 pp., Technion City, Haifa

Poulain P.M., Barbanti R., Font J., Cruzado A., Millot C, Gertman I., Griffa A., Molcard A., Rupolo V., Le Bras S., and Petit de la Villeon L., *2007*; "MedArgo: a drifting profiler program in the Mediterranean Sea", Ocean Science, **3**, 379–395

Sladkevich M., Glozman M., Keren Y., Levin A., and Kit E., *2013*: "Rutenberg Power Station and Ashkelon Desalination Plant: I. Statistical Analysis of Waves; II. Engineering Assessment of Brine and Warm Water Spreading", CAMERI report P.N.781/13, Technion City, Haifa.

Sladkevich M., Glozman M., Levin A., Keren Y., and Kit E., *2011*: "Spreading of Warm Water Issued from the Hadera Power Station Diluted with Brine Released from the Hadera Desalination Plant", CAMERI report P.N.747/11, Technion City, Haifa.

7 – COASTAL CURRENTS

Currents in the sea are, to a great degree, due to density gradients. In the surface layer, currents are mainly due to wind stress and, to a lesser degree, waves. In the coastal zone wind is responsible for the creation of waves and currents. In the surf zone close to the shore, waves arriving obliquely to the shore are the cause of the longshore current.

In the coastal area and more generally over the continental shelf, water is well mixed and of almost uniform density over depth, particularly in winter. During summer, flow decreases with depth due to density gradients. The continental shelf extends from the shoreline to a depth of approximately 100 m, where the pronounced continental slope begins. The Israeli shelf is relatively narrow: 20 Km at Ashkelon to about 10 Km near Atlit (*Kunitsa et al., 2005*).

A background current due to the water mass circulation in the Mediterranean is always present. In the Eastern Mediterranean, the background current circulates counterclockwise and parallel to the coastline (south to north along Israel's coast) with a mean velocity of about 15 to 25 cm/s. Its activity is observed mainly way offshore, in the region where the water depth is 20 m or more. The values of tidal currents within the study area are, in general, quite low, reaching about 5 cm/s (*Stiassnie, 1987*).

Stronger currents in the coastal area are generated mainly by waves and wind. *Stiassnie* (1987) indicates that wave induced currents occur within the breaker zone, flowing mainly parallel to the coastline (longshore currents induced by waves approaching obliquely to the bathymetry contour lines), but sometimes also narrow currents flowing offshore may occur (rip currents). The maximum theoretical values of the longshore current may reach 1.5 to 2.0 m/s during storms.

However, outside the surf zone, the longshore current is estimated to diminish rapidly to a few centimeters per second at about 15 m water depth (*Stiassnie, 1987*).

A program for measuring the current regime in the Israeli continental shelf was initiated by IOLR in 1987. Currents were measured directly by an array of current meters moored to the seafloor in several coastal stations at different times and indirectly by measuring sea bottom pressure at several locations, to a depth of 120 m. During the last years of last century, measurements were also made on the continental slope to a depth of 500 m. opposite Hadera (*Rosentraub, 1995, Kunitsa et al., 2005*).

The ISRAMAR website http://isramar.ocean.org.il/isramar_data/CastMap.aspx keeps historical data collected from cruises on, among other measurements, horizontal currents. Data access and download is subject to agreement with IOLR.

Moreover, historical records of currents over Israel's continental shelf are offered (for diverse periods of operation between 1987 and 1996) for more than 20 offshore stations located at different places south of Haifa, opposite Hadera, Netanya, Ashdod and Ashkelon, and for depths ranging from 30 m to more than 500 m, as displayed at the ISRAMAR Internet website: http://isramar.ocean.org.il/CurrentsBuoy/default.asp. Although choice of stations and time period is interactive, only an example of a tabular histogram is displayed.

Three-last-day hourly measurements of currents are offered online at Hadera station (sea depth where the instrument is anchored is 27 m), where velocity is measured 11 m below sea surface (http://isramar.ocean.org.il/isramar2009/Hadera/), as seen in Fig. 7.1. The graph is updated 8 times daily. The horizontal scale shows local time, the ordinate indicates speed (knots in right hand side, m/s in left hand side). Arrows indicate measured current speed and direction and the cyan curve represents speed, as a function of time. The graph shows a typical summer situation where flow is predominantly towards the north with speed below 25 cm/s. Currents are also measured continuously at Ashdod and Ashkelon.

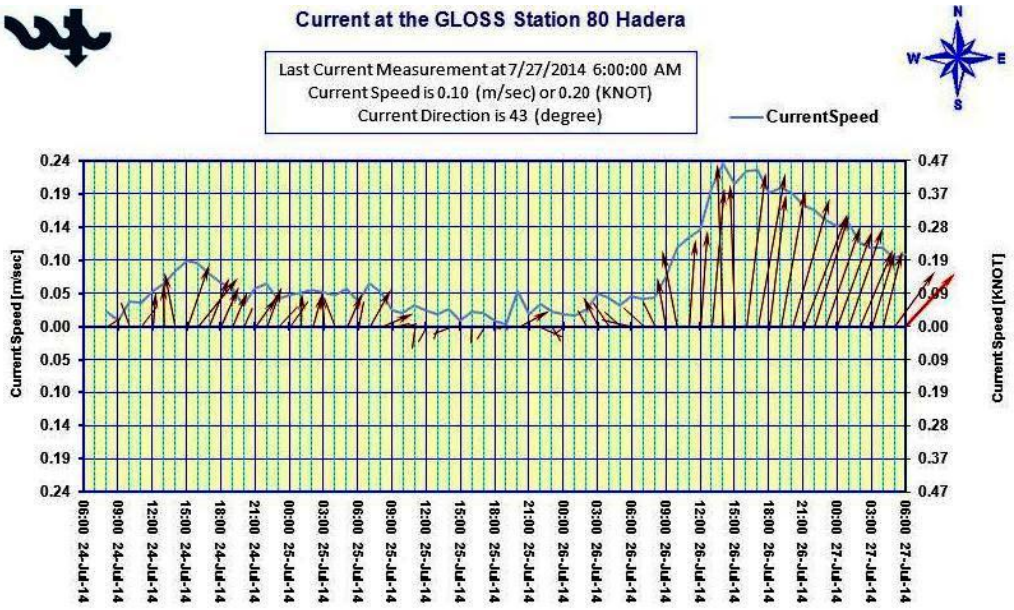

Fig. 7.1 – Three-last-days hourly current measurements at Hadera station. Source: ISRAMAR website http://isramar.ocean.org.il/isramar2009/Hadera/.

Another source of measurements is the survey performed by OCEANA Marine Research Ltd. on behalf of the Israel Ports Company, IPC (Israel Ports and Railways Authority at that time), in whose framework current meters were deployed. A very comprehensive report based on these measurements was prepared by *Kit et al.* (2001). The results were partially presented at a conference in Girona (*Kit & Sladkevich, 2001).*

CAMERI had access to the historical time series of currents recorded at some stations by IOLR and OCEANA, on behalf of IPC. As an illustrative example of one of the studies, Fig, 7.2 shows the location of measuring stations in the vicinity of Ashdod.

Some stations were in shallow water (10-15 m) and others in somewhat deeper water (about 25 m). For the former, measurements were taken at 0.7 m from seabed. For the rest, currents were measured at 1m intervals from about 2-4 m below sea surface to about 0.5 m above the local seafloor. The data coverage for OCEANA's measurements during 1995-1998 is low. The coverage of IOLR's measurements (2001-2010) reaches almost 80% and the latest IOLR measurements (2009-2010) have time coverage of above 98%.

While OCEANA utilized S-4 (and later S-4A) current meters, which allow a measurement of the local current at approximately 70 cm above the seafloor, IOLR employed seafloor anchored ADCP (Acoustic Doppler Current Profiler) instruments, that measure water current velocities (speed and direction) using the Doppler effect related to the variation of sound velocity propagation in water in the presence of currents (*Levin et al., 2012*). A description of the measurement technique and data processing by the IOLR can be found in e.g. *Rosentraub and Bishop* (2010), and is summarized in an Appendix in *Levin et al.* (2012).

CAMERI performed statistical analysis of currents from the various measured data near the sea surface and near the seafloor at Ashdod, Haifa and other locations along the coast. Some analysis results are presented as example, to show the distribution and order of magnitude of current velocity in the coastal area.

Consider the hourly averaged current records at Ashdod stations Asd1, Asd2, and Asd3 combined, during the 9 year period 01.04.2001-31.03.2010. These three stations are relatively close together (see Fig. 7.2). The sea is about 24.5 m deep. The velocities are recorded from about 3.5 m below sea surface (near surface) to about 22.5 m depth (near bottom) at 1 m intervals. Rose diagrams of near-surface and near-bottom currents are plotted in Fig. 7.3.

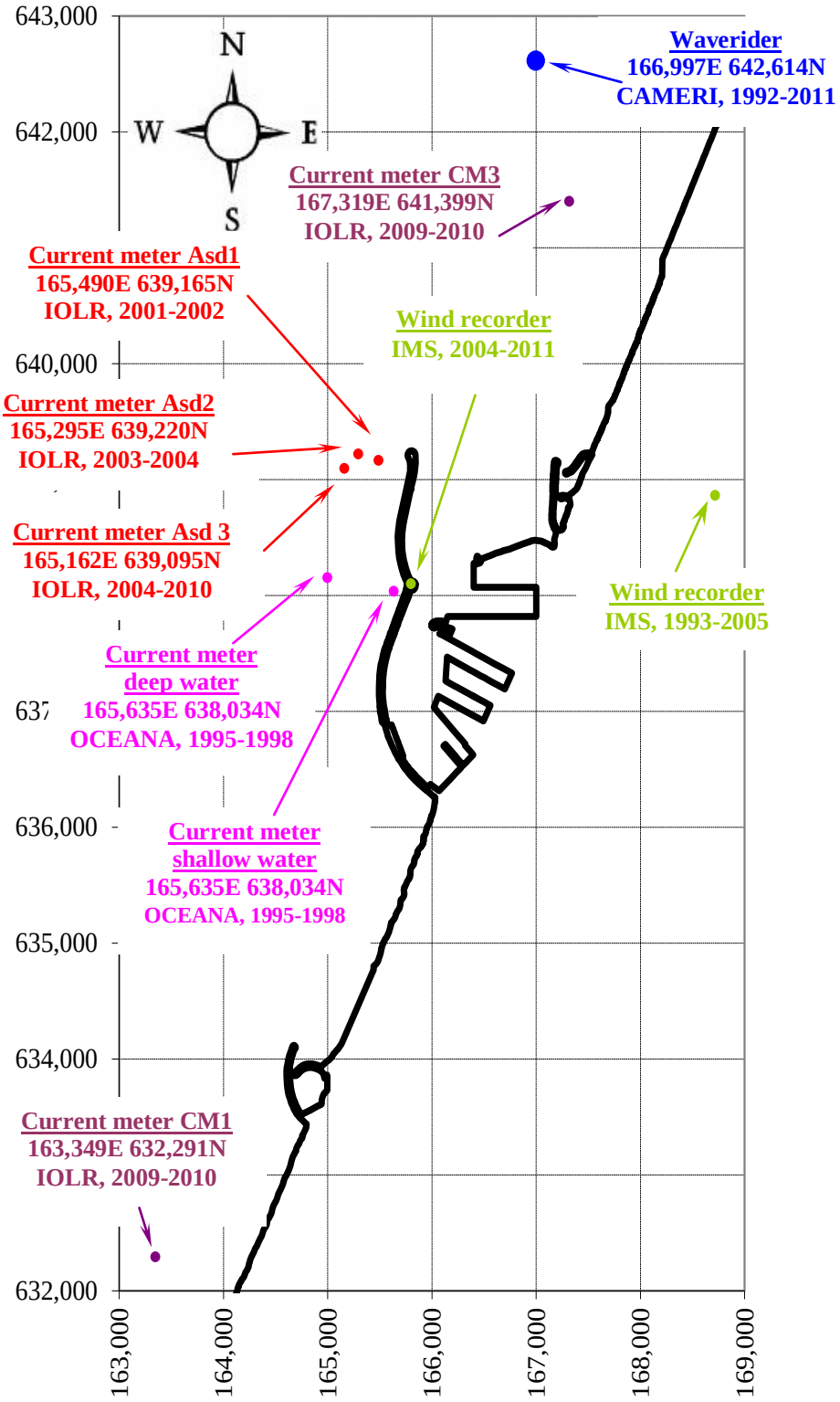

Fig. 7.2 – Locations of current measuring stations and other stations in the vicinity of Ashdod. Coordinates in meters correspond to the New Israeli Grid, NIG. Source: *Levin et al.* (2012)

There is a very pronounced majority of records corresponding to the current from south to north along the shore. About 58% of the near-surface currents and 57% of near-bottom currents correspond to the N-NE sectors. Also, about 20% of the near-surface and 13% of near-bottom currents flow in the opposite (southern) direction, i.e. sectors SSW-SW.

The strongest currents were recorded during the winter season. The largest near-surface and near-bottom speeds were ~120 cm/s and ~85.0 cm/s, respectively.

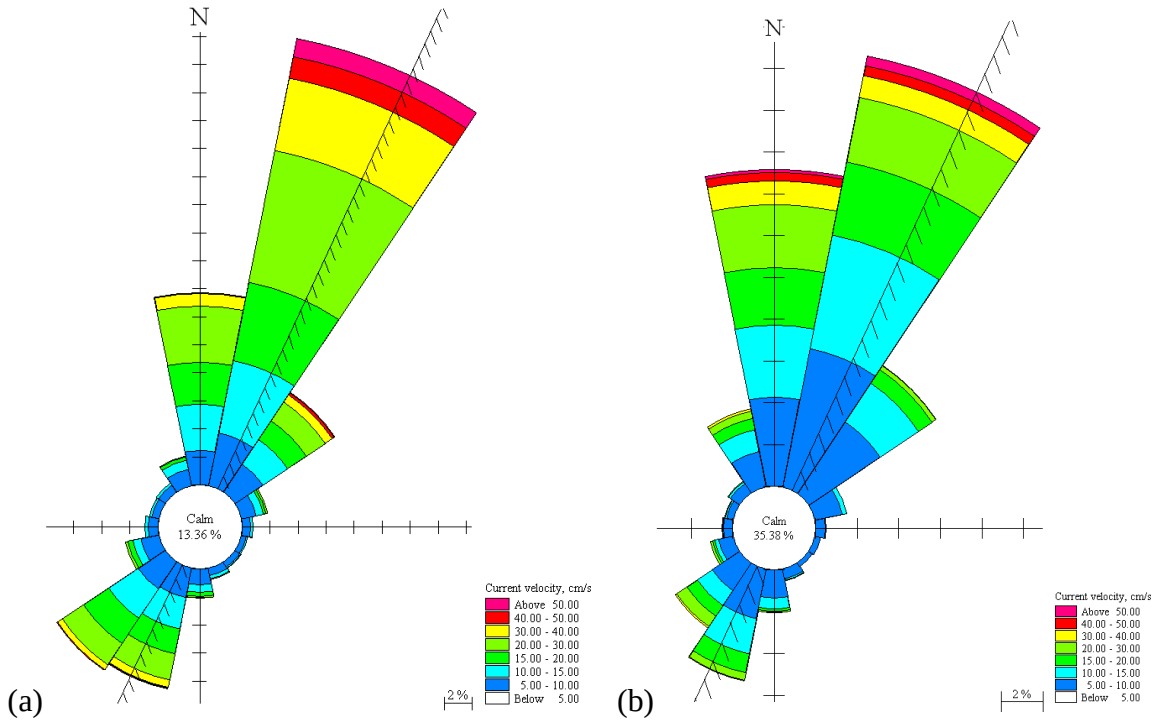

Fig. 7.3 – Annual current rose diagrams: (a) near-surface and (b) near-bottom (stations Asd1, Asd2 and Asd3, 01.04.2001-31.03.2010). Source: *Levin et al.* (2012).

Fig. 7.4 shows current speed and direction profiles corresponding to the strongest current recorded close to the surface (30.01.2008 00:00). This event is linked to the wave storm event with highest significant wave height H_{m0}=6.7 m, peak period T_p=12.5 s and direction (clockwise from north) *Dir*=277.1° in deep water (29.01.2008 17:56, storm duration was 82 hr) and with the strongest hourly averaged annual wind 19.2 m/s blowing from 277.8° (29.01.2008 18:00). The agreement in time of the peak events clearly indicates the cause-effect linkage between winds, waves, and currents.

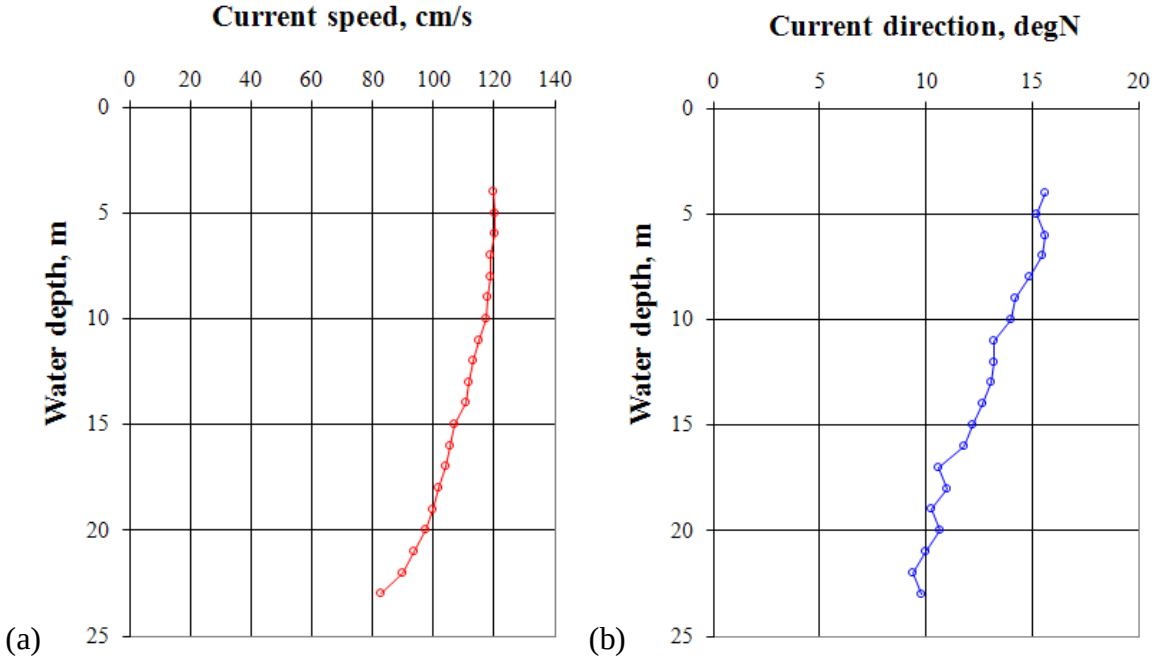

Fig. 7.4 – Depth profiles of (a) current speed and (b) current direction, corresponding to the strongest current recorded close to the surface at station Asd3 (30.01.2008 00:00). Source: *Levin et al.* (2012).

During the summer season, the largest near-surface and near-bottom speeds recorded were ~62 cm/s and ~46 cm/s, respectively.

Most of the time (90%), the speed of the near-surface current does not exceed 15-35 cm/s and the speed at the near-bottom current does not exceed 10-25 cm/s. The larger speeds occur near the sea surface. The largest near-surface and near-bottom speeds recorded occur during winter. The predominant direction is along the coast. With obvious differences due to local geographical and topographical features, the situation at Ashdod is representative for other locations along the Israeli coast.

References

ISRAMAR Internet website: http://isramar.ocean.org.il/isramar2009/

Kit E. et al., *2001*; "Joint analysis of Current, Wind and Wave data collected in Ashdod area between May 1995 and July 1998 - Final Report", CAMERI report P.N. 539, 340 pp.,Technion City, Haifa

Kit E. and Sladkevich M., *2001*: "Structure of Offshore Currents on Mediterranean Coast of Israel", 6th Workshop on Physical Processes in Natural Waters. Casamitjana, X. (ed.), Girona, Spain, 97-100

Kunitsa D., Rosentraub Z. and Stiassnie M., *2004*; "Estimates of winter currents on the Israeli continental shelf", Coastal Engineering, **52**/1, 93-102

Levin A. et al., *2012*; "Processing of Hydrographic Data at the Ashdod Region", CAMERI report P.N. 736, 271 pp., Technion City, Haifa

Rosentraub Z., *1995*; "Winter currents on the continental shelf of Israel", D.Sc. thesis, Technion, Haifa (in Hebrew, with English abstract)

Rosentraub Z. and Bishop Y., *2010*; "Development of a New Container Terminal at Haifa Port: Current Measurements at Station HFA3- Year 1", Quarterly report No.2, 7 June 2009 – 2 September 2009, IOLR Report H5/2010

8 - SEA WATER LEVEL AND TIDES

The sea level variations in the Mediterranean from 1999 to 2006 are shown in Fig. 8.1. Sea level is rising significantly in the Ionian Sea, with 12 cm increase registered on the Levantine coast since 1992 (*UNEP/MAP, 2012*). However, causes are not yet known and a cause effect relationship with climate change has not yet been established. Although the Israeli coast is painted red, indicating a large yearly increase in sea level, a detailed analysis of available data for Ashdod and Tel Aviv show otherwise, as explained in detail in *Levin et al.* (2012).

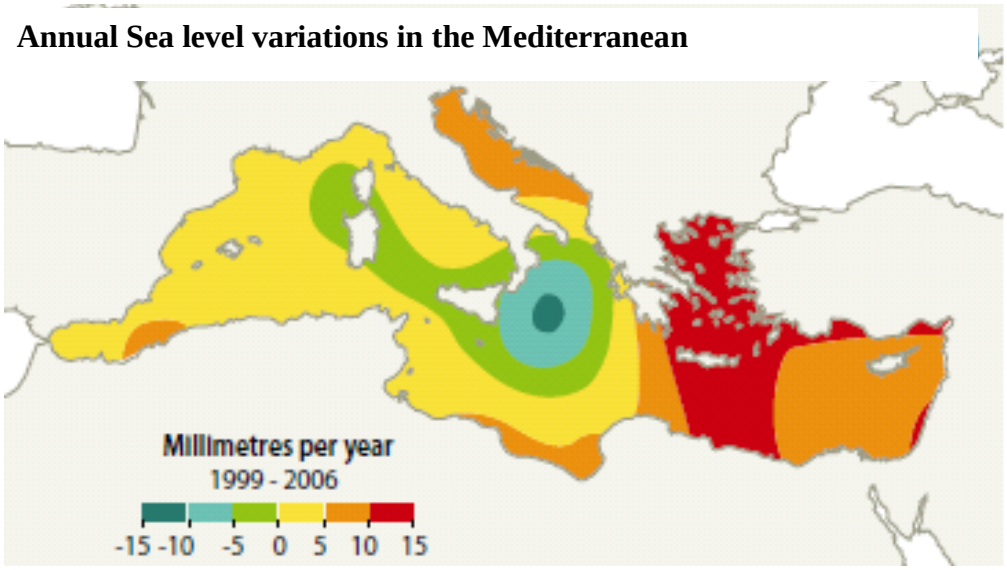

Fig. 8.1 – Mediterranean Sea level variations (mm/year) from 1999 to 2006. Source: *UNEP/MAP* (2012)

At Mediterranean scale, the mean sea level has various components:

(a) A nearly static component (almost constant in time) determined by the distribution of earth mass, reflecting the spatial variations in the Earth's gravitational field. This results by hills and valleys on the sea surface, reaching tens of meters. There is, for example, a 50 m permanent "hole" in the sea surface, over a 1500 Km long region between Nice and Crete (*OCA/CNES, 2000*).

(b) An inter-annual component, which is dominated by climate change. Research suggests that the mean level of the Mediterranean is increasing by 7-8 mm/year. However, observations are not conclusive.

(c) A seasonal component, showing high sea level at the end of summer and low sea level at the end of winter. The difference between both is about 20 cm. It is assumed that half of it is due to dilatation or contraction of the upper sea layers due to temperature (steric effect), and the other half is due to complex seasonal variations of rain and evaporation and to variations in flow to and from the Atlantic Ocean.

(d) Diurnal and semi-diurnal tidal component, with variations in sea level of the order of 10 cm in most areas. In some shallow areas of the north Adriatic and the Tunisian coast, tides may reach over half a meter.

Concerning the Israeli coast, measured sea level data can be obtained at the Internet site of the Survey of Israel (SOI) http://www.soi.gov.il. SOI's tide gauges are located at Akko, Tel-Aviv, Ashdod and Ashkelon. A tide gauge at Haifa was discontinued. Data covers the years 2000-2011, but is incomplete. Other organizations such as the Israeli Port and Railways Authority (now Israeli Ports Company), the Israel Meteorological Service (IMS) and Israel Oceanographic and Limnological Research (IOLR) have also been involved in sea level monitoring during different

periods. There are two stations, at Hadera and Ashdod, operated by IOLR in the framework of the European MEDGLOSS program. No information from these stations is currently accessible. Statistical monthly highest, lowest and mean levels at Hadera and Ashdod, however, can be obtained interactively at http://medgloss.ocean.org.il/statistic.asp.

The Mediterranean coast of Israel is characterized by water level fluctuations due to the local tides. As with most of coastlines, the Levant coast is subjected to semidiurnal tides. Moreover, the diurnal constituents near 24 hours are important as well. The primary lunar and solar constituents have periods that differ only slightly so that the relative phases, and, consequently, the amplitude of the combined tide, change fortnightly. Longer term constituents are monthly and semiannual.

The mean value of the Mediterranean Sea level defines the vertical datum of the geodetic network in Israel (ILSD). In general, the nominal values of the mean low water, MLW (the hydrographic zero usually used for navigation charts), mean sea-level, MSL, and mean high water, MHW, must be determined over a datum Epoch period (averaging period of 19 years that accounts for the sun periodicity of 18.6 years). As long as there were no continuous records covering such a long period, definitive answer regarding the position of these levels relative to the topographic zero of the national land survey (ILSD) could not be given.

Blank (1998) digitized 19 years of hourly data recorded at Ashdod during 1966-1984. After correcting for errors, he managed to determine these levels at Ashdod. The calculated MLW was 11.92 cm below the ILSD, while the MSL and MHW were 2.73 cm and 17.77 cm above the ILSD, respectively. These estimates took into account the fact that the locations of the Ashdod benchmark and monitoring site were changed twice: once upon moving from the Eshkol settling basin to the Ashdod Port on January 1968 (rising +6 cm thereafter according to *Goldsmith and Gilboa, 1985*); and once again at an unknown date (record lost) upon moving from the inner part of the port to its entrance sector (*Rosen, 1998*). The next MSL estimate performed by *Shirman* (2004) provides the average tide level at 5.9 cm relative to the vertical Israeli datum in the period 1958-2001. The most recent assessment of the MSL published in the SOI website (http://www.soi.gov.il) is at 12 cm above the ILSD in 2006.

In general, the astronomical tide in the area usually varies between 0.4 m during spring tides, and 0.15 m during neap tides. However, extreme levels may occur due to extreme meteorological conditions (*Stiassnie, 1987*). The approximate average recurrence of extreme sea levels as provided by *Stiassnie* (1987) and *Rosen* (1998) are gathered in Table 8.1. The differences between these two estimates (3-4 cm) seem to be due to the different reference datum specified by the authors, i.e. MSL by *Stiassnie* (1987) and ILSD by *Rosen* (1998). As mentioned earlier, in the 1966-1984 period used by *Rosen* (1998) for his assessment, the approximate position of the MSL according to *Blank* (1998) was about 2.73 cm above the ILSD.

Table 8.1 – Average recurrence of extreme sea levels

Average Return Period years	**Low Sea Level, m**		**High Sea Level, m**	
	Rosen, 1998 relative to the ILSD	Stiassnie, 1987 relative to the MSL	Rosen, 1998 relative to the ILSD	Stiassnie, 1987 relative to the MSL
1	-0.38	-0.41	+0.64	+0.60
50	-0.74	-0.79	+1.04	+1.00
100	-0.87	-0.90	+1.10	+1.06

Fig. 8.2 presents annually based values of low, high and average sea levels at Ashdod during 1966-1984 (*Rosen, 1998*) and during 2000-2009 as measured by SOI. Although some gradual rise in average sea level is obtained in the period 1966-1984, the mean seawater level in the period 2000-2009 seems to be quite stable.

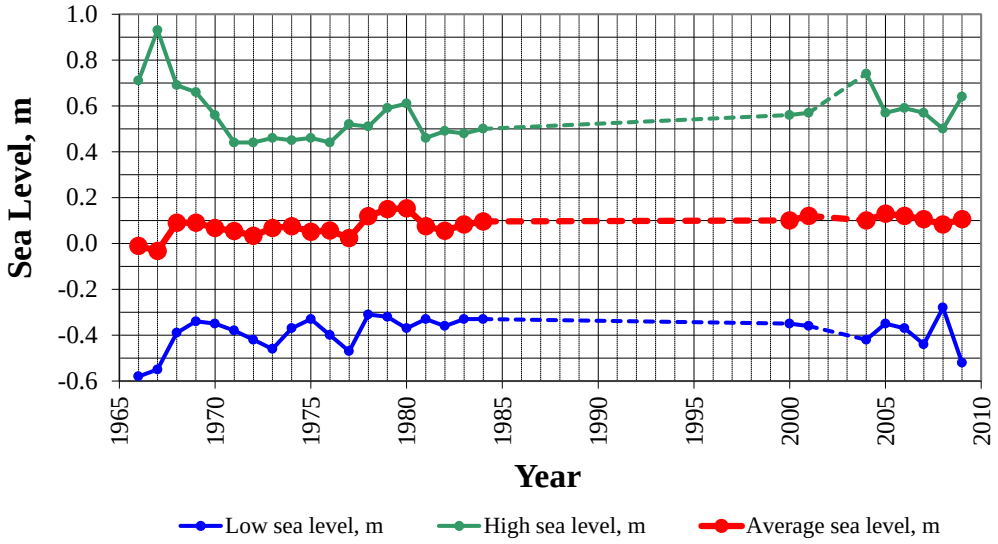

Fig. 8.2 – Sea levels at Ashdod measured relative to the ILSD during 1966-1984 (based on the data presented in the IOLR report, *Rosen, 1998*) and during 2000-2008 (based on the sea level measurements published by SOI in the website: http://www.soi.gov.il). Dashed lines indicate missing data. Source: *Levin et al.* (2012)

Shirman and Melzer (2002) and *Shirman* (2004) analyzed the data from Ashdod, Yafo, Tel-Aviv and Ashkelon for the period 1958-2001. In order to clarify the differences between sea level changes along the Israeli coast, records from different stations were compared. The comparison showed that the astronomical tide waves appear at the same phase and have almost the same amplitude at all stations. The average tide level for the entire period investigated was about 6 cm relative to the ILSD.

According to the study "East Mediterranean sea level changes over the period 1958-2001" conducted by *Shirman* (2004), the yearly MSL reached its highest value at the beginning of the sixties (Fig. 8.3). After that, the MSL fell sharply to a local minimum in the mid seventies. A gradual rise of the sea level was observed since 1973 falling again after 1980. A new rise began in 1990.

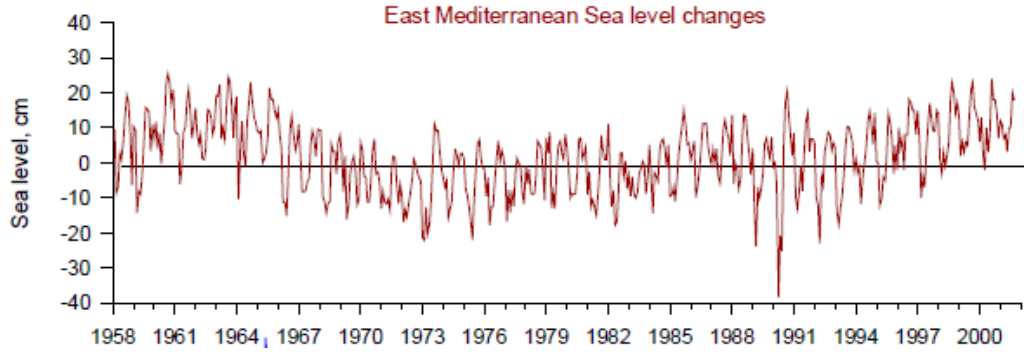

Fig. 8.3 – East Mediterranean Sea level during 1958 – 2001. The monthly mean values are relative to the Yafo datum. Source: *Shirman and Melzer* (2002)

Shirman and Melzer (2002) concluded that between the years 1973 and 2000 there are indications that the sea level rose about 15 cm. Monthly mean values at the Ashdod and Tel-Aviv

stations during 1990-2001 are reproduced from their work in Fig. 8.4, showing a gradual increase in Mediterranean Sea level of about 10 mm/year. However, during the last decade no increase of sea level has been noticed at the Ashdod or Tel-Aviv stations. The monthly mean values at the Ashdod and Tel-Aviv stations during 1999-2009 are plotted in Fig. 8.5 revealing almost constant trend that is coincident with the annual mean sea level presented in Fig. 8.2. SOI presents a similar conclusion indicating that the MSL between 2000 and 2005 was stable with no noticeable changes in the annual mean value (http://www.soi.gov.il). Although slightly different from each other in detail, sea level measurements at the all stations along the Israeli shoreline reveal the same tendencies.

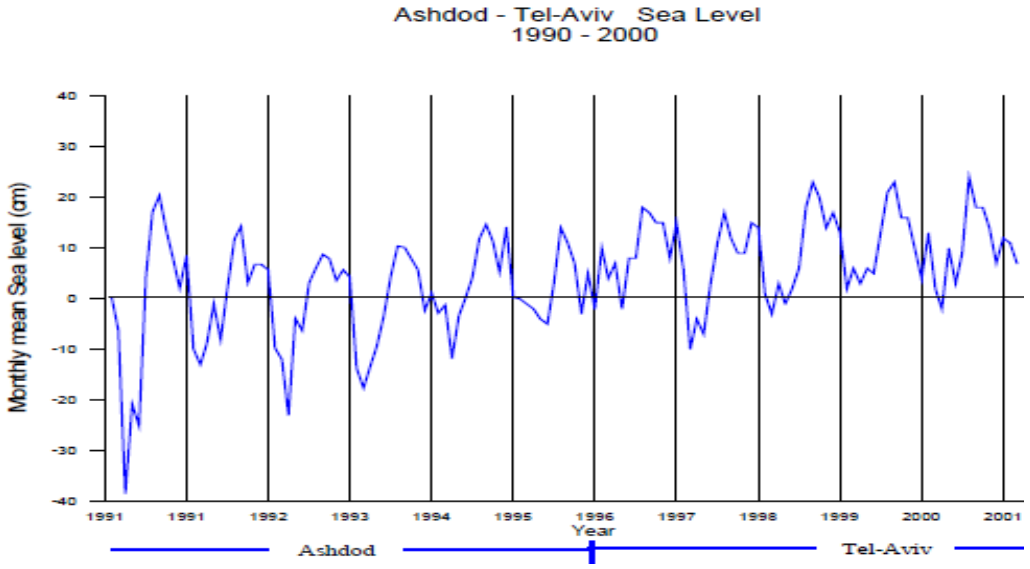

Fig. 8.4 – Monthly mean sea level values at Ashdod and Tel-Aviv stations during 1990-2000. Source: *Shirman and Melzer* (2002).

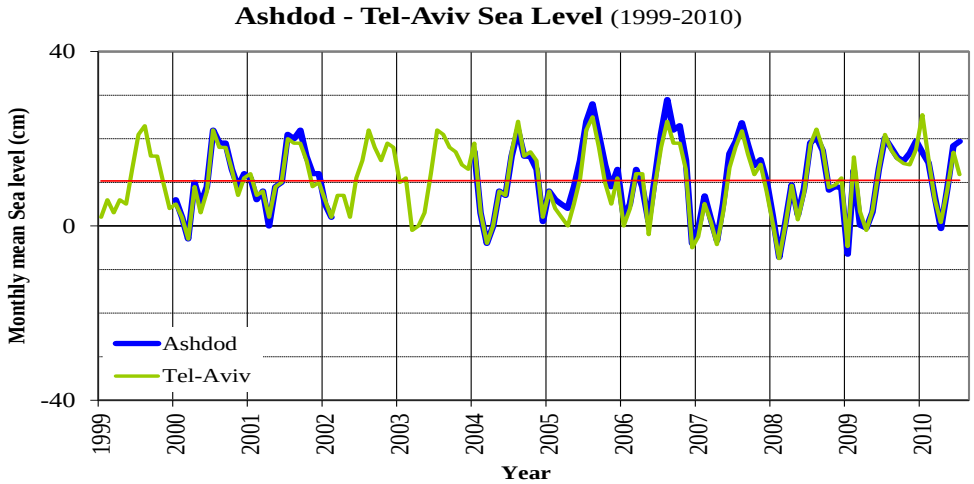

Fig. 8.5 – Monthly mean sea level values at Ashdod and Tel-Aviv stations during 1999-2010. The trend line is plotted in red. Based on sea level measurements published by SOI, (website http://www.soi.gov.il). Source: *Levin et al.* (2012)

Other relevant studies and sea level forecasts are described in *Levin et al.* (2012).

In summary, according to recent research literature the forecasted worldwide average rate of sea-level rise is 0.6–0.7 cm per year and the regional one is about 0.7–0.9 cm per year; this means a 35–45 cm rise during the next 50 years. However, SOI sea-level records at Ashdod as well

as at Tel-Aviv show that the mean seawater level along Israel's Mediterranean coast remained quite stable in since 1999. These results are inconsistent with the worldwide and regional trends up to the beginning of the 2000s and forecasts of sea-level rise thereafter. Obviously, the period 1999-2010 is too short for the purpose of providing a reliable forecast for the coming 50 years, and continued study is required.

References

Blank Y., *1998*: "Long-Term Analysis of Sea-levels at Ashdod, and the Astronomical Tide and Meteorological Contributions to the Sea-level", Graduation Thesis in Physics, Ministry of Education, Culture and Sport, in Hebrew.

Goldsmith V., and Gilboa M., *1985*: "Development of an Israeli Tidal Atlas and Comparison with Other Mediterranean Tidal Data", IOLR report H8/85, Haifa

Levin A. et al., *2012*; "Processing of Hydrographic Data at the Ashdod Region", CAMERI report P.N. 736, 271 pp., Technion City, Haifa

OCA/CNES, *2000*; "The Mediterranean Sea". Extract from: The Geonauts inquire the oceans educational CD, 7 pp. Found as pdf file in the Internet.

Rosen D. S., *1998*: "Sea-Levels Climate", IOLR Report No.H3/98, Submitted to building and planning department, PRA-Israel.

Shirman B., *2004*: "East Mediterranean sea level changes over the period 1958–2001", Isr. J. Earth Sci., **53**: 1–12.

Shirman B. and Melzer Y., *2002*: "Mediterranean Sea Level Changes over the Period 1961-2000", FIG XXII International Congress, Washington, D.C. USA.

Stiassnie M., *1987*: "Safe Heavens for Avoidance of Dangerous Weather and Sea State in Mediterranean, Ashdod Port", CAMERI report P.N.188/87, Technion City, Haifa

Survey of Israel; Internet site http://soi.gov.il

UNEP/MAP, *2012*; "State of the Mediterranean Marine and Coastal Environment", 2012 United Nations Environment Program / Mediterranean Action Plan, Barcelona Convention, Athens, 2012, 96 pp.

9 – BED SEDIMENT AND GRANULOMETRY

Seabed sediment characteristics have been measured and analyzed at different locations along the coast of Israel. Detailed survey campaigns have been carried out by several organizations and researchers along the coastal area (and in deeper water), that examine the composition of seabed and transported sediment material. *Levin et al.* (2012a) and *Levin et al.* (2012b) present a comprehensive account and summary of these surveys and studies from 1970 to 2010, with reference to the Ashdod and Haifa areas, respectively.

Testing of seabed material at the Ashdod region has been conducted by different institutions, like e.g. Laboratoire Central D'Hydraulique de France (LCHF), Technion Research and Development Foundation Ltd, and Israel Oceanographic and Limnological Research (IOLR). *Levin et al.* (2012a) considered data collected during the OCEANA Marine Research Ltd. thorough survey carried out in 1995-1996 on behalf of the Port and Railways Authority (now IPC) and a more recent survey carried out by IOLR (*Gertner, 2009*).

Based on median grain size d_{50} in the Ashdod region provided by these sources, the seabed sediment in that area can be classified as sandy soil with low content of fines. The median grain size d_{50} gradually decreases from the beach offshore, usually d_{50}~0.2-0.4 mm close to the shoreline, d_{50}=0.11-0.17 mm for 10-20 m water depths and about 0.10-0.14 mm in waters more than 20 m deep. In several places along the coastline, non-uniform, unstable rocky beaches with many holes and presence of shell residues are found. Northward the Ashdod port, the sand median grain size is sometimes larger than 1.0 mm (*Levin et al., 2012a*).

Concerning the Haifa area, *Levin et al.* (2012b) addresses the work reported in *Golik* (1999), *Zviely* (2006), *Gertner* (2008) and others. Three segments are considered:

- In the *Carmel Coast* the seabed sediment is mainly fine sand with a narrow grain size distribution. The median grain size d_{50} usually ranges from 0.125 to 0.25 mm. Along the shore (water depths 0 to 1 m), the sand is somewhat coarser, with d_{50}~0.35 mm. The particle size generally decreases offshore and northward. More recent sampling indicates a rocky seabed already at 15 m water depth.
- In *Haifa Bay* the beach and seabed sediment up to 10 m water depth is mainly fine sand with a narrow grain size distribution. d_{50} usually ranges from 0.125 to 0.25 mm. Particle size generally decreases offshore and northward. In some places the sediment is coarser, which can be associated with the presence of shells fragments and broken rocky seabed. According to *Gertner* (2008) the sediment at 25 m water depth contains a relatively large fraction of clay.
- Along the *Carmel headland* the beach and the seafloor are exposed. The sand, if any, is coarse or very coarse and highly variable in grain size. The *Bat Galim* rocky shore, covered in some places by medium and coarse sand, changes to finer sand toward the port facilities. According to *Gertner* (2008) the shoreline sediment is largely biogenic. The sand that settles along the Haifa Port main breakwater is usually fine with d_{50}<0.25 mm.

These conditions may vary locally, like for instance the changes due to the recent expansion of the main port breakwater and other marine structures. Updated monitoring measurements are given in *Levin et al.* (2014).

Like for Ashdod and Haifa, specific and particular features apply, for example, to the Netanya coast (see e.g. *Levin et al., 2011*).

References

Gertner Y., *2008*: "Environmental Impact Assessments, Outline Plan 13/bet/gimel – Deepening of Haifa Port Entrance Channel, Outline Plan 13/bet/gimel – Extension of Haifa Port Main Breakwater, Grain Size Analysis of Sediment from Haifa Bay and the South Coast of Haifa", IOLR Report H20/2008, Haifa

Gertner, Y., *2009*; "Granulometric and Mineralogical Survey of the sand in the vicinity of Ashdod Port", Israel Oceanographic and Limnological Research IOLR, Report H21/09, 9 pp. Haifa, (in Hebrew)

Golik A., *1999*: "Haifa Port Expansion Project, Environmental Impact Assessment, Task 1.2.9 – Grain Size Distribution of Sea Bottom Sediment, Final Report", IOLR Report H16/99, HPEIA report 26, Haifa.

Levin A., et al., *2011*; "Netanya Coast and Cliff Protection: *Hydrographic Conditions and Marine Sediment Characteristics*", CAMERI Interim Report P.N.746, 91 pp., Technion City, Haifa

Levin A. et al., *2012a*; "Processing of Hydrographic Data at the Ashdod Region", CAMERI report P.N. 736, 271 pp., Technion City, Haifa

Levin A. et al., *2012b*; "Processing of Hydrographic Data for the Haifa Region", CAMERI report P.N. 737, 329 pp., Technion City, Haifa

Levin A. et al., *2014*; "Monitoring activities after completion of works for deepening the marine entrance channel to Haifa Port", CAMERI report P.N. 799, 162 pp., Technion City, Haifa (in Hebrew)

Zviely D., *2006*: "Sedimentological Processes in Haifa Bay in Context of the Nile Littoral Cell", Ph.D. Dissertation in Hebrew, Tel Aviv University, Israel.

10 – SEDIMENT TRANSPORT

Most of Israel's Mediterranean coast and coastal seabed is sandy. The primary source of this sand is the river Nile delta. The sand transport occurs mainly alongshore, within a relatively narrow strip between the shoreline and kurkar reefs.

There are clear indications that sediment transport towards the north occurs even at water depths greater than 24 m (*Golik, 1993, Kit et al., 1979*). For example, longshore sand transport under the coal unloading terminal at Hadera caused sand accumulation at the northern bank of the terminal's underwater trench. This forced the Israel Electric Company, IEC, to conduct dredging works in order to warrant safe mooring of the ships at the terminal (*Kit and Khalfin 2002*).

Within the surf zone, sand is primarily transported by longshore currents induced by breaking waves. Beyond the breaker zone, wind-induced currents dominate, governing the sand transport. The direction of wave-induced sediment drift depends on the direction of incident waves with respect to the shore normal. The orientation of the Israeli coastline, combined with local climatic conditions, favors transport of the sand from south to north (*Levin et al., 2012*). However, there are periods when waves cause north to south currents. The difference between the (yearly) sand fluxes from the south and that from the north is called net sediment transport, while the sum is the gross transport.

The 140 Km long coastline from Ashkelon to Haifa is relatively smooth. The shore normal orientation (measured clockwise from North) slowly varies from ~306° at Ashkelon to ~277° at the southern coast of Haifa. Wave heights and consequently wave energy vary only slightly along the coast. Assuming that incident wave directions do not change noticeably along the coast; the gross transport is expected to vary slowly as well.

Quantitative estimations of sediment transport patterns along the Israeli shore have been made by several researchers from different institutions (e.g. *Golik, 1999*; *Perlin and Kit, 1999*; *HR Wallingford 1996a, 1996b, 1999*; *Zviely, 2006*; *Zviely et al., 2007, 2009*). An indicative region for assessment of alongshore littoral drift is the Haifa Port main breakwater, which served (before the construction of the Polynom harbor) as a trap for Nile River sand traveling northward. The mean annual amount of sand drifting towards Haifa Bay can be roughly assessed through estimation of the sediment volume settled along the port's main breakwater (at least 60,000-70,000 m^3/year) plus some volume of sand bypassing the breakwater. The most updated estimate of sand accumulation along the main breakwater of the Haifa Port is given in *Zviely* (2006) and *Zviely et al*. (2007). Other quantitative assessments of drifting and trapped sand can be made from the amounts of sediment annually dredged from port and marina entrance channels as well as from power station settling basins.

At present, the different researchers dealing with sediment transport in Israel agree that the annual gross transport is approximately 300,000-400,000 m^3.

Following a geological analysis of the Israeli Mediterranean beaches, *Emery and Neev* (1960) presented the pattern of sediment fluxes shown in Fig. 10.1. This sediment flux pattern seems very plausible, in general, if the appropriate source for a current beyond the surf zone can be well-defined. *Emery and Neev* (1960) assumed that the offshore fluxes in deeper water are related to the so called general Mediterranean current. However, as suggested by *Kit and Sladkevich* (2001), and shown by *Kunitsa* (2000) and *Kunitsa et al.* (2005), the background Mediterranean currents diminish rapidly to a few centimeters per second at about 15 m water depth and are of no relevance in the littoral zone. Based on an extensive analysis of currents in the Ashdod area (measured in a survey by OCEANA Marine Research Ltd.), *Kit and Sladkevich* (2001) showed that there are clear indications of noticeable northerly currents generated by wind in the region beyond the surf zone.

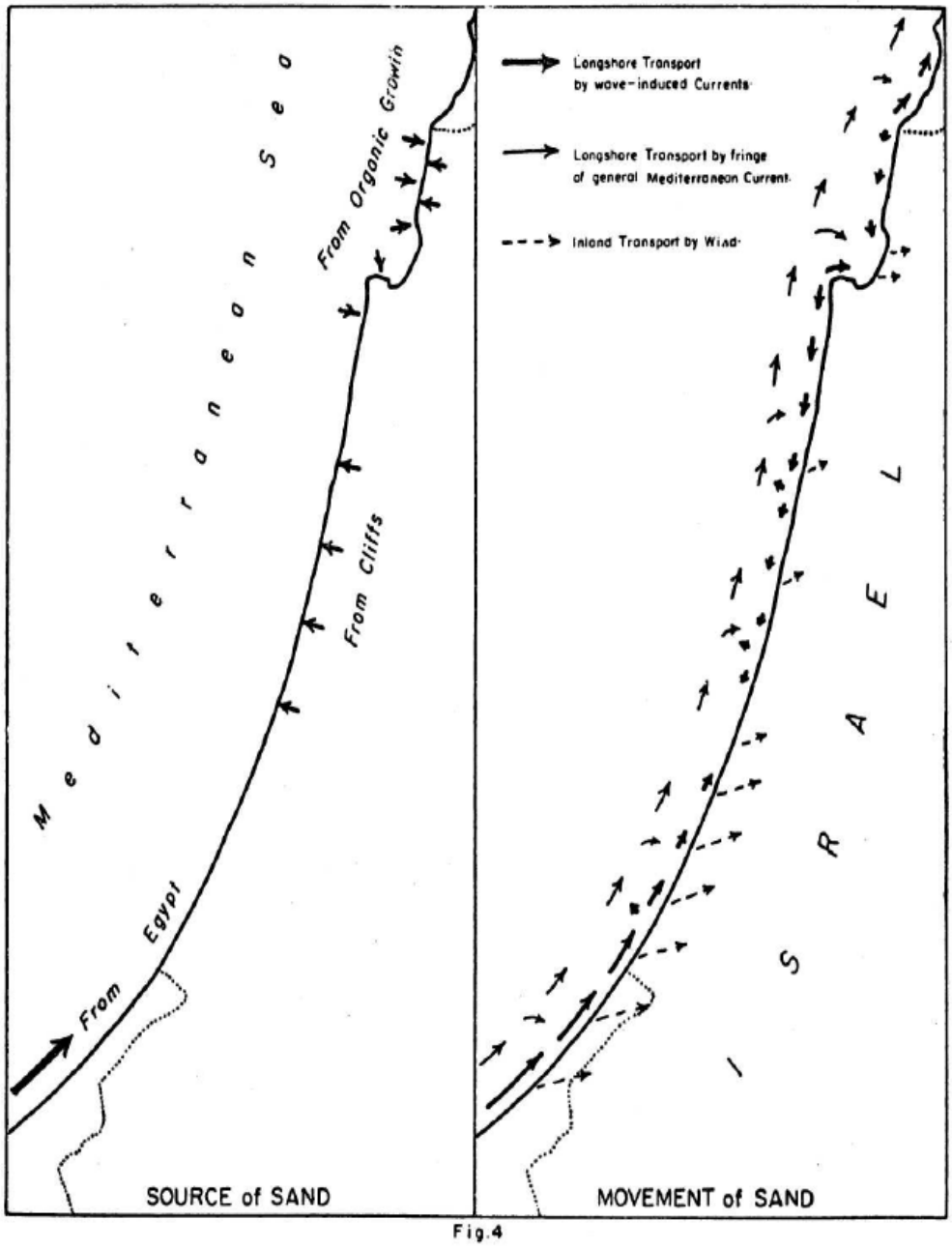

Fig. 10.1 – Hypothetical sand transport patterns along the Israeli Mediterranean coast as proposed by *Emery and Neev* (1960)

At water depths beyond about 5 m, wind-induced south-to-north currents transport about 100,000 m^3 of sand annually along the Israeli Mediterranean coast from Ashkelon to Haifa Bay.

According to a study of the Herzelia coast summarizing the above considerations, the expected littoral sand transport in that region can be considered as consisting of:

- wave-induced; gross transport ~300,000-350,000 m^3/year with net transport close to zero, and
- wind-induced; northward transport of 100,000 m^3/year.

The above values are used for calibration of mathematical models in studies by CAMERI researchers.

Goldsmith and Golik (1980) indicate the presence of four distinct zones of longshore sediment transport (from southwest to northeast) along the Mediterranean coast of Israel:

(1) Western Zone (El Arish to Rafah), where all wave approach directions cause transport to the northeast, and therefore net transport equals gross transport.

(2) Central Zone (Rafah to Haifa), which is characterized by converging longshore transport nodal points that shift along the coast in response to changes in wave direction and, to a lesser extent, wave period (i.e., north of the nodal point longshore transport is directed to the south, and south of the nodal point transport is directed to the north). For waves from azimuth 282.5°, the nodal point is at Netanya and for azimuth 315° at Rafah, the southern border of the central zone.

(3) Haifa Bay, a 20 Km long shoreline segment having significantly lower wave energy than the other coastal zones for all wave conditions except 5 s waves from the northwest which cause southern transport. Even for southwest 9 s waves, the sediment transport in this area is essentially zero due to wave refraction, so this area may be considered a sediment sink.

(4) Northern Zone (Akko to Rosh Hanikra) which is subject to intense wave refraction over the near-shore Akhziv Canyon, resulting in great variably of local longshore transport for most wave conditions.

The above local redistribution of longshore sediment transport along the south-eastern Mediterranean coast explains many observed shoreline phenomena. For example, the lack of quartz sediment north of Akko, derived from the Nile River and Kurkar cliffs to the south, appears to be due to Haifa Bay, which acts as sediment sink for northward moving sand. The large differences in sediment transport between the Bardawil Lagoon (Western Zone) and Gaza (Central Zone), as evidenced by the differing sand accumulations on the southern sides of coastal constructions in these two zones, is attributed to the increasing importance of waves from the northwest in causing southwestern transport along the coast northeast of Rafah. The lack of strong indicators of transport direction (such as sediment accumulations differentially on one side of the structures) along the coast of Tel-Aviv and to the north is due to the continuously changing directions of longshore transport with changing wave conditions in the Central Zone.

References

Emery K.O. and Neev D., *1960*; "Mediterranean Beaches of Israel", Geological Survey Bulletin, 26, 1-24

Goldsmith V. and Golik A., *1980*; "Sediment transport model of the southeastern Mediterranean coast", Marine Geology, **37**/1-2, 147-175

Golik A., *1993*: "Indirect Evidence for Sediment Transport on the Continental Shelf of Israel", Geo-Marine Let. **13**, 159-164

Golik A., *1999*: "Haifa Port Expansion Project, Environmental Impact Assessment, Task 1.2.9 – Grain Size Distribution of Sea Bottom Sediment, Final Report", IOLR Report H16/99, HPEIA report 26, Haifa

HR Wallingford, *1996a*: "Ashdod Sedimentological Study. Model Set up and Validation", Project manager: Dr. M.P. Dearnaley, Report EX 3403.

HR Wallingford, *1996b*: **"**Ashdod Sedimentological Study", Project manager: Dr. M.P. Dearnaley, Final Report EX 3518**.**

HR Wallingford, *1999*: "Hayovel Port Stage A. Coastal Nourishment with Dredged Material", Project manager: Dr. M.P. Dearnaley, Report EX 4025.

Kit E. and Khalfin I., *2002*: "Assessment of Expected Impact of Sandbar Dredging Formed to the North of Coal Unloading Terminal on the Neighboring Marine Environment and Submarine Trench", Ramot at Tel Aviv University Project No 1573, 35 pp, submitted to IEC.

Kit E. and Sladkevich M., *2001*: "Structure of Offshore Currents on Mediterranean Coast of Israel", 6th Workshop on Physical Processes in Natural waters. Casamitjana, X. (ed.), Girona, Spain, 97-100

Kit E., Rosen D., and Vajda M., *1979*; "Consultation Regarding Coal Spillage in the Surroundings of the Coal Unloading Terminal Off-shore Hadera and Assessment of the Feasibility of Pollution of Neighboring Beaches by Coal", CAMERI report P.N. 59, Technion City, Haifa, 38 pp, submitted to the IEC (in Hebrew)

Kunitsa D., *2000*: "Forecasting the Regime of Currents on the Israeli Continental Shelf", Ph.D. thesis, Technion, Haifa.

Kunitsa D., Rosentraub Z., Stiassnie M., *2005*; "Estimates of winter currents on the Israeli continental shelf", Coastal Engineering, **52**/1, 93-102

Levin A. et al., *2012*; "Processing of Hydrographic Data at the Ashdod Region", CAMERI report P.N. 736, 271 pp., Technion City, Haifa

Perlin A. and Kit E., *1999*; "Longshore sediment transport on Mediterranean Coast of Israel", *ASCE Journal of the Waterways, Port, Coastal and Ocean Division*, **125**/2, 80-87

Zviely D., *2006*; "Sedimentological Processes in Haifa Bay in Context of the Nile Littoral Cell", Ph.D. Dissertation, Tel Aviv University, Israel, (in Hebrew).

Zviely D., Kit E., Klein M., *2007*; **"**Longshore sand transport estimates along the Mediterranean coast of Israel in the Holocene", *Marine Geology*, **238,** 61-73

Zviely D., Kit E., Rosen B., Galili E., Klein M., *2009*; "Shoreline Migration and Beach-Nearshore Sand Balance Over the Last 200 Years in Haifa Bay (SE Mediterranean)", GeoMar Lett., **29**, 93-110

11 – TSUNAMI

Tsunami is a natural phenomenon developing in the sea that can be caused by an offshore earthquake due to a co-seismic displacement of the ocean bottom, by landslides occurring at sea trenches or continental shelf slopes triggered by earthquakes, by volcanic eruption in the coastal area or due to other reasons such as meteorite impacts on the sea, offshore nuclear explosions, etc.

A strong tsunami can lead to total disaster in the region affected, destroying buildings, marine structures and entire villages, and causing the loss of many thousands of lives. Therefore, tsunamis are being studied intensively, using advanced numerical models for the description of tsunamigenic sources, tsunami propagation in open Ocean, tsunami transformation in coastal regions, development of run-up and inundations. These are subjects of great importance.

A comprehensive report was prepared by CAMERI researchers to describe the potential threat of a devastating tsunami in Israel (*Kit et al., 2010*). The report contains a very detailed literature survey describing most of the known tsunami events that affected the Mediterranean coast of Israel during the last two millennia and even prior to that period. It includes practically all papers, reports and documents dealing with historical tsunamis and with tsunami prediction models applied to the Eastern Mediterranean in general and to the coast of Israel in particular *(Beisel et al.* 2009*).*

The analysis of historical records for the last two millennia in the Eastern Mediterranean reveals a considerable number of devastating tsunamis caused by local earthquakes at the Dead Sea Transform Faults and remote earthquakes that occurred within Aegean Sea, Hellenic and Cyprus arcs and even at such remote locations as Sicily, Italy. Recent paleoseismic studies, employing the most advanced technologies (like GPS for determining the relative velocities of plates and radioisotopes for geological dating) and supported by archeological data, were able to locate the sources of extreme events with good precision and to estimate their recurrence times.

The engineering aspects of the problem are discussed, based on the lessons provided by careful studies of consequences caused by recent disasters such as the Indian Ocean tsunami in 2004 and the Katrina hurricane in 2005. *Kit et al.* (2010) deals with determining the potential of disastrous tsunamis near the Israeli coast and suggests measures for damage mitigation.

The list of topics considered in *Kit et al.* (2010) is as follows:

- Local and remote sources of potential tsunamis in Israel;
- Important historical events;
- Probabilistic and statistical approaches to estimate tsunami potential and impact;
- Classification of issues related to tsunami generation and propagation modeling, ranked according to their importance: (a) description of tsunami sources (seismic and others), (b) tsunami expected occurrences (statistical approaches), (c) modeling of tsunami generation mechanisms, (d) modeling of tsunami propagation in open ocean, (e) tsunami propagation in the coastal region and on the continental shelf, tsunami run-up and inundation maps;
- Tsunami engineering – lessons from recent disasters: PNG (Papua New Guinea, 1998), Indian Ocean 2004 tsunami, Hurricane Katrina 2005;
- Tsunami mitigation measures – design of structures capable of withstanding earthquakes and tsunamis;
- Tsunami warning system – real time alerts and advices, education for population awareness, communication links and appropriate broadcasting system; agencies, operational guides, handbooks and brochures – Federal Emergency Management Agency (FEMA), Tsunami Risk Assessment and Strategies for European Region (TRANSFER), Japan Meteorological Agency (JMA), etc.;

- Recent tsunami computations for the Mediterranean coast of Israel due to co-seismic and landslide induced free surface perturbations: Coastal and Marine Engineering Research Institute (CAMERI), United Research Services (URS) for the Geological Survey of Israel (GSI) and Israel Oceanographic and Limnological Research (IOLR);

The main conclusions in the *Kit et al.* (2010) report are:

- Although the Eastern Mediterranean is currently the most quiescent region in the Mediterranean Sea, very devastating local and remote earthquakes and tsunamis can strike Israel and the neighboring countries during the present or next centuries. These conclusions, as well as the analysis of potential tsunami threat, are based on the thorough review of a great number of recently published papers on the subject. The studies presented in these papers employed modern technologies as well as paleoseismic and archaeological approaches as mentioned before.
- Three disastrous events (in the years 551, 1202 and 1303) are discussed in *Kit et al.* (2010) with greater emphasize. It is shown with a great degree of confidence that similar events could occur during this or the next century. Therefore, there is a vital necessity for design and construction of tsunami detection and warning systems, and wide dissemination of tsunami awareness by appropriate public education. Any further research on tsunamis and their sources is of great value but the focus should be primarily on tsunami prediction, detection and alert dissemination.
- Regarding marine structures, there is a reasonable probability that buildings, coastal structures and other facilities designed to withstand earthquakes, would survive tsunamis as well.

References

Beisel S., Chubarov L., Didenkulova I., Kit E., Levin A., Pelinovsky E., Shokin Y., Sladkevich M., *2009*; "The 1956 Greek tsunami recorded at Yafo, Israel, and its numerical modeling", Journal of Geophysical Research, Vol. 114, C09002, 18 pp

Kit E., Levin A., Sladkevich M., *2010*; "Comprehensive Report on: *Investigation of Tsunami Hazard in Israel – Eastern Mediterranean*", CAMERI report submitted to DHV as Appendix to *Engineering Assessment of Tsunami Hazard*, 66 pp.

12 – BEYOND MEASUREMENTS; THE USE OF NUMERICAL MODELS

The greater understanding of the physics of complex flow processes has led to detailed and sophisticated mathematical formulations. The mathematical representation is mostly deterministic and Eulerian, in the form of partial differential equations expressing the conservation laws and equations of state. The initial and boundary conditions for the equations governing the circulation flow in the ocean are zero velocity at land boundaries, friction formulas at the seafloor and diverse interface conditions at the sea surface. Internal mixing and various scale turbulence expressions are adopted. The horizontal and vertical scales are widely different. In the Mediterranean, the average depth of 1.5 Km compared to 3800 Km length is like a 25 cm long strip of (0.1 mm) thin paper.

Numerical flow models are discrete approximations (in time and space) to the governing (continuous) mathematical formulations on gridded space. Finite difference formulations use normally a rectangular grid covering the horizontal extent of the model while flexible mesh approaches employ an unstructured free form triangular/quadrangular mesh of varying resolution, allowing the use of a locally denser grid in areas of steep gradients or where finer resolution is desired. The vertical dimension is partitioned using a specified division in depth, or considers a determined number of so called sigma layers, proportionally distributed according to local depth and sea level. This latter approach features the same number of layers in areas of deep and shallow sea. Moreover, the position of sigma layers varies in time with sea surface variations. In the time dimension, numerical schemes are divided in explicit and implicit. While in implicit schemes the time step is independent of the spatial discretization, in explicit schemes the time step is limited by the spatial resolution because of stability considerations. For shallow water coastal areas, models are two dimensional, and consider only (averaged over depth) horizontal flow.

Of course, a numerical model cannot resolve flows, eddies and other variables at a scale below the grid size. The grid size is always determined as a compromise between better resolution and limited computer resources. The sheer amount of computational effort for a large number of grid points means long run times. Long run times, in turn, make a model impractical.

Any model necessitates detailed knowledge of the boundary conditions as function of time, sources and sinks also as function of time, and the initial conditions in the entire water body. Of particular difficulty are the free surface boundary conditions, necessitating an interface providing wind stress, precipitation and evaporation, pressure and heat exchange with the atmosphere, etc. Also the initial condition is unknown and usually taken from a calibrated model's former run.

Any model also needs calibration in order to be useful. Model calibration is essential and consists of a trial-and-error iterative process in which model results are compared with available observations, then model parameters are corrected and a new run is performed, until a satisfactory agreement is achieved. The more observations are available for comparison the better the calibration basis and the more reliable model results are for attempting forecast runs. Nevertheless, there is no guarantee that model behavior follows nature's behavior. Models are best suited to discover trends, to verify conjectures, to compare between alternatives with otherwise identical conditions, etc. They are invaluable in reliable forecasting, only if continuously calibrated and verified.

There are also some Lagrangian numerical models, with random components of dispersion, employed mainly to simulate the spreading of oil slicks and other pollutants, or to simulate the path of drifters in surface currents. These models need as background the flow field variation in time, generally from an Eulerian flow model, among other things.

Many ocean circulation models, coastal flow models, wind-wave models and atmospheric models are in use, mostly for research and forecasting purposes. Operational systems employ all of the above plus the capability to acquire and incorporate observed measured data automatically and in real time. These data are necessary for improving the quality of the models by further calibration

and verification, real time correction of boundary and interface conditions, so as to produce ever more reliable atmospheric and marine forecasts at land and sea.

Wind

The European Center for Medium range Weather Forecasting, ECMWF, based in England, is an inter-governmental body merging information from its 34 member states. The information is both observations and results from atmospheric models running at the members' national meteorological services. The data is collected and merged in the center's facilities, employing one of the largest supercomputers in Europe running atmospheric models. Model results are distributed in a unified detailed regional forecast for Europe and the Mediterranean. Israel is a co-operating state in ECMWF. *Richardson et al.* (2013) presented an evaluation of the system's forecasts including the changes introduced to the system in 2012-13. A recent study by *Levi and Carmona* (2013) analyzed the ECMWF system 4 forecasting skill for the Mediterranean by comparing model forecasts to measured results since many years back. In general, predictability was high. Warming trends were correctly predicted but values were under-predicted. Israel's Meteorological Service (IMS) is doing research and using a regional forecasting model, HRM, based on the German Meteorological Service model for workstations and adapted by the IMS to the conditions in the south eastern Mediterranean. Details about resolution and such can be found in the IMS Internet website: http://www.ims.gov.il/IMSEng/RESEARCH.

Waves

Wave numerical models are mainly associated with the names WaveWatch, used by the American National Oceanic and Atmospheric Administration (NOAA), National Weather Service (NWS) and National Centers for Environmental Prediction (NCEP), and WAM (in many variations, see e.g. *Hasselman et al., 1988, Komen et al., 1994*), as employed by many research and operational forecasting systems throughout Europe. Other names are: SWAN, developed at the Delft University of Technology, and NSSM, the U.S. Navy Standard Surf Model.

Fig. 12.1 shows a wave climate forecast for the Eastern Mediterranean from the University of Athens, employing the Triton wave forecasting package based on WaveWatch III.

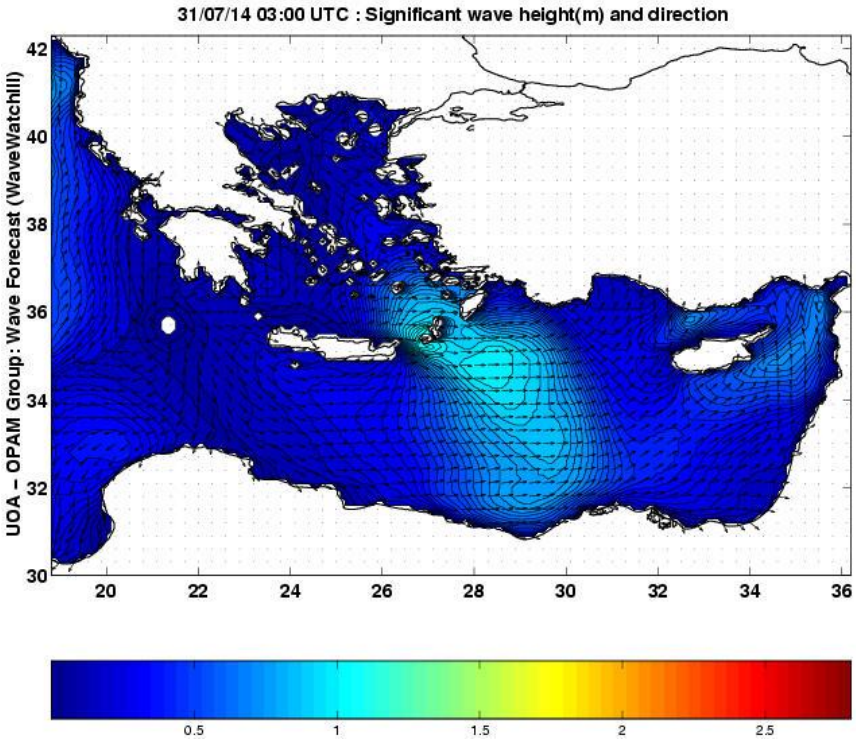

Fig. 12.1 – Wave climate (significant wave height and direction) forecast for the Eastern Mediterranean, Source: http://pelagos.oc.phys.uoa.gr/page10.html

Currents

Concerning ocean **circulation** models the most popular are associated with the names:

- Princeton Ocean Model, POM,
- Regional Ocean Model System, ROMS, developed at Rutgers University and UCLA,
- Hybrid Coordinate Ocean Model, HYCOM, which allows changing the depth coordinate locally between z-level, terrain following sigma layers and isopycnic layers. HYCOM is employed by the U.S. Navy, among others,
- Nucleus for European Modeling of the Ocean, NEMO, developed at the Laplace Institute in France,
- The unstructured grid Finite Volume Community Ocean Model, FVCOM, from the University of Massachusetts at Dartmouth and Woods Hole Oceanographic Institution,
- MIT's General Circulation Model, MITgcm.

A more comprehensive list can be found in the Wikipedia link: http://en.wikipedia.org/wiki/List_of_ocean_circulation_models.

Several Mediterranean countries have continuously functioning numerical model based operational ocean circulation forecasting systems coupled to other forecasting models. The European Union project MFSTEP promoted the development of such systems covering the entire Mediterranean, with focus on regional features. These are associated with the Italian MFS (*Pinardi and Coppini, 2010*), CYCOFOS in Cyprus (*Zodiatis et al., 2005*), ALERMO in Greece, etc. The Mediterranean Operational Oceanography Network, MOON, served as umbrella organization for collecting and redistributing the local and sub-regional forecast data. MOON was recently merged into the Mediterranean Operational Network for the Global Ocean Observing System, MONGOOS, (see websites http://www.mongoos.eu/ and http://www.capemalta.net/medgoos/index.html).

Fig. 12.2 shows the ALERMO forecast of (daily average) flow velocities for the Eastern Mediterranean at 5, 30 and 360 m below sea surface.

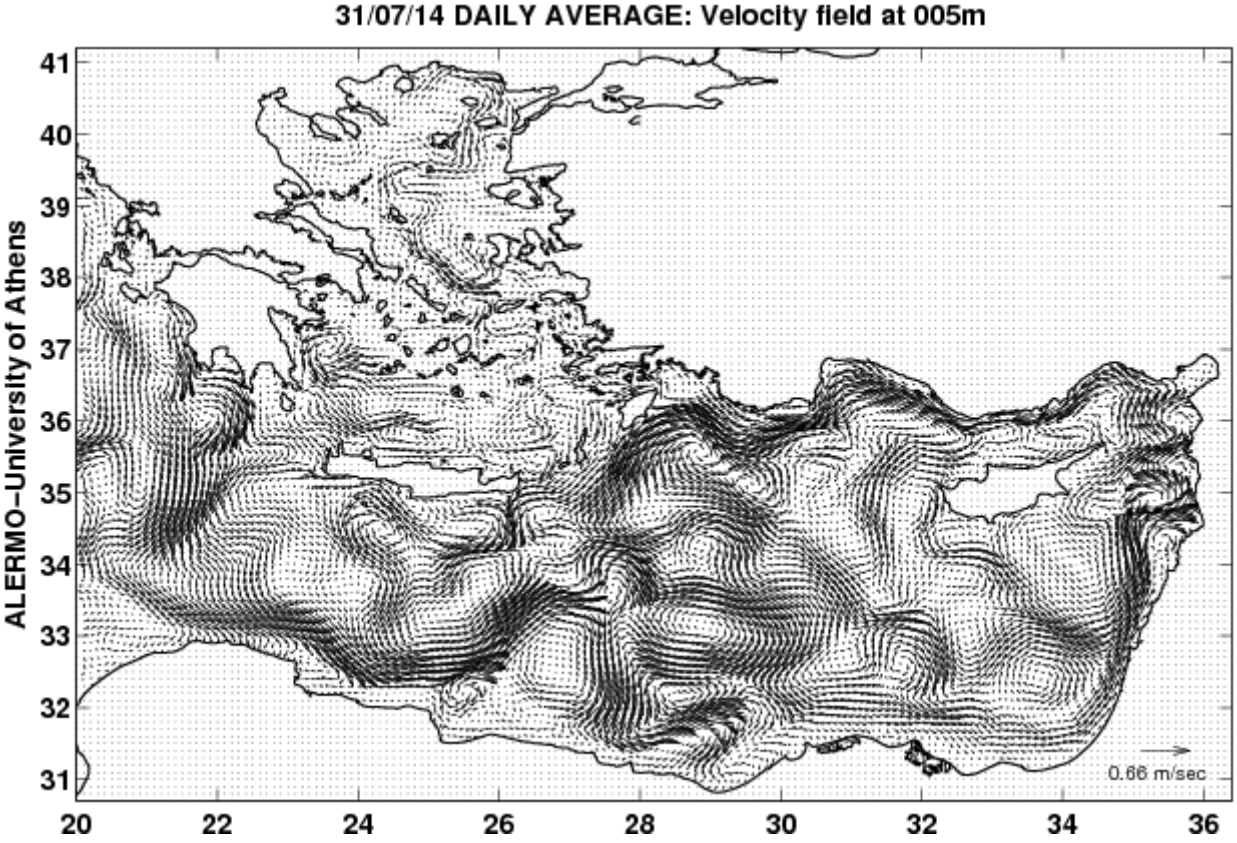

(a)

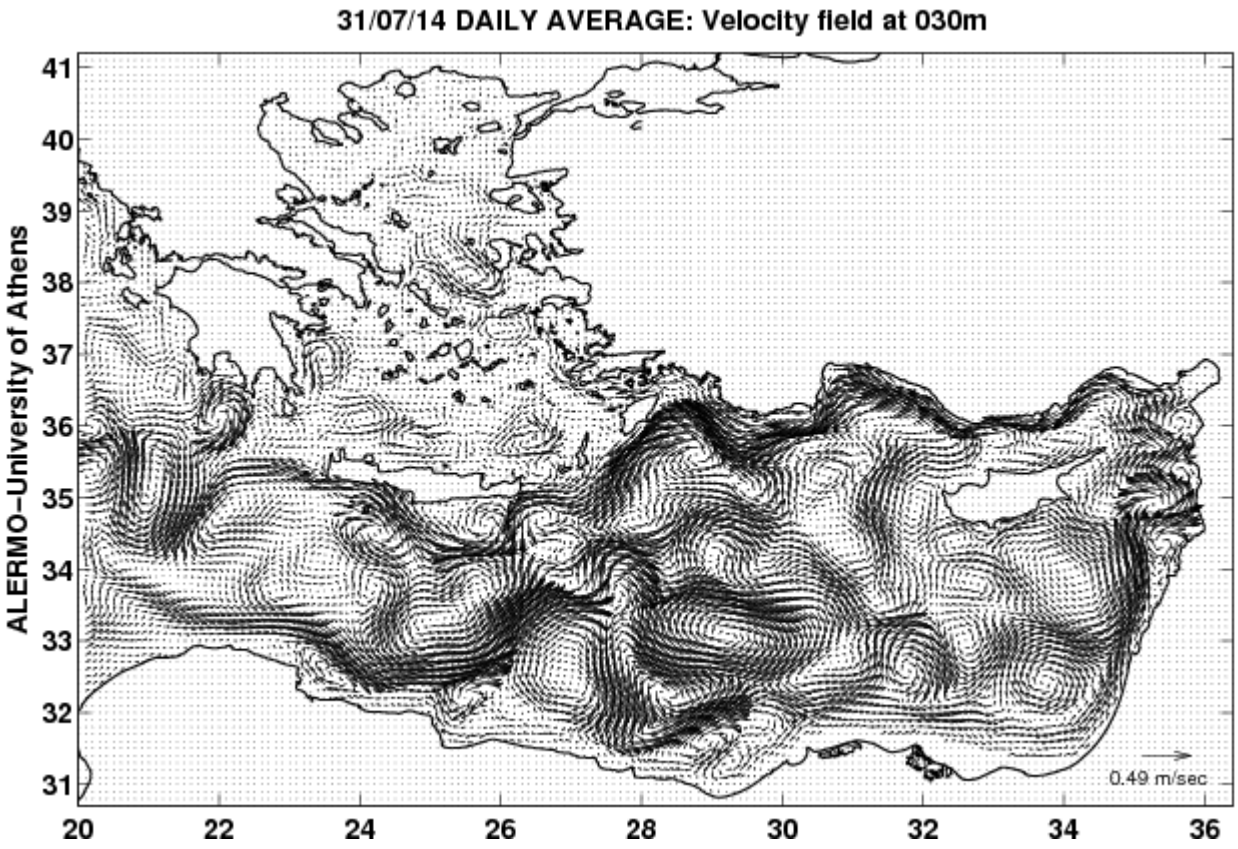

(b)

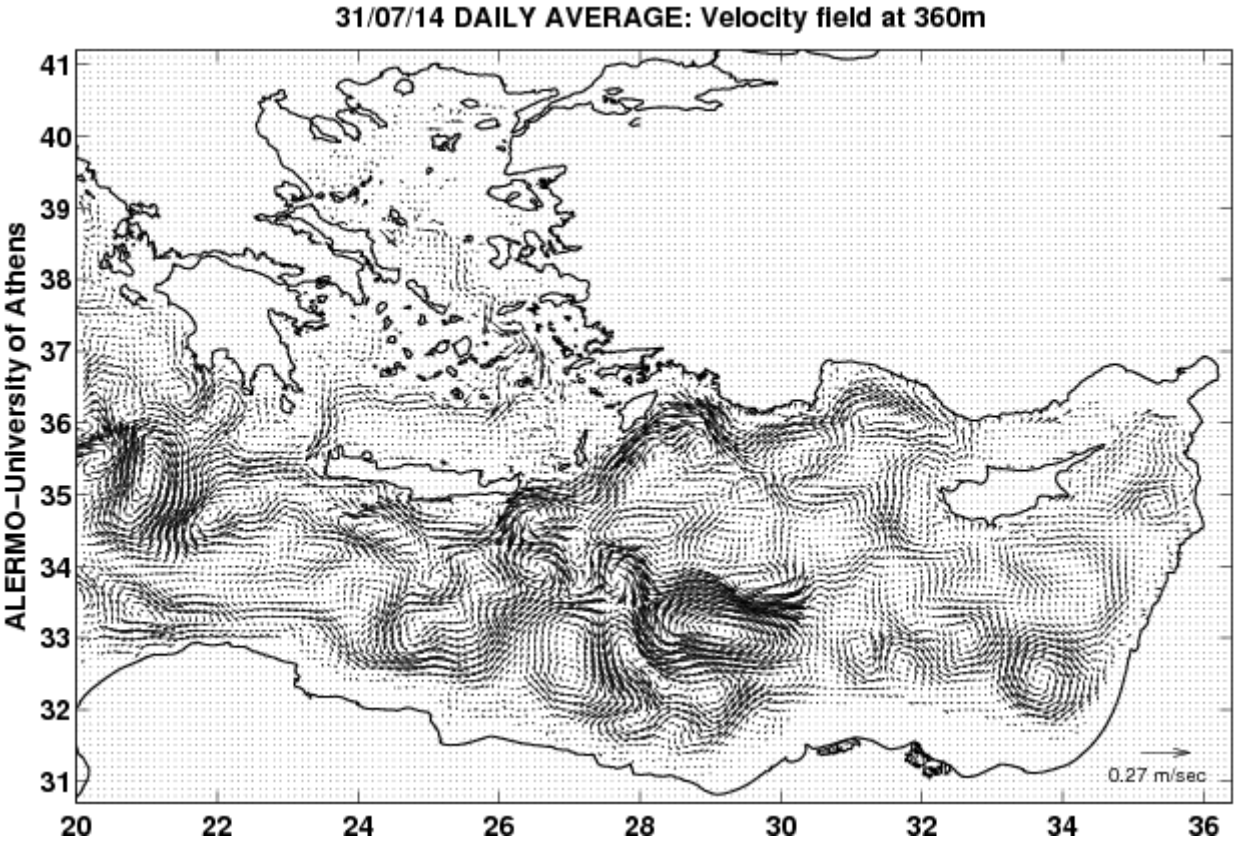

(c)

Fig. 12.2 – ALERMO forecast of average daily flow velocity in the Levantine Sea at (a) 5 m depth, (b) 30 m depth and (c) 360 m depth. Note the different velocity scale at the lower right corner of each plot. Coordinates are longitude and latitude in arc-degrees. Source: ALERMO website http://pelagos.oc.phys.uoa.gr/mfstep/bulletin/

Use in Israel

Concerning the implementation of a quasi real time forecasting system for most of Israel's EEZ at IOLR, many elements are operational. *Brenner et al.* (2007) made an evaluation study of the hydrodynamics (POM) and wave (WAM) models implemented at IOLR for the south-eastern Mediterranean, testing their behavior for diverse wind and other atmospheric forcing at sea surface. Several sources of atmospheric forcing were assessed, based on their availability and their impact on the quality of the ocean model forecasts. The various sources included operational forecast centers, other research centers, as well as running an in-house regional atmospheric model. For waves, higher spatial and temporal resolution of the winds are essential for improving the forecasts in terms of significant wave height and correct prediction of the time of occurrence of high wave events. For the hydrodynamics, using the predicted wind stress and heat fluxes directly from an atmospheric model can potentially produce pretty good short range ocean forecasts. *Brenner et al.* (2007) also describe a high resolution nested version of the model, which proved to be stable under a variety of forcing conditions and time scales, thus indicating the robustness of the selected nesting strategy.

IOLR/ISRAMAR is the governmental organization that provides on line wave forecasts, running an operational WAM model in conjunction with other European similar services, and with SELIPS (South Eastern Levantine Israeli Prediction System, based on POM) as ocean circulation model (see http://isramar.ocean.org.il/isramar2009/selips/description.aspx). Both employ SKIRON (the weather forecasting model at the University of Athens) as the source for wind and other atmospheric forcing. The models provide 4 day forecasts for flow velocity, salinity and temperature at depths 5m, 30m, 50m, 100m and 300m, as well as sea surface level forecasts, computed at grid points with horizontal resolution of about 1 Km.

The WAM model at IOLR produces a five day forecast of wave climate for the entire Mediterranean and the Levantine Basin, presented at three hour intervals. Fig. 12.3 shows the WAM model forecast for the Levantine basin at a certain time. The forecast map can show an animation of the five day forecast. The display can be significant wave height and the SKIRON wind forcing used, or significant wave height and direction.

Also, the five day WAM model forecast is provided as a three hour time series at a point selected interactively. Fig. 12.4 shows the time series for significant wave height and wave period. The climate/wind forcing, also shown at the selected point, is provided by the SKIRON system. The plots were extracted from the ISRAMAR website for the WAM wave forecast for the Levantine basin.

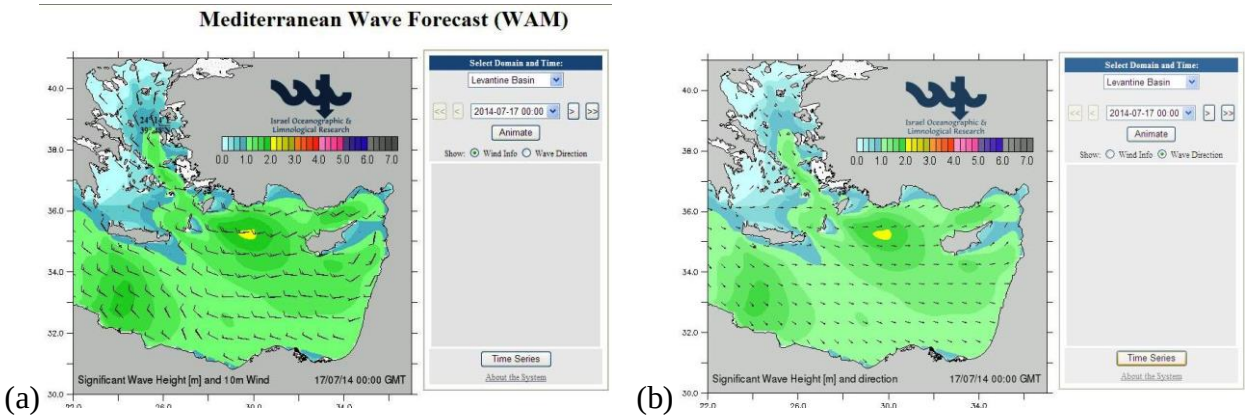

Fig. 12.3 – Wave climate forecast for the Levantine basin (a) Significant wave height in meters and (SKIRON) 10 m wind used as forcing; (b) Significant wave height and direction. Source: http://isramar.ocean.org.il/isramar2009/wave_model/default.aspx?model=wam&region=coarse#

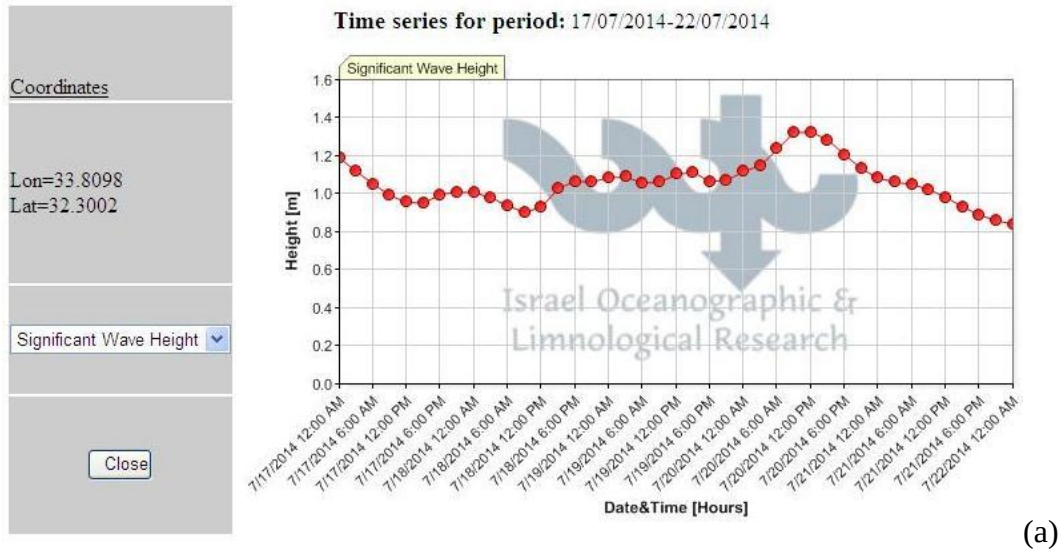

(a)

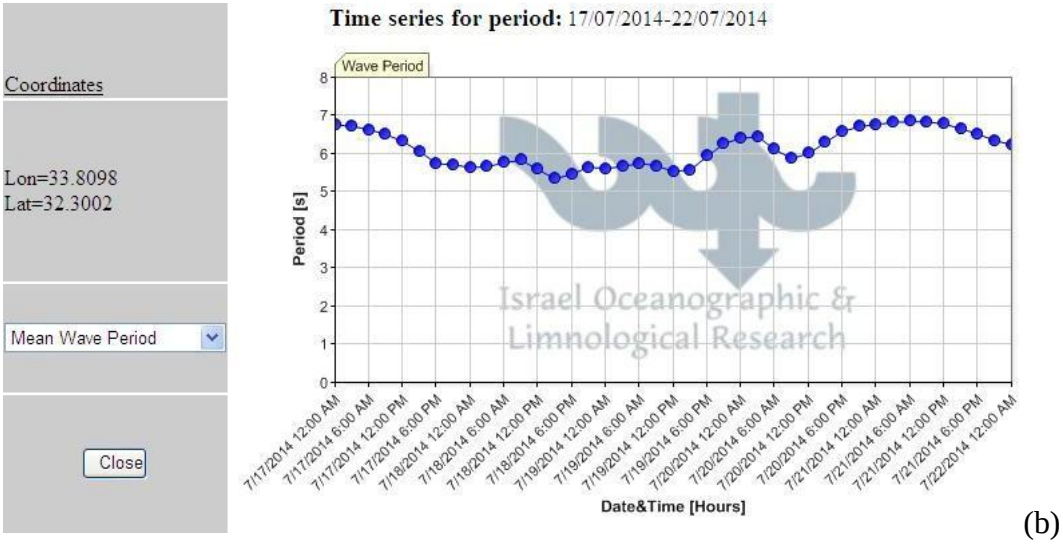

(b)

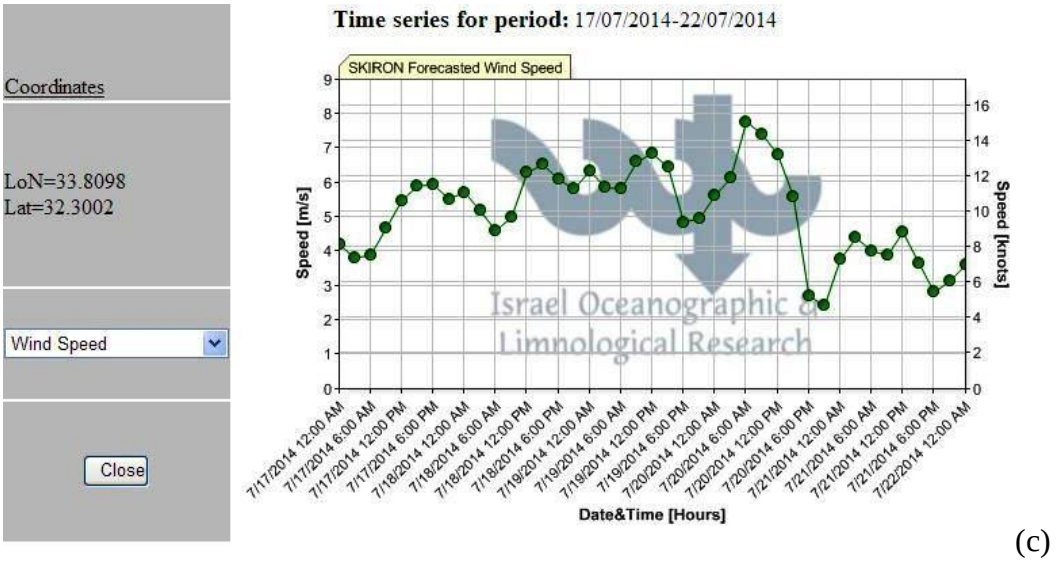

(c)

Fig. 12.4 – Wave climate model forecast (based on WAM) and SKIRON wind forcing: Time series of (a) Significant wave height, (b) wave period and (c) 10 m wind speed, at a selected point in the South Eastern corner of the Levantine Sea. Source: ISRAMAR website: http://isramar.ocean.org.il/isramar2009/wave_model/default.aspx?model=wam&region=coarse#

A finer grid is used for wave forecasts at the coastal zone, and particularly for Haifa, using the SWAN system, with SKIRON wind forcing. The forecast is for three days at 3 hour intervals.

Fig. 12.5 presents an example of the SELIPS forecast results, as extracted from ISRAMAR's website. The figure shows the distribution of potential temperature five meters below sea surface, for a selected time. The arrows represent computed flow speed and direction at computational grid points at that depth. The layer can be selected at given intervals down to 300 m depth. SELIPS forecasted sea surface level in the Levantine basin is plotted, for the same selected time, in Fig. 12.6.

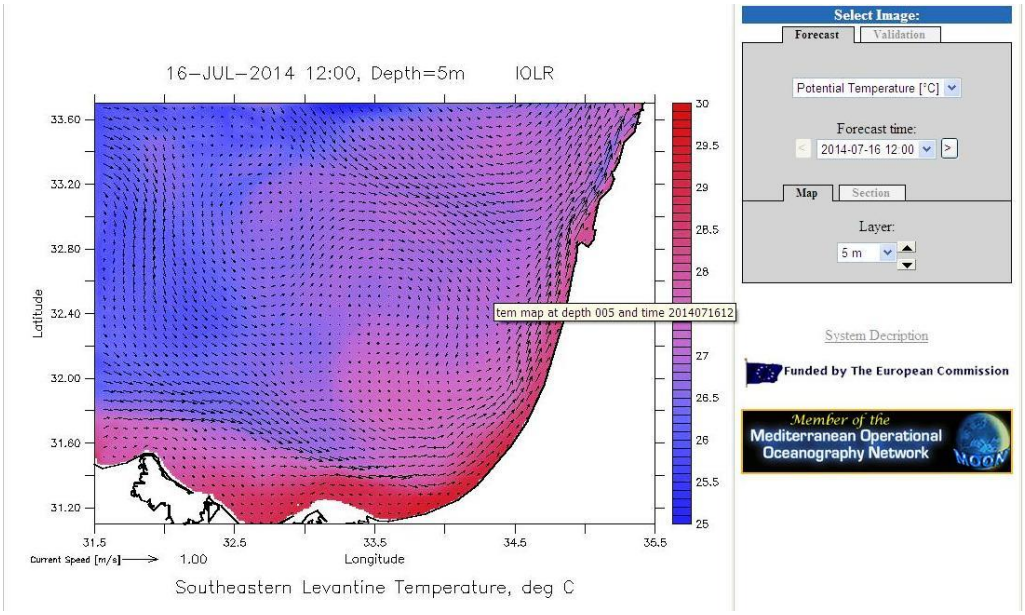

Fig. 12.5 – Temperature and flow velocity fields 5 m below sea surface forecasted by SELIPS at a selected time. Source http://isramar.ocean.org.il/isramar2009/selips/

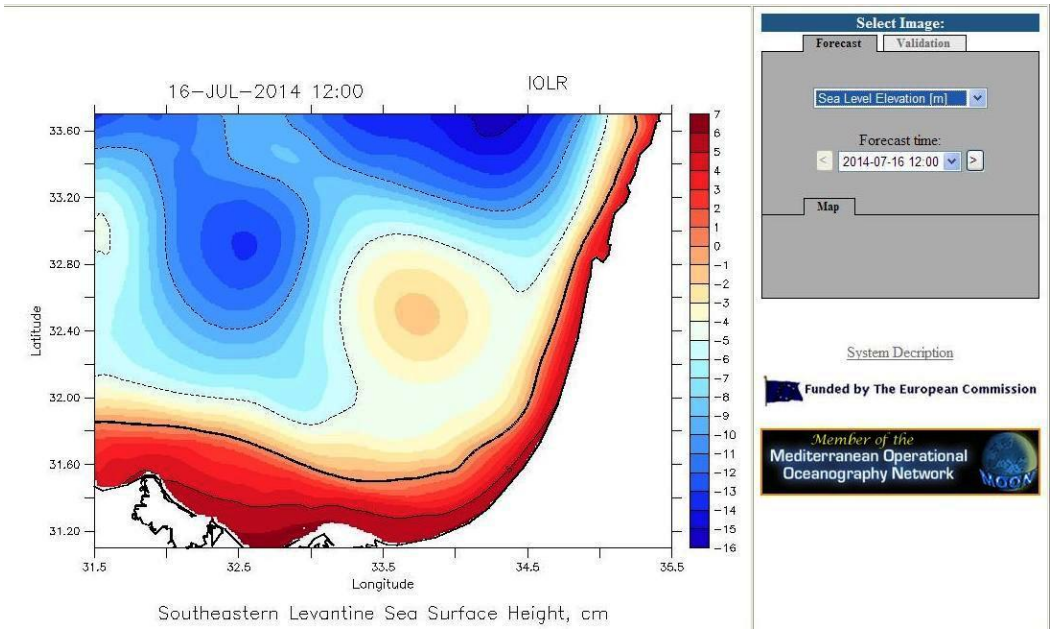

Fig. 12.6 – SELIPS forecast of sea surface level at the same selected time.
Source: http://isramar.ocean.org.il/isramar2009/selips/

CAMERI also utilizes hydrodynamic numerical models, designed for coastal waters. The models are two dimensional and are mostly suited for areas in the vicinity of the shoreline, to resolve flow around marine structures like harbors, marinas, breakwaters and the like. The systems used are CAMERI-3D and MIKE 21/3 FM. The latter system has been developed by the Danish Hydraulic Institute, DHI, and is one of the most accepted worldwide. The software consists of a series of interrelated compatible application modules that deal with hydrodynamics, sediment transport, coastal morphology, etc., sharing the same rectangular grid or flexible mesh covering the area of interest, common data formats, a common user interface and shared utility service routines.

In a typical coastal application involving an area of a few tens of square kilometers, the horizontal grid size may vary from, say, 5-30 m in the area of interest to 100-300 m in the outer borders of the model (see, for example, *Khudyakova et al., 2012*)

To finalize this section and in order to get an idea of the complexity of the Mediterranean currents pattern, the YouTube clip at https://www.youtube.com/watch?v=BeurUq0cRaM presents a visualization of an 11 month flow simulation constrained with measured data. The clip was prepared at NASA's Goddard Space Flight Center Scientific Visualization Studio. The time period for this visualization is 16 Feb 2005 through 16 January 2006. One second in the clip corresponds to about 2.75 days in the simulation. The colors of the flows represent their depths. White represents near surface flow while deeper currents are bluer. The flow field was produced by running a simulation using the MIT general circulation model (MITgcm), constrained with satellite and other data. Unfortunately, flow in the Levantine basin is not shown in the clip. Besides the capability of visualizing huge amounts of data in a compact and understandable fashion, the clip illustrates the power of numerical flow models and data synthesizing software.

References

Brenner S., Gertman I., Murashkovsky, A., *2007*; "Preoperational ocean forecasting in the southeastern Mediterranean Sea: Implementation and evaluation of the models and selection of the atmospheric forcing", Journal of Marine Systems, **65**, 268-287

Hasselman K. et al. (The WAMDI group), *1988*; "The WAM model – A third Generation Wave Prediction Model", American Meteorological Society, Journal of Physical Oceanography, **18**, 1775-1810

Levi Y. and Cremona I., *2013*; "ECMWF system-4 predictability over the Mediterranean basin", Powerpoint presentation, Israel Meteorological Service, 38 slides. Found as pdf file in the Internet.

Khudyakova V. et al., *2012*; "Netanya coast and cliff protection study – Model calibration", CAMERI interim report P.N. 755, 101pp.,Technion City, Haifa

Komen G.J., Cavaleri L., Donelan M., Hasselmann K., Hasselmann S., Janssen P.A., *1994*; "Dynamics and Modeling of Ocean Waves", Cambridge University Press, Cambridge. 554pp.

Pinardi N. and Coppini G., *2010*; "Operational oceanography in the Mediterranean Sea: the second stage of development", Ocean Science, 6, 263-267

Richardson D.S. et al., *2013*; "Evaluation of ECMWF forecasts, including 2012-2013 upgrades", ECMWF Technical Memorandum 710, 55pp. Found as pdf file in the Internet.

Zodiatis G., Lardner R., Hayes D.R., Georgiou G., *2005*; "CYCOFOS - An operational oceanographic forecasting and observing system for the Eastern Mediterranean Levantine basin: The Cyprus coastal ocean forecasting and observing system", Fourth EuroGOOS Conference Proceedings, 503-599

13 – NEW TECHNOLOGIES FOR OCEAN MEASUREMENTS

Remote measurements from satellites (temperature, chlorophyll)

Remote sensing of surface temperature and chlorophyll concentration that relies on satellite-based technologies became a very powerful method for determination of these important parameters in the coastal regions and in the open ocean. In particular, the **Coastal Zone Color Scanner** (or **CZCS**) was a multi-channel scanning radiometer aboard the Nimbus 7 satellite, predominately designed for water remote sensing. Nimbus 7 was launched 24 October 1978, and CZCS became operational on 2 November 1978. It was only designed to operate for one year (as a proof-of-concept), but in fact remained in service until 22 June 1986.

CZCS measured reflected solar energy in six channels, at a resolution of 800 meters. These measurements were used to map chlorophyll concentration in water, sediment distribution, salinity, and the temperature of coastal waters and ocean currents. CZCS lay the foundations for subsequent satellite ocean color sensors, and formed a cornerstone for international efforts to understand the ocean's role in the carbon cycle.

Reflected solar energy was measured in six channels to sense color caused by absorption due to chlorophyll, and sediments in coastal waters. Data from the scanning radiometer were processed, with algorithms developed from the field experiment data, to produce maps of chlorophyll absorption. The temperatures of coastal waters and ocean currents were measured in a spectral band centered at 11.5 micrometers. Observations were made also in two other spectral bands, 0.520 micrometers for chlorophyll correlation and 0.750 micrometers for surface vegetation.

LiDAR bathymetry or Airborne Laser Bathymetry & Topography System (ALBTS)

Airborne laser bathymetry offers the hydrographic community a very rapid and thorough wide area coverage solution for charting and data acquisition in shallow waters and along the coastal zone. Its non-impact technology provides the perfect solution for imaging delicate environments and for sensitive ecosystems. In particular, LiDAR bathymetry can survey those areas that are either denied to vessel based systems or where the risks are too great.

The basic laser sounding principle is similar to acoustic methods. A pulse of laser light is transmitted from the ALBTS towards the water surface in a predefined pattern. The red laser light is reflected at the water surface whereas the green laser light penetrates into the water volume. The green laser light is reflected in the water volume and from the seabed. A portion of the reflected light is collected in the ALBTS receivers. The water depth is equal to the time elapsed between the two echo pulses, multiplied by the speed of light in water. Typical water depth penetration is in the range 20-40m but, in good conditions, depths as great as 70m are possible.

There is a common and widely circulated miscomprehension that airborne ALBTS surveys are expensive. The confusion arises over the day rate of an airborne ALBTS system compared to, say, a vessel based swath system. In fact, ALBTS bathymetry is 25-30% the cost of a conventional swath survey when the economies of scale come into play. The cost break comes when site areas reach the 8-10km^2 level, thereafter, the cost of a ALBTS survey compared with a conventional acoustic swath survey rapidly falls 35% at 50km^2 and about 25% at 100km^2. Just as acoustic swath systems cannot do everything, so neither can ALBTS. The greatest advantages to the data user community come when the two methods are integrated. More details can be found in the paper by Danson (2006).

High frequency radars for wave heights and surface velocity measurements

This is well established as a powerful tool for measuring the pattern of surface currents over an area out to a range of about 30 km., with an accuracy of about ± 3 cm/s in all conditions. Much has been claimed for its potential for measuring directional wave spectra out to ranges of perhaps 150 km. Although substantial progress has been made, the development has still had a rather limited success.

The radio wavelength used are in the range 10 m to 300 m (30 MHz to 1 MHz).The first developed for this specific purpose was the CODAR (Coastal Oceans Dynamics Applications Radar) intended for measuring both waves and currents). The OSCR (Ocean Surface Current Radar) was developed specifically for current measurement, and has been found to be very useful in this application, but it can also be used for wave measurement. Longer wavelength HF radar was developed at the University of Birmingham mainly for wave measurement. The most recent is the WERA (WEllen Radar) developed by the University of Hamburg. The radars used are coherent radars.

To simplify the explanation the radars are considered as continuous transmission radars arranged to illuminate only one approximately rectangular path of the sea-surface, though in fact, a grid of such patches can be view simultaneously. Energy is backscattered from the waves on the sea surface and is subject to a small Doppler shift (generally less than 1 Hz.). In 1955 D.D. Crombie showed that the radar echo from a patch of the sea surface contained two main spectral lines, one positively and one negatively Doppler shifted from the transmitter frequency. These lines correspond to echoes from Bragg resonant waves travelling towards and away from the radar. With no current, the Doppler shifts are equal to the frequency of the Bragg resonant wave, and are therefore in the range 0.1 to 0.6 Hz approximately. If a component of the surface current is flowing towards the radar, it will increase the Doppler shift of the approaching wave and decrease that of the receding wave. The current component can be calculated from the difference. Two radars looking at the same area of sea from different directions allow two component of the current to be measure. More details can be found in the monograph by Tucker and Pitt (2001).

Although around the world, more systems of this kind are being installed, no one system has been purchased in Israel until recently. Very soon the things are going to be changed dramatically due to an initiative of a new faculty at Tel Aviv University Dr Yaron Toledo. He is supported in part by the seed money from Tel Aviv University and got support from two foundations, among them Israel Scientific Foundation, to purchase and install two system (WERA type) that will enable him to provide data coverage (currents and waves) for the most of the Israeli Mediterranean EEZ. It can provide a huge boost in regards to the abilities to measure spatial distribution of currents and waves including locations where platforms for gas/oil production are placed.

References

Edwin Danson Understanding LiDAR bathymetry for Shallow Waters and Coastal Mapping, TS 19 – Hydrography II, *Shaping the Change XXIII FIG Congress* Munich, Germany, October 8-13, 2006

M.J. Tucker and E.G. Pitt 2001 Waves in Ocean Engineering, Elsevier, Amsterdam-London-New York.

CONCLUDING REMARKS

It is obvious that carrying out an important mission related to the development of the Israeli Mediterranean EEZ requires first of all to measure or to compute the circulation currents, to assess the waves and to determine the temperature and salinity fields in the Eastern Mediterranean. The detailed data can be found by employing advanced computations models. However, the validation of the velocity and temperature fields may be performed *only* using measured data obtained from remote measurements employing various types of radars e.g. radar for SST measurements using e.g. Sea-viewing Wide Field-of-view Sensor (SeaWiFS) of NASA, HF radar, SAR or INSAR for currents and waves. The latter two can be airborne (using specially equipped planes) or from satellites. HF radar uses antennas located at the coast. As mentioned, Dr. Yaron Toledo, new faculty at School of Mechanical Engineering, of Tel Aviv University is on the way to develop this ability in Israel.

Until recently, most of the efforts of CAMERI scientists were to operate near-shore coastal models at water depths not exceeding 30-50 m. These models were used to provide coastal designers dealing with coastal projects initiated by IPC, IEC and related to Desalination Plants (DP) with solutions optimization and to carry out EIA requested by the Ministry of Environmental Protection. Recently CAMERI researches made a significant progress in acquiring and development of a deep-water coupled wave-currents model *for the first time in Israel*. The expansion of modeling suits to the Israeli Mediterranean EEZ enables to meet the new requirements caused by offshore activities as a consequence of gas and oil production. The development of modern advanced numerical models, in particular, wave-current coupled models will be carried out through collaboration with Universities and institutions around the world who have already acquired proven experience in the field.